FUNDAÇÃO OSWALDO CRUZ

INSTITUTO DE PESQUISAS GONÇALO MONIZ

Curso de Pós-Graduação em Biotecnologia em Saúde e Medicina Investigativa

TESE DE DOUTORADO

ATIVIDADE ANTIMALÁRICA, ESPECTRO E MECANISMO DE AÇÃO DE COMPOSTOS DE RUTÊNIO E PLATINA COM A CLOROQUINA

TAÍS SOARES MACEDO

Salvador – Bahia
2016

FUNDAÇÃO OSWALDO CRUZ

INSTITUTO DE PESQUISAS GONÇALO MONIZ

Curso de Pós-Graduação em Biotecnologia em Saúde e Medicina Investigativa

ATIVIDADE ANTIMALÁRICA, ESPECTRO E MECANISMO DE AÇÃO DE COMPOSTOS DE RUTÊNIO E PLATINA COM A CLOROQUINA

TAÍS SOARES MACEDO

Orientadora: Profª Drª Milena Botelho Pereira Soares
Co-orientador: Prof. Dr. Diogo Rodrigo Magalhães Moreira

Tese apresentada ao Curso de Pós-Graduação em Biotecnologia em Saúde e Medicina Investigativa para obtenção do grau de Doutora.

Salvador – Bahia
2016

"ATIVIDADE ANTIMALÁRICA, ESPECTRO E MECANISMO DE AÇÃO DE COMPOSTOS DE RUTÊNIO E PLATINA COM A CLOROQUINA."

TAÍS SOARES MACEDO

FOLHA DE APROVAÇÃO

COMISSÃO EXAMINADORA

Dra. Marilda de Souza Gonçalves
Pesquisadora Titular
IGM/FIOCRUZ

Dra. Márcia Cristina Aquino Teixeira
Professora Adjunta
UFBA

Dra. Elisalva Teixeira Guimarães
Professora Assistente
UNEB

AGRADECIMENTOS

Gostaria de expressar os meus sinceros agradecimentos a todas as pessoas e instituições que contribuíram para a realização deste trabalho.

À Fundação de Amparo à Pesquisa do Estado da Bahia – FAPESB pela bolsa de Doutorado concedida.

Ao Programa de Pós-Graduação em Biotecnologia em Saúde e Medicina Investigativa do Centro de Pesquisas Gonçalo Moniz – CPqGM (FIOCRUZ), em especial ao Laboratório de Engenharia Tecidual e Imunofarmacologia – LETI, pela acolhida durante o doutorado, pela logística e infra-estrutura fornecida para a realização do trabalho.

À minha orientadora, Dra. Milena Botelho Pereira Soares, pelos ensinamentos e principalmente pela grande oportunidade e confiança, sem as quais nada disso teria acontecido.

Agradeço imensamente ao meu co-orientador, Dr. Diogo Rodrigo de Magalhães Moreira, pela confiança, paciência, pelos importantes ensinamentos, experiências, amizade, apoio e incentivo, sem os quais este trabalho não teria sido possível. O que seria de mim neste doutorado sem você? Muito obrigada!

Neste contexto, não poderia deixar de agradecer a professora e amiga Dra. Fabiana Regina Nonato, pelo grande incentivo ao longo de toda minha vida acadêmica, pela amizade, por tudo e sempre. Nona, muito obrigada!

À toda excelente equipe e amigos do Laboratório de Engenharia Tecidual e Imunofarmacologia – LETI pelos importantes conhecimentos e momentos compartilhados, especialmente à Msc. Nanashara Coelho de Carvalho e Msc. Cássio Santana Meira que me receberam de braços abertos e gentilmente me ensinaram e auxiliaram na rotina do laboratório.

À Msc. Maria Menezes, por ter passado seus conhecimentos sobre a cultura de *Plasmodium*, gentilmente me ensinando e auxiliando no início quando comecei a trabalhar com os parasitas.

Neste contexto, agradeço aos alunos de iniciação científica: Helena Mariana Teixeira, Marcelo da Paixão e Camila Couto pela grande ajuda em etapas importantes para o desenvolvimento do trabalho, pela amizade e momentos compartilhados. Obrigada!

Ao Laboratório de Tecnologia Farmacêutica do Farmanguinhos/FIOCRUZ, nas pessoas da Juliana Johansson Medeiros, Ana Claudia Tavares e Kátia Menezes pelo fornecimento da Cloroquina e demais antimaláricos que viabilizou a preparação dos complexos.

A Prof. Antoniana Ursine Krettli da Fiocruz/Minas pelo envio da cultura de 3D7. Aos pesquisadores do Departamento de Química da Universidade Federal de São Carlos: Prof. Alzir Azevedo Batista, Msc. Wilmer José Villarreal Peña, Msc. Legna Andreina Colina Vegas e Drª. Marilia Barbosa pelo envio dos compostos.

Agradeço imensamente a toda minha família, em especial aos meus pais, Francisco e Bernadete, e meu namorado Vagner, pela extraordinária ajuda, grande incentivo, apoio, paciência, pelo amor dedicado e compreensão. Amo vocês!

Um agradecimento especial as amigas, que de longe ou perto, sempre me apoiaram: Msc. Camilla Reis, Msc. Nanashara Carvalho, Msc. Joicelene Lima e Dra. Vanessa Matos. “We are the champions, my friends. And we’ll keep on fighting ’till the end...”

Aos meus gatos e cachorros, pelos momentos de alegria, distração e conforto quando me sentia cansada. Obrigada meus preciosos!

Agradeço as minhas culturas de *Plasmodium* por me ensinarem a arte da paciência e mostrarem que nem sempre as coisas são do jeito que planejo.

Aos membros da Banca Examinadora por aceitarem o convite e pelas contribuições prestadas ao presente trabalho. A Ana Maria Fiscina Vaz Sampaio da Biblioteca de Ciências Biomédicas Eurydice Pires de Sant'Anna, CPqGM – FIOCRUZ, pela ajuda e correções realizadas na tese, colocando-a dentro das Normas da ABNT.

A todos que eu não tenha mencionado e que colaboraram na realização deste trabalho, me ajudando ao longo deste caminho, os meus mais profundos agradecimentos.

MACEDO, Taís Soares. Atividade antimalárica, espectro e mecanismo de ação de compostos de rutênio e platina com a cloroquina. 65 f. il. Tese (Doutorado) – Fundação Oswaldo Cruz, Instituto de Pesquisas Gonçalo Moniz, Salvador, 2016.

RESUMO

INTRODUÇÃO: A malária é uma das doenças infecciosas de maior incidência e que mais leva a óbito no mundo. Os medicamentos disponíveis são capazes de combater o parasita no ciclo intraeritrocítico, no entanto há cepas resistentes ao tratamento com quinolinas e artemisininas. Além disso, os medicamentos em uso clínico não eliminam as formas sexuadas do parasita, responsáveis pela transmissão, nem os hipnozoítos, fase hepática latente causadora das recidivas da doença. Em virtude disso, é necessário identificar novos fármacos antimaláricos. Dentre as classes de moléculas com potencial terapêutico antimalárico, os complexos com metais de transição se destacam como possíveis candidatos. **OBJETIVO:** Identificar potenciais fármacos antiparasitários para o tratamento da malária, com base em moléculas do tipo complexos metálicos com a cloroquina. **MATERIAL E MÉTODOS:** Em relação ao metal utilizado, o átomo de rutênio está presente nos compostos MCQ, FCQ, BCQ, FFCQ e a platina nos compostos WV-90, WV-92, WV-93, WV-94. Dois complexos sem a presença da cloroquina na sua composição, FCL e WV-48, também foram testados como antimaláricos. **RESULTADOS:** A inibição do crescimento *in vitro* no ciclo eritrocítico das cepas 3D7 (sensível à cloroquina) e W2 (resistente à cloroquina) do *Plasmodium falciparum* revelou que os complexos sem cloroquina não apresentaram atividade em concentrações inferiores à 3.0 µM. Entretanto, a incorporação da cloroquina na composição de complexos de platina e rutênio resultou em compostos com atividade antiparasitária em concentrações abaixo de 1.0 µM. Portanto, a presença da cloroquina se mostrou essencial para a atividade antimalárica. Quando a potência e seletividade *in vitro* dos complexos metálicos foram comparadas à cloroquina, observou-se que nenhum dos complexos metálicos apresentou potência ou seletividade superiores às da cloroquina. Em trofozoítos, os complexos de rutênio apresentaram uma ação parasiticida mais rápida que a cloroquina, enquanto que os complexos de platina apresentaram uma ação mais lenta que os de rutênio, mostrando um perfil mais similar à cloroquina. Tal como a cloroquina, os complexos de platina e de rutênio inibiram a polimerização da hemina em β-hematina. Os complexos de rutênio exerceram ação parasiticida em cultura de trofozoítos através da produção de ROS, enquanto que os complexos de platina não induzem de maneira significativa tal produção. Os complexos de platina reduziram a viabilidade da mitocôndria em trofozoítos. Ao contrário da cloroquina, que apresenta um espectro de ação restrito ao ciclo eritrocítico do *Plasmodium*, tanto os complexos de rutênio quanto os de platina apresentaram um espectro de ação mais amplo, reduzindo a viabilidade de gametócitos do *P. falciparum* e inibindo a carga parasitária em células infectadas com esporozoítos do *P. berguei*. Em camundongos infectados com a cepa NK65 do *P. berghei* o tratamento com complexo MCQ reduziu em 95.1% a parasitemia e em 40% a taxa de mortalidade quando administrado na dose de 50 mg/kg por via intraperitoneal. **CONCLUSÃO:** Os dados aqui apresentados são de extrema relevância na compreensão de compostos inorgânicos, em especial complexos metálicos, como candidatos a agentes antimaláricos.

Palavras-chave: *Plasmodium*, Malária, Complexos Metálicos, Cloroquina, Multiestágio

MACEDO, Taís Soares. Antimalarial activity, spectrum and mechanism of action of ruthenium and platinum complexes with chloroquine. 65 f. il. Thesis (Doctor) – Fundação Oswaldo Cruz, Instituto de Pesquisas Gonçalo Moniz, Salvador, 2016.

ABSTRACT

INTRODUCTION: Malaria is one of the infectious diseases of highest incidence and mortality in the world. Drugs currently available are efficacious against parasites in the blood stage, however there are strains resistant treatments based on quinolones and artemisinines. In addition, these drugs do not eliminate neither the asexual forms responsible for human-to-vector transmission nor the dormant hypnozoites resident in the liver, which are responsible for the relapse of disease. In view of this, novel antimalarial drugs are needed. Among the classes of compounds which holds therapeutic potential, complexes with transition metals are considered of great promise. **OBJECTIVE:** Identify potential antiparasitic drugs for the malaria treatment, based on metal complex molecules with chloroquine. **MATERIAL AND METHODS:** Regarding the employed metal, the atom of ruthenium is present in MCQ, FCQ, BCQ and FFCQ compounds, while a platinum atom is present in WV-90, WV-92, WV-93 and WV-94 complexes. Two complexes lacking chloroquine, FCL and WV-48, were also tested as antimalarial agents. **RESULTS:** The inhibitory activity of *in vitro* parasite growth in the erythrocytic cycle of 3D7 (chloroquine-sensitive) and W2 (chloroquine-resistant) strains of *P. falciparum* revealed that complexes lacking chloroquine were devoid activity in concentration up to 3.0 µM. In contrast, incorporating chloroquine in complexes of platinum and ruthenium resulted in compounds with antiparasitic activity in in concentration up to 1.0 µM. Therefore, the presence of chloroquine in the composition of metal complexes is essential for antimalarial activity. When *in vitro* potency and selectivity indexes of metal complexes were compared to chloroquine, none complexes presented superior potency and selectivity than chloroquine. In trophozoites, ruthenium complexes presented faster killing activity than chloroquine, while platinum complexes displayed slow speed of action than ruthenium complexes, being platinum complexes similar to chloroquine. Like chloroquine, both platinum and ruthenium complexes were able to inhibit polymerization of hemin into β-hematin. Ruthenium complexes achieved parasiticidal activity against trophozoites by inducing the production of reactive oxygen species, while platinum complexes were devoid such property. Yet, platinum complexes reduced the mitochondrial viability in trophozoites culture. Unlike chloroquine, which presents a spectrum of action limited to erythrocytic stage, both ruthenium and platinum complexes displayed a wide spectrum of action, by reducing cell viability of gametocytes of *P. falciparum* and inhibiting parasite burden in cells infected by sporozoites of *P. berghei*. Mice infected by NK65 strain of *P. berghei* and treated with MCQ presented highest efficacy among tested complexes, by reducing in 95.1% blood parasitemia and in 40% mortality rate when given in a dose of 50 mg/kg by intraperitoneal route. **CONCLUSION**: The presented data are very important in understanding of inorganic compounds, in particular metal complexes as candidate antimalarial agents.

Key-words: *Plasmodium*, Malaria, Metal Complexes, Chloroquine, Multistage

SUMÁRIO

LISTA DE ILUSTRAÇÕES

1 INTRODUÇÃO

1.1 ASPECTOS GERAIS DA MALÁRIA

A malária é uma doença infecciosa causada por protozoários pertencentes ao filo Apicomplexa, família Plasmodiidae, gênero *Plasmodium*. Existem cerca de 200 espécies de plasmódio que podem infectar aves, répteis e mamíferos (DRONAMRAJU, 2006). Destas, cinco espécies são capazes de infectar o homem: *P. falciparum*, principal responsável pela mortalidade associada à doença, com um ciclo eritrocítico de 48 horas; *P. vivax* e *P. ovale*, também com um ciclo de 48 horas; *P. malariae*, com um ciclo eritrocítico de 72 horas e *P. knowlesi*, com um ciclo de 24 horas (COX-SINGH, 2008; CRAWLEY et al., 2010; OMS, 2015).

O *P. vivax* é encontrado principalmente na Ásia, América Latina e algumas partes da África; o *P. ovale* se distribui principalmente na África e Ilhas do Pacífico Ocidental; o *P. malariae* é encontrado em todos os continentes, o *P. falciparum* distribui-se pelas Américas, África e Ásia, e o *P. knowlesi* é encontrado no sudeste asiático (CARTER; MENDIS, 2002; COX-SINGH, 2008; ASKLING et al., 2012).

A doença é transmitida para o hospedeiro vertebrado através da picada de mosquitos do gênero *Anopheles*. Este inclui cerca de 400 espécies, porém 60 espécies são capazes de transmitir o plasmódio em condições naturais. Apenas as fêmeas dos anofelinos, que possuem o hábito hematófago, são responsáveis pela transmissão da malária (BRUCE-CHWATT, 1980).

Originada provavelmente no continente africano, desde a antiguidade a malária vem sendo uma das principais tormentas da humanidade. Também conhecida como paludismo, maleita, febre terçã ou quartã, a doença acompanhou as migrações humanas por outras regiões do mundo. Tais migrações foram o fator chave na disseminação global da doença. O nome malária teve sua origem na Itália do século XVIII, a partir da expressão "*mal aria*" que significa mau ar ou ar insalubre, por acreditarem, naquela época, que a doença era causada por emanações e miasmas provenientes dos pântanos (BRUCE-CHWATT; ZULETA, 1980; SCHLAGENHAUF, 2004).

Charles Louis Alphonse Laveran, médico do Exército Francês, foi o responsável pela descoberta do agente causador da malária. Em 1880, ao observar o sangue de indivíduos infectados, o médico identificou protozoários flagelados, aos quais deu o nome de *Oscillaria malariae*, hoje reconhecidos como gametócitos de *P. falciparum* (SCHLAGENHAUF, 2004).

A malária é a doença parasitária que causa a maior taxa de mortalidade no mundo. De acordo com a Organização Mundial da Saúde – OMS (2015), no ano de 2015 ocorreram cerca de 214 milhões de casos com 438 mil mortes.

A doença, por séculos interferiu no desenvolvimento econômico e continua sendo um grande problema social, econômico e, principalmente, de saúde pública em diversos países. Segundo Carter e Mendis (2002), a malária é hoje uma das grandes doenças da pobreza. Nenhuma nação rica é afetada por sua presença endêmica. Na Europa, nos Estados Unidos da América e em partes da China, há regiões inteiras que não teriam alcançado seu atual grau de prosperidade se não tivessem, primeiramente, erradicado a malária. Por outro lado, em muitos outros países, incluindo os mais pobres do mundo, a magnitude do problema da malária é simplesmente devastadora.

As manifestações clínicas da malária incluem febre alta, calafrios e sintomas de gripe. A periodicidade dos acessos febris está relacionada com o ciclo eritrocítico das espécies de plasmódio. Tradicionalmente, a malária causada por *P. vivax* e *P. ovale* é conhecida como malária terçã benigna, enquanto que a causada por *P. malariae* é a malária quartã e a que tem como agente etiológico o *P. falciparum* é a terçã maligna (CARTER; MENDIS, 2002).

Estimativas apontam que 1-2% dos casos de malária podem evoluir para a forma grave da doença, caracterizada por anemia grave, acidose metabólica e sintomas relacionados ao seqüestro de eritrócitos infectados, devido ao fenômeno de citoaderência dos parasitos ao endotélio dos capilares, obstruindo a microcirculação de diversos tecidos. A malária cerebral, responsável por grande parte dos óbitos registrados, é causada pela obstrução dos capilares no cérebro (MACKINTOSH et al., 2004).

1.2 CICLO DE VIDA DO *PLASMODIUM* SP. EM HUMANOS

O ciclo biológico do *Plasmodium* sp. se divide em duas fases distintas: uma fase onde ocorre a reprodução sexuada no hospedeiro definitivo invertebrado (Figura 1), e outra fase assexuada (esquizogonia), que ocorre no hospedeiro vertebrado (Figura 2). A fase assexuada pode ser subdividida no ciclo exoeritrocítico ou hepático, que ocorre no fígado, e o ciclo eritrocítico ou intraeritrocítico, que se desenvolve no interior dos eritrócitos.

Ao realizar o repasto sanguíneo, a fêmea infectada do mosquito inocula, juntamente com sua saliva, esporozoítos móveis na derme do hospedeiro humano (VANDERBERG; FREVERT, 2004; AMINO et al., 2006). Os esporozoítos invadem os vasos da derme, alcançam a corrente sanguínea e migram para o fígado, invadindo os hepatócitos, onde se diferenciam e, pelo processo de esquizogonia, originam os merozoítos (TAVARES et al., 2013). Os esquizontes maduros liberam os merozoítos teciduais através de um processo de brotamento de vesículas, denominado merossomas, que após atingirem a corrente sanguínea, repletos de parasitas, liberam os merozoítos (STURM et al., 2006). Estes invadem as hemácias e iniciam o ciclo intraeritrocítico, responsável pela sintomatologia clínica da malária. O tempo de diferenciação dentro dos hepatócitos varia de acordo com a espécie: cerca de uma semana para *P. falciparum*, *P. vivax* e *P. knowlesi* e duas semanas para *P. ovale* e *P. malariae*. Além disso, no caso das espécies *P. vivax* e *P. ovale*, ocorre a formação de hipnozoítos, forma latente do parasito que se mantém no fígado sem iniciar o processo de esquizogonia, e que é responsável por recaídas meses após a infecção (ANTINORI et al., 2013).

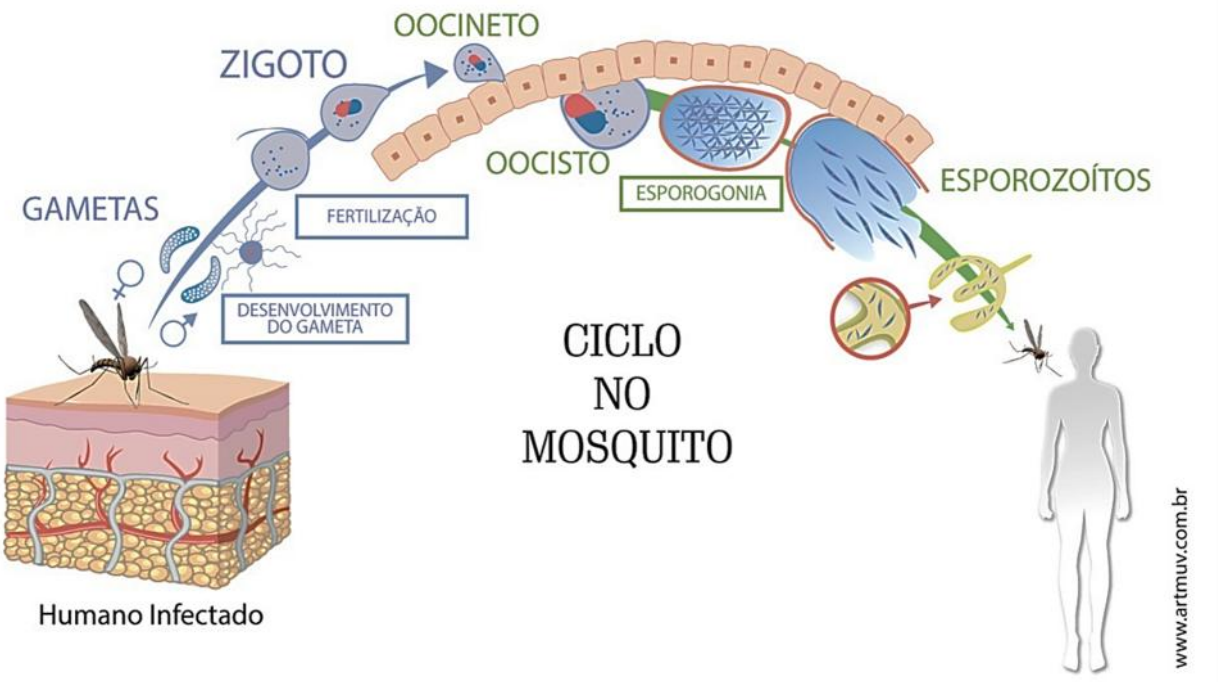

Figura 1. Ciclo sexuado do *Plasmodium* sp.

No interior do eritrócito, os merozoítos passam por etapas de diferenciação, crescimento e multiplicação. Primeiramente, ocorre a diferenciação em trofozoíto jovem, que apresenta uma morfologia semelhante a um anel. O amadurecimento do trofozoíto é acompanhando de crescimento

e aumento do metabolismo, sendo o estágio trófico do parasito. É nesta fase que a hemoglobina do eritrócito é digerida pelo parasito para ser utilizada como fonte de aminoácidos. A degradação da hemoglobina gera como produto o grupamento heme que é oxidado em ferriprotoporfirina IX, o qual é tóxico aos parasitos, e por isso é polimerizado em um composto inerte, denominado hemozoína (pigmento malárico), impedindo que a toxicidade do grupamento prejudique os parasitos (HEMPELMANN et al., 2003; MILLER et al., 2013).

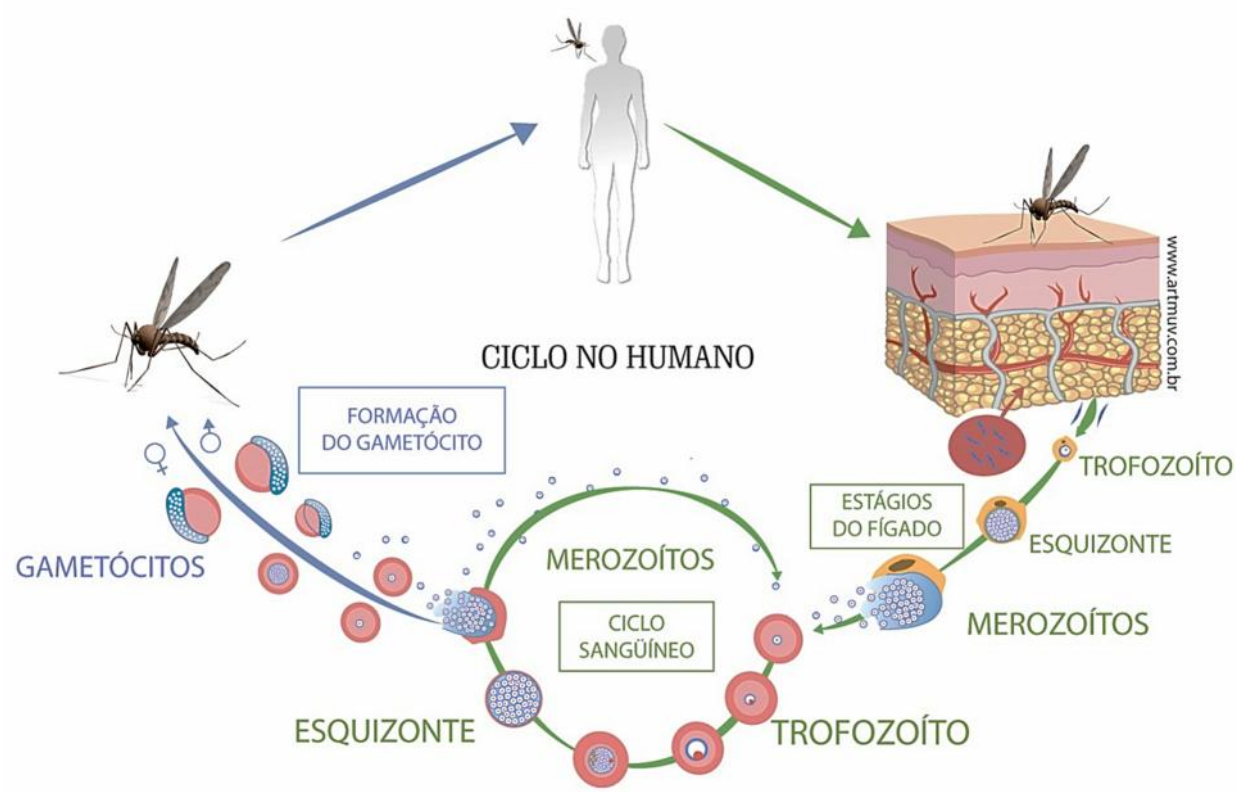

Figura 2. Ciclo assexuado (esquizogonia) do *Plasmodium* sp.

Após este estágio de trofozoíto, sucessivas divisões nucleares sem citocinese resultam na formação dos esquizontes (TUTEJA, 2007). O rompimento destes esquizontes eritrocíticos libera novos merozoítos que irão infectar outros eritrócitos. A liberação dos merozoítos e conseqüente rompimento das hemácias coincidem com os picos de acessos febris característicos da doença. Este ciclo é bastante regular e a duração é característica para cada espécie de plasmódio (GARCIA et al., 2001).

Após um período de liberação de merozoítos sanguíneos, alguns se diferenciam dando origem a formas sexuadas, os gametócitos masculinos (microgametócitos) e femininos (macrogametócitos). A fêmea do anofelino, ao realizar o repasto sanguíneo em um indivíduo infectado, ingere esses

gametócitos. Dentro do lúmen do intestino médio do mosquito, inicia-se a fase sexuada do ciclo biológico do plasmódio. A gametogênese ocorre pela exflagelação dos gametócitos. A fecundação entre os gametas (microgameta e macrogameta) dá origem ao zigoto diplóide. Este, após divisão meiótica, origina uma forma móvel e haplóide, denominada oocineto. O oocineto penetra nas células epiteliais do intestino médio, passando a ser chamado de oocisto. O oocisto se multiplica por um processo de divisão assexuada (esporogonia), dando origem aos esporozoítos que migram através do sistema hemolinfático até alcançarem as glândulas salivares do mosquito, estando prontos para infectar um novo hospedeiro (WHITE, 2003).

1.3 EPIDEMIOLOGIA DA MALÁRIA

De acordo com o relatório mundial da malária, publicado pela Organização Mundial da Saúde (2015), existem atualmente cerca de 106 países e territórios com transmissão da malária em curso e 9 países em fase de prevenção da reintrodução da doença. Entre 2000 e 2015, casos de malária foram reportados para a África, Sudeste da Ásia, região do Pacífico Ocidental, países do Leste do Mediterrâneo, países da América Latina e alguns países do Leste Europeu (Figura 3).

Globalmente, estima-se que 3.2 bilhões de indivíduos estão em risco de adquirir malária. A OMS estimou para 2015 a ocorrência de 214 milhões de casos de malária com 438 mil mortes. A maioria dos casos (88%) e de mortes (90%) ocorreu na região da África, e a maioria das mortes (95%) foram em crianças com menos de 5 anos de idade (OMS, 2015).

Apesar dos números, os dados publicados no referido relatório, apontam que as taxas de mortalidade da doença diminuíram cerca de 48 % em todo o mundo entre 2000 e 2015. Houve uma redução de 66% das mortes na Região Africana entre 2000 e 2013, e 95% em crianças menores de 5 anos de idade, no ano de 2015.

A maior parte dos casos é causada por *P. falciparum*. Apenas 9% são devidos ao *P. vivax*, embora a proporção dos casos para este último parasita, fora do continente Africano, seja de 50%. Mais de 78% das mortes por malária ocorrem em cerca de apenas 15 países e 80% dos casos estimados ocorrem em 15 países, com a República Democrática do Congo e Nigéria respondendo juntos por 35% do total estimado (OMS, 2015).

No Sudeste Asiático, aproximadamente 1,6 bilhões de indivíduos correm algum risco de adquirir malária nos 10 países endêmicos e 1 bilhão de indivíduos estão em alto risco. *P. falciparum* é o

responsável pela maioria dos casos na região, mas no Nepal, Sri Lanka e República Democrática da Coréia, a maior parte dos casos são devido ao *P. vivax* (OMS, 2015).

Na Região das Américas, a OMS (2015) estima que cerca de 112 milhões de indivíduos em 21 países estão sob algum risco de adquirir malária. *P. vivax* é o principal agente etiológico na região, enquanto que o *P. falciparum* é responsável por menos de 30 % dos casos, sendo a proporção de mais de 50% na Guiana e Guiana Francesa e 100% na República Dominicana e no Haiti. O número de casos confirmados de malária na região caiu de 1,2 milhões em 2000 para 390 mil em 2014. Três países foram responsáveis por 77% dos casos em 2013: Brasil (37%), Venezuela (23%) e Colômbia (17%).

Foram relatadas 79 mortes por malária na região das Américas, em 2014, um declínio de 80% em comparação com o ano de 2000. O Brasil é responsável por quase metade das mortes devido à malária nas Américas (OMS, 2015). Segundo dados do Ministério da Saúde, no Brasil a transmissão da malária está quase que restrita à Região Amazônica, área endêmica para a doença no país. A Amazônia possui características geográficas e ecológicas altamente favoráveis à interação do parasito e do mosquito vetor, com os fatores socioeconômicos, políticos e culturais, determinando um nível de endemicidade (BRASIL, 2015). Desde o início da década de 1990, a Amazônia Legal registra elevada incidência de malária (SANTOS et al., 2013).

Em 2013, foram notificados 178.613 casos de malária no Brasil, uma redução de 2,4% em comparação a 2012. Destes, 169.570 (94,9 %) tiveram como local provável de infecção a Região Amazônica, 89 casos a Região Extra-amazônica e 8.924 casos com local provável de infecção em outro país. Dos casos notificados, cerca de 82% foram causados por *P. vivax* e 18% por *P. falciparum*. Apesar da redução relatada, a malária ainda representa um grande problema de Saúde Pública no país (BRASIL, 2015).

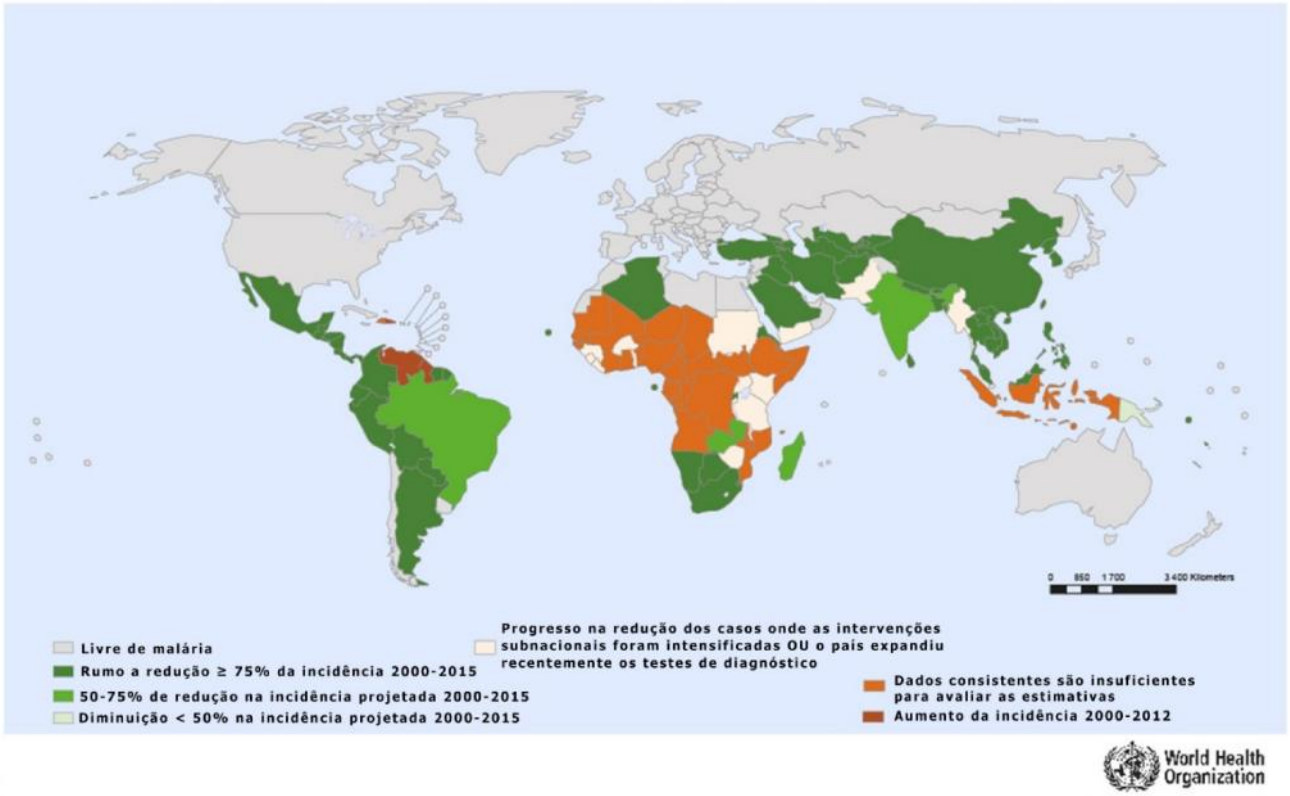

Figura 3. Estimativas da incidência de malária no mundo. Adaptado de: OMS, 2012 (http://www.who.int/malaria/publications/world_malaria_report_2012/en/).

1.4 FÁRMACOS ANTIMALÁRICOS E O PROCESSO DE RESISTÊNCIA

O controle e tratamento da malária se baseiam principalmente na quimioterapia. Os medicamentos antimaláricos atuam inibindo etapas no ciclo evolutivo do plasmódio. Desta forma, os principais antimaláricos podem ser classificados pelo seu alvo de ação no ciclo biológico do parasito. A maioria dos antimaláricos utilizados na clínica são esquizonticidas, agindo nos estágios sanguíneos assexuados do parasito, responsáveis pelas manifestações clínicas da doença. Existe também o fármaco que atua no estágio hepático (hipnozoítos), evitando recidivas. Além disso, a abordagem terapêutica de pacientes residentes em áreas endêmicas visa também à redução de fontes de infecção, pelo uso de fármacos que eliminam os gametócitos, formas sexuadas dos parasitos (BUSTAMANTE et al., 2009; PEATEY et al., 2012).

O tratamento da malária com o uso de determinados antimaláricos depende de alguns fatores como a espécie de plasmódio, o grau da infecção, a idade do paciente, história de exposição anterior à infecção, gestação.

A quinina (Figura 4) foi o primeiro antimalárico caracterizado estruturalmente e purificado em 1820 a partir da casca de árvores do gênero *Cinchona* (Rubiaceae), nativo da América do Sul. A descoberta da quinina marcou a primeira utilização bem sucedida de um composto químico para tratar uma doença infecciosa. Este fármaco apresenta ação esquizonticida e é também gametocitocida para *P. vivax* e *P. malariae*. É eficaz contra o *P. falciparum*, sendo usada isoladamente em áreas onde as cepas dessa espécie ainda não desenvolveram resistência, ou em associação com antibióticos para aquelas áreas com comprovada resistência a este antimalárico. No Brasil, a quinina continua sendo utilizada como fármaco de segunda escolha para a malária causada por *P. falciparum* não grave ou complicada, em associação com doxiciclina ou tetraciclina (BRASIL 2001; 2010; ACHAN et al., 2011). A quinina permaneceu como suporte no tratamento da malária em todo mundo até a década de 1920, quando antimaláricos sintéticos mais eficazes se tornaram disponíveis. O mais importante destes antimaláricos foi a cloroquina, que tem sido extensivamente utilizada, principalmente a partir de 1940 (ACHAN et al., 2011).

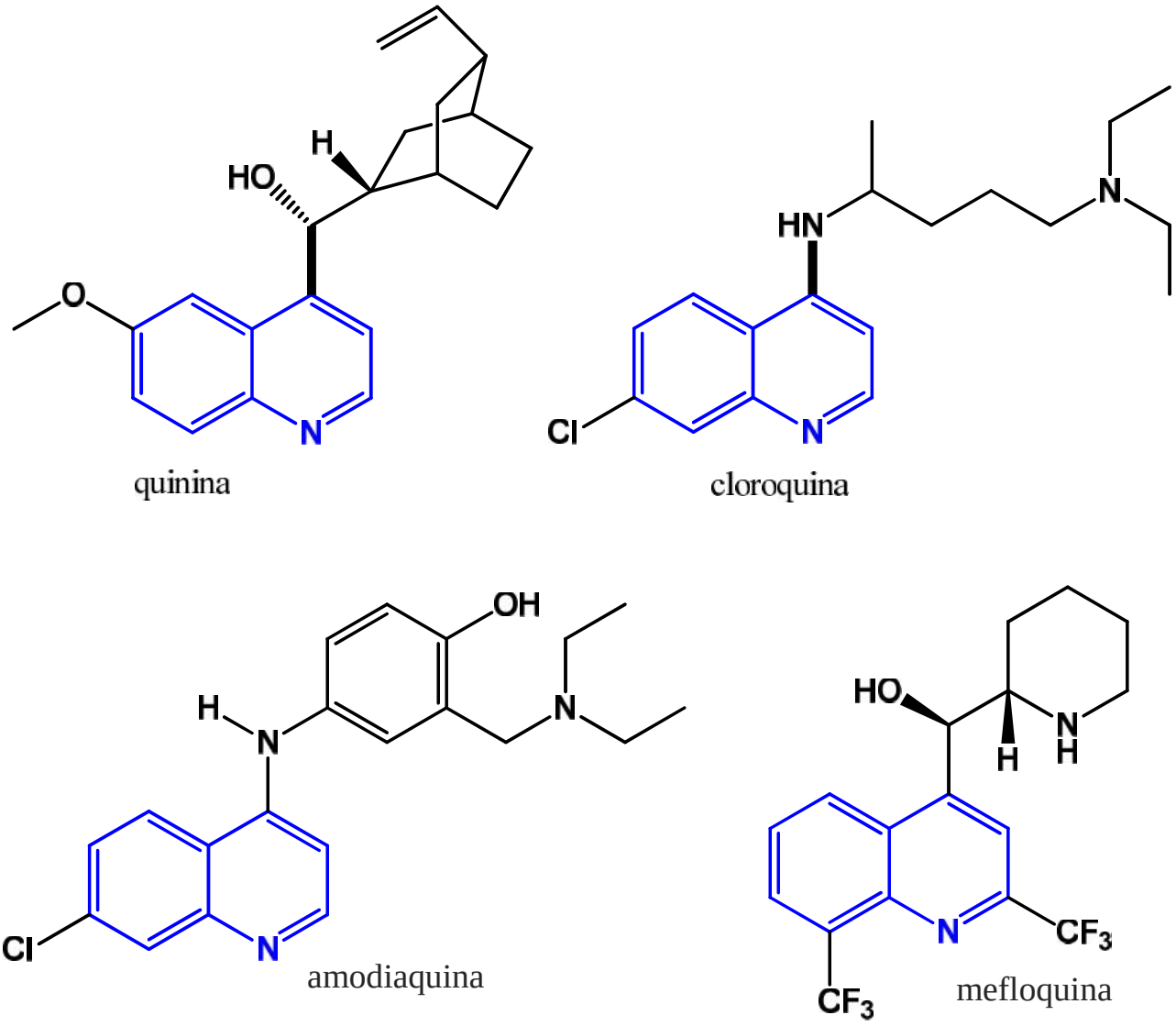

Figura 4. Estrutura química da quinina, cloroquina, amodiaquina e mefloquina.

A cloroquina é uma 4-aminoquinolina com rápida atividade esquizonticida para todas as espécies e gametocitocida para *P. vivax* e *P. malariae*. Este fármaco foi utilizado mundialmente durante décadas como monoterapia no tratamento e profilaxia da malária em áreas endêmicas. Atualmente, poucas cepas de *P. falciparum* são ainda sensíveis à cloroquina. Com o surgimento de resistência por parte do *P. falciparum*, novos antimaláricos foram sintetizados e usados em substituição à cloroquina, como por exemplo a amodiaquina e a mefloquina. Porém, a cloroquina continua sendo empregada em combinação com outros fármacos para o tratamento de *P. falciparum* ou como esquizonticida de escolha no tratamento da malária humana causada por outras espécies de plasmódio (CRUZ et al., 2009; AGUIAR et al., 2012).

A amodiaquina é uma 4-aminoquilonina com estrutura química semelhante à cloroquina, difere em um anel aromático *p*-hidroxil anilino inserido em sua molécula (Figura 4). Assim como a cloroquina, a amodiaquina tem ação antipirética e anti-inflamatória e apresenta efeito esquizonticida para todas as espécies e gametocitocida para *P. vivax* e *P. malariae*. Porém, na maior parte das áreas endêmicas do mundo, o *P. falciparum* já é resistente à amodiaquina (BRASIL 2001; 2010). Além disso, este fármaco não é mais recomendado para a terapia da malária causada pelo *P. falciparum*, devido à sua hepatotoxicidade (GIL, 2008).

A atividade antimalárica mais provável das 4-aminoquinolinas está relacionada com o anel quinolínico, responsável por impedir a polimerização do heme ao se ligar a ele, o que causa a inibição da polimerização do heme. Durante o ciclo eritrocítico, o parasito da malária digere, enzimaticamente, a hemoglobina da hemácia hospedeira dentro de uma organela ácida especializada chamada de vacúolo digestivo (Figura 5). Neste processo, grande quantidade de heme é liberada e convertida em um cristal insolúvel, não reativo e atóxico para o plasmódio, a hemozoína (GOLDBERG et al., 1990). As 4-aminoquinolinas parecem ser capazes de formar uma ligação com o heme, inibindo a formação da hemozoína e formando um complexo reativo e tóxico ao parasito (FISH, 2004; OLAFSON et al., 2015).

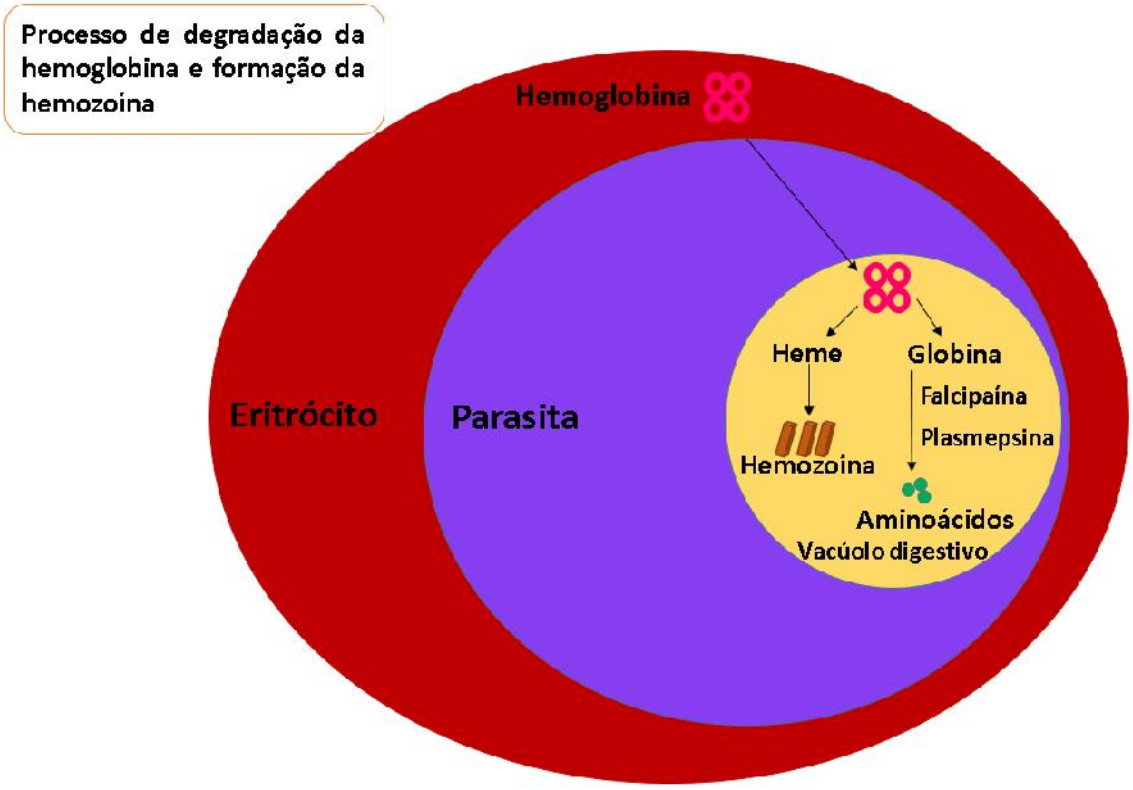

Figura 5. Biossíntese da hemozoína.

Outro antimalárico de destaque é a mefloquina (Figura 4) , um 4-quinolinometanol quimicamente relacionado com a quinina. É um potente esquizonticida sangüíneo, de ação prolongada contra todas as espécies, inclusive cepas de *P. falciparum* resistente às 4-aminoquinolinas. Não tem ação contra as fases hepáticas dos parasitos e é eficaz contra os gametócitos de *P. vivax*. A meia-vida da mefloquina é prolongada, variando entre 10 a 40 dias em adultos. Efeitos adversos como dores abdominais, cólicas, náuseas, vômitos, diarréia podem aparecer. Entretanto, o principal temor com relação ao uso da mefloquina está relacionado ao seu potencial para induzir manifestações neuropsiquiátricas graves (BRASIL 2001; 2010).

A lumefantrina (Figura 6) é quimicamente relacionada com a quinina, mefloquina e halofantrina. É um aril-aminoálcool com ação esquizonticida. Tem o seu uso recomendado pela OMS em combinação com derivados da artemisinina (OMS, 2015). Segundo a OMS (2013), a combinação lumefantrina/artemeter representou 77 % do volume de fármacos combinadas para o tratamento da malária, adquiridas pelo setor público e privado em 2012. Já a halofantrina foi desenvolvida ainda durante a Segunda Guerra Mundial. É um metanol de fenantreno com ação esquizonticida sangüínea sobre todas as espécies de plasmódio, mas não age contra gametócitos ou sobre as fases hepáticas dos parasitos. Este fármaco tem sido pouco utilizado em programas de controle da malária devido ao seu custo elevado, à variabilidade de sua biodisponibilidade, sua resistência cruzada com a mefloquina e ao fato de haver relatos de cardiotoxicidade em certos grupos de risco após a dosagem padrão (WINSTANLEY et al., 2001).

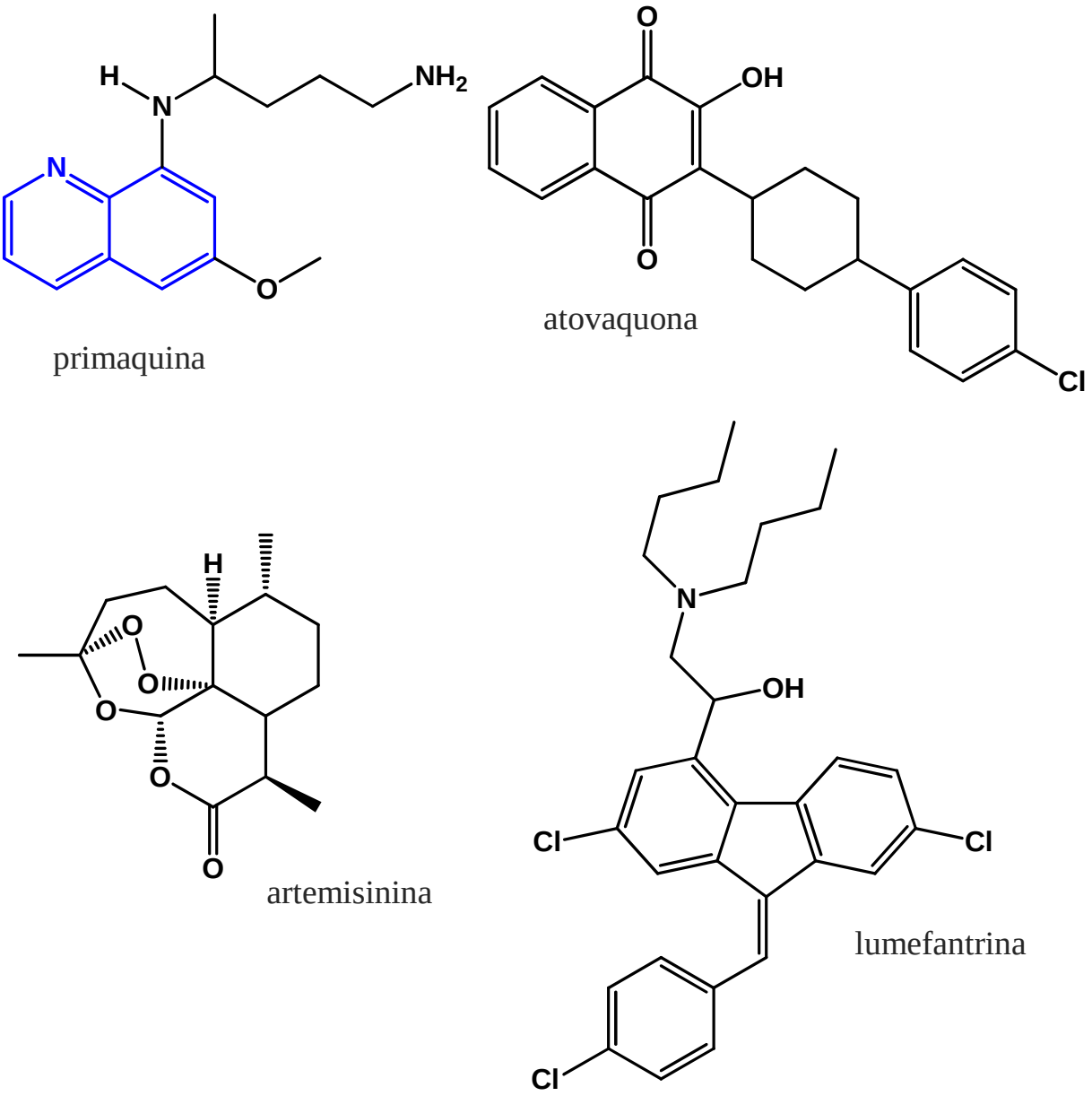

Figura 6. Estruturas químicas da lumefantrina, primaquina, artemisinina e atovaquona.

A primaquina é uma 8-aminoquinolina (Figura 6) ativa contra gametócitos de todas as espécies de malária humana e o único fármaco utilizado na clínica com comprovada eficácia contra hipnozoítos do *P. vivax* e *P. ovale* (OMS, 2015). Este efeito hipnozoiticida da primaquina é função da dose total e não da duração do tratamento. Existem variações geográficas quanto à sensibilidade de hipnozoítos de *P. vivax* à primaquina. A primaquina atua também contra as fases assexuadas sangüíneas, mas para isto é necessária a administração de doses elevadas (BRASIL 2001; 2010). De acordo com Oliver (2008), doses de primaquina mais elevadas que a terapêuticas produzem metabólitos oxidativos, responsáveis por causar hemólise e anemia hemolítica aguda

em indivíduos com deficiência de glicose-6-fosfato desidrogenase. Sendo assim, o monitoramento dos pacientes é recomendado antes do tratamento com primaquina.

A atovaquona é uma hidroxinaftoquinona (Figura 6) eficaz contra o *P. falciparum*, inclusive com ação frente as cepas resistentes à cloroquina (FRY; PUDNEY, 1992). Este fármaco atua principalmente no complexo citocromo *bc1*, inibindo a cadeia transportadora de elétrons na mitocôndria do parasita (DA CRUZ et al., 2012). Porém, a utilização como monoterapia pode induzir uma resistência a este fármaco, sendo esta conferida por mutações pontuais no gene do citocromo *b*. Apesar da resistência à atovaquona se desenvolver rapidamente, quando combinada com um segundo fármaco, tal como o proguanil (a combinação utilizada no medicameto malarone) ou tetraciclina, a resistência se desenvolve mais lentamente. A atovaquona está sendo usada mais amplamente para o tratamento de infecções oportunistas em pacientes imunocomprometidos (LOOAREESUWAN S et al., 1996; BLOLAND, 2001).

A artemisinina (Figura 6) e seus derivados semi-sintéticos, tais como diidroartemisinina, artemeter, arteeter e artesunato, são lactonas sesquiterpênicas com um peróxido como ponte de ligação. Estas têm o princípio antimalárico isolado da *Artemisia annua* L. (Asteraceae), uma planta medicinal que tem sido utilizada há mais de mil anos na China. Estes fármacos são esquizonticidas sangüíneos potentes e de ação rápida, eliminando o parasito e melhorando os sintomas em menos tempo que a cloroquina ou a quinina. A artemisinina é pouco solúvel em óleo ou água e, após derivação do composto precursor, foi possível produzir a diidroartemisinina, os derivados solúveis em óleo (artemeter) e os derivados mais solúveis em água (artesunato de sódio e ácido artelínico). A artemisinina e seus derivados são recomendados pela OMS como tratamento de primeira escolha em combinação (Terapia Combinada da Artemisinina) com outros fármacos antimaláricos, como mefloquina, lumefantrina e amodiaquina ou com antibióticos, como doxiciclina, para tratar a malária por *P. falciparum* e *P. vivax* em áreas de resistência à cloroquina. A Terapia Combinada da Artemisinina visa principalmente a redução do aparecimento de cepas resistentes do plasmódio (AGUIAR et al., 2012; BRASIL 2001; OMS 2015). Contudo, nos últimos anos, a resistência do *P. falciparum* à artemisinina e derivados tem sido detectada em cinco países: Camboja, Laos, Mianmar, Tailândia e Vietnã (OMS, 2015).

A resistência aos medicamentos antimaláricos é um problema recorrente, sendo descrita para duas das cinco espécies de parasitas da malária que naturalmente infectam os seres humanos, *P. falciparum* e *P. vivax*. A resistência é definida como a capacidade de sobrevivência ou multiplicação de algumas cepas, apesar da administração e absorção de um fármaco, em doses

iguais ou mesmo maiores àquelas usualmente recomendas e que estejam dentro dos limites de tolerância do paciente (BRASIL, 2006). Os casos de resistência aparecem principalmente entre cepas de *P. falciparum*. Na década de 1970 e 1980, a resistência do *P. falciparum* a medicamentos, como a cloroquina e a sulfadoxina-pirimetamina, tornou-se comum, dificultando o controle da malária e revertendo os ganhos na sobrevivência infantil (OMS, 2015). A resistência a outros fármacos como amodiaquina, quinina e mefloquina foram surgindo e ainda tem sido registrada para diferentes cepas e em diferentes níveis nas áreas endêmicas.

Muitos fatores podem contribuir para o desenvolvimento de resistência ou multiresistência aos fármacos antimaláricos, tais como padrões de uso do fármaco, propriedades intrínsecas do fármaco utilizada, uso incorreto e indiscriminado, fatores individuais do hospedeiro, características do parasita e também do vetor, bem como fatores ambientais (WINSTANLEY, 2001). Estes fatores, isolados ou em combinação, podem promover a seleção de um ou mais indivíduos constituintes de uma população parasitária carreando uma ou mais mutações que proporcionam uma vantagem seletiva na presença de concentrações do fármaco que, em condições normais, inibiriam a proliferação da fração sensível da população parasitária (PETERS, 1990).

Em geral a resistência parece ocorrer através de mutações espontâneas, que conferem resistência nos alvos onde os antimaláricos atuam, tal como ocorre para atovaquona, ou em transportadores envolvidos na distribuição do antimalárico no parasito a exemplo dos genes envolvidos no transporte e efluxo de antiparasitários (CHERUIYOT et al., 2014; MBOGO et al., 2014). Um dos exemplos mais conhecidos é o *P. falciparum chloroquine resistance transporter (pfcrt),* principal determinante de resistência à cloroquina que codifica uma proteína de transporte localizada na membrana do vacúolo digestivo do parasito. A acumulação reduzida de cloroquina no vacúolo digestivo está ligada a polimorfismos no *pfcrt*, e esta descoberta levou à hipótese de que este gene controla o acesso da cloroquina ao seu destino. Os parasitas resistentes à cloroquina acumulam quantidades substancialmente mais baixas deste fármaco em seu vacúolo digestivo do que os parasitas sensíveis. A redução das concentrações da cloroquina no vacúolo digestivo chega a ser inferior aos níveis exigidos para inibir a polimerização do heme (SANCHEZ et al., 2010).

O gene *Plasmodium falciparum multidrug resistance* 1 (*pfmdr 1)* codifica a proteína Pgh1 (glicoproteína homóloga 1), estruturalmente homóloga à glicoproteína P de células tumorais. A Pgh1 é expressa na membrana do vacúolo digestivo do parasito, ao longo do seu desenvolvimento intraeritrocítico. Os polimorfismos nos aminoácidos 86, 184, 1034, 1042 e 1246 do *pfmdr1*, além

de conferir resistência à cloroquina, alteram a suscetibilidade *in vitro* para outros fármacos antimaláricas, incluindo a quinina, halofantrina, mefloquina e artemisinina (VENKATESAN et al., 2014)

Nos últimos anos, a resistência do parasita à artemisinina foi detectada em cinco países da sub-região do Grande Mekong, na Ásia. Segundo a OMS (2015), muitos fatores contribuem para o surgimento e propagação da resistência, porém neste caso o uso da artemisinina como monoterapia parece ser a principal causa. Os pacientes, quando tratados com uma monoterapia à base de artemisinina, podem interromper o tratamento prematuramente após o rápido desaparecimento dos sintomas da malária. Isto resulta em tratamento incompleto e podem causar a persistência de parasitas no sangue. Sem um segundo medicamento administrado como parte de uma combinação (como é fornecido com uma Terapia Combinada da Artemisinina), estes parasitas resistentes sobrevivem e podem ser transmitidos para mosquitos e, em seguida, para outros indivíduos. Em virtude dos fatos descritos acima, é evidente que o desenvolvimento de novos fármacos úteis ao tratamento da malária é necessário.

1.5 DESENVOLVIMENTO DE FÁRMACOS ANTIMALÁRICOS COM AÇÃO EM MÚLTIPLOS ESTÁGIOS

Para a erradicação da malária, há uma necessidade do desenvolvimento de antimaláricos com espectro de ação amplo, apresentando atividade não só nos estágios sanguíneos assexuados, mas também contra os gametócitos e outras fases sexuadas, responsáveis pela transmissão. Além disso, a busca por fármacos capazes de exercer ação antiparasitária frente aos esporozoítos, prevenindo assim a infecção, bem como compostos com atividade contra os estágios hepáticos do plasmódio é necessária (FRANKE-FAYARD et al., 2004; CEVENINI et al., 2013; D'ALESSANDRO et al., 2014).

Os gametócitos correspondem a um dos estágios sexuados, produzidos no hospedeiro vertebrado e transmitidos para o mosquito durante o repasto sanguíneo. Há um consenso atual que os fármacos antimaláricos que atuam nesta fase do ciclo do parasita são capazes de bloquear a transmissão da doença (DECHY-CABARET; BENOIT-VICAL, 2012; PEATEY et al., 2012).

Um mosquito infectado pode inocular, no hospedeiro vertebrado, os esporozoítos, que são a forma infectante do plasmódio. Os esporozoítos então migram para o fígado do hospedeiro,

passando por uma fase hepática obrigatória no ciclo de vida do parasita. Portanto, fármacos que agem sobre os esporozoítos podem impedir o estabelecimento da infecção. Além disso, busca-se também o desenvolvimento de novos fármacos, capazes de atuar nos hipnozoítos, forma hepática latente bastante recorrente nas espécies *P. vivax* e *P. ovale*, responsável por recidivas da doença (BUSTAMANTE et al., 2009; WASSMER et al., 2015). Cabe aqui ressaltar a importância do desenvolvimento de fármacos antiparasitários com ação nos hipnozoítos do *P. vivax*, que é de ocorrência no Brasil (BUSTAMANTE et al., 2009; FERREIRA; CASTRO, 2016).

Exceto a primaquina, os antimaláricos disponíveis atuam majoritariamente nas fases eritrocíticas do plasmódio. De fato, a primaquina é considerada um fármaco com ação multiestágios, apresentando atividade gametocitocida e também nos estágios hepáticos do parasita (WHITE, 2013). Todavia, a primaquina apresenta uma eficácia limitada, além de provocar efeitos colaterais que limitam o seu uso (CRUZ et al., 2012; CABRERA; CUI, 2015).

Diante da importância de descobrir novos fármacos com eficácia na eliminação de diferentes fases do plasmódio, o desenho químico e triagem de moléculas tem se tornado constante nos últimos anos (RODRIGUES et al., 2012).

Durante os esforços para identificação de compostos antimaláricos que atuem na fase hepática da doença, o decoquinato (Figura 7) foi um dos primeiros compostos identificados com eficácia e potência superior à primaquina. Este composto é uma quinolona sintética e foi descoberto após a triagem *in vitro* com esporozoítos. Além de apresentar potência similar à artemisinina nos estágios eritrocíticos, o decoquinato reduziu a carga parasitária em células hepáticas infectadas com esporozoítos e também promoveu a cura de camundongos infectados. O decoquinato inibe enzimas mitocondriais do parasito, interferindo na cadeia respiratória (DA CRUZ et al., 2012).

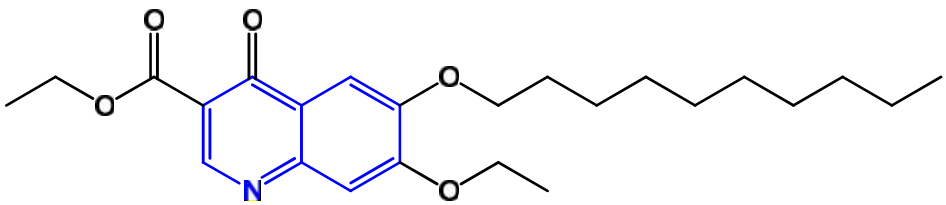

Figura 7: Estrutura química do decoquinato, um novo candidato à fármaco antimalárico com ação potente frente a fase hepática.

Seguindo o decoquinato, Nilsen et al. (2013) descobriram a quinolina EQL-300 (Figura 8), um candidato a fármaco antimalárico com espectro de ação multiestágio mais amplo que o decoquinato. O composto foi descoberto após sucessivas modificações moleculares de uma classe de quinolina-3-diarileteres. Este candidato a fármaco apresentou atividade antiparasitária nos estágios hepáticos, sanguíneos e nos estágios de transmissão não apenas no vertebrado, mas também no mosquito. Embora o EQL-300 seja estruturalmente distinto do decoquinato, este composto também apresentou mecanismo de ação via inibição de enzimas do citocromo *c* da mitocôndria do *P. falciparum*.

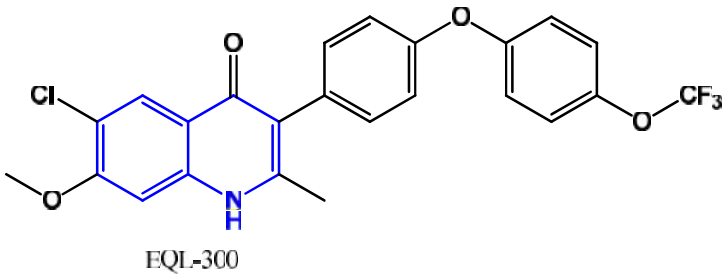

EQL-300

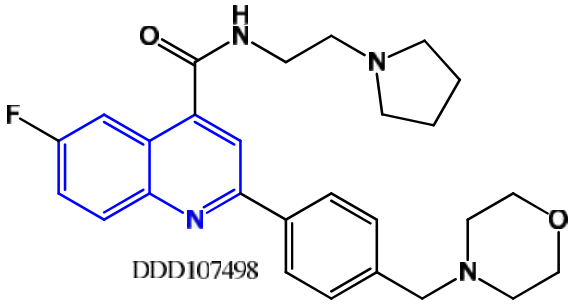

DDD107498

Figura 8: Estruturas químicas do EQL-300 e DDD107498, novos candidatos à fármacos antimaláricos com amplo espectro de ações.

Diferente do decoquinato e do EQL-300, que são antimaláricos de ação multiestágios, porém com potência inferior nos estágios não-sanguíneos, a quinolina DDD107498 (Figura 8) foi descoberta recentemente como um antimalárico com atividade em nanomolar nos três principais estágios de desenvolvimento do parasita: sanguíneo, hepático e nos estágios sexuados no mosquito (BARAGANÃ et al., 2015). O composto DDD107498 é uma quinolina que contém um grupo químico carboxamida que foi identificado após sucessivas triagens *in vitro*, nos estágios sanguíneos do plasmódio, e modificações moleculares. O composto apresentou atividade antiparasitária superior ao artesunato, atuando em cepas com diferentes níveis de resistência. Além disso, o DDD107498 foi capaz de curar a infecção *in vivo*, no estágio sanguíneo, e apresentou atividade profilática em camundongos infectados com esporozoítos. Diferente do

decoquinato e do EQL-300, que atuam principalmente inibindo as enzimas do citocromo *c* da mitocôndria do plasmódio, o DDD107498 é um inibidor de síntese protéica (BARAGANÃ et al., 2015).

1.6 COMPLEXOS METÁLICOS COM CLOROQUINA

A estrutura química das quinolinas tem sido utilizada para o planejamento químico e triagem da atividade antimalárica de novos compostos. De fato, uma característica química em comum dos compostos decoquinato, EQL-300 e DDD107498 é a presença da quinolina, destacada na cor azul na Figura 7 e 8. Os compostos quinolínicos estão presentes não somente nos novos compostos candidatos a fármacos, mas também nos fármacos antimaláricos em uso, à exemplo da primaquina, cloroquina, amodiaquina e mefloquina. Muito embora a cloroquina, a amodiaquina e a mefloquina possuam ação antiparasitária principalmente no estágio sanguíneo da infecção, há novos compostos quinolínicos com espectro de ação em mais estágios do ciclo evolutivo do plasmódio. Portanto, é possível realizar modificações estruturais em quinolinas visando aumentar o espectro de ação. Em virtude disso, a realização do planejamento químico e triagem da atividade antimalárica de novos compostos derivados de quinolinas representa uma linha de pesquisa promissora.

Uma estratégia em potencial tem como base a incorporação de um metal de transição na estrutura de compostos quinolínicos com atividade já conhecida, resultando na formação de um complexo metálico. Por definição, um complexo metálico consiste em um átomo metálico de transição, circundado quimicamente por moléculas orgânicas ou inorgânicas, conhecido como ligantes. Tem-se como exemplos clássicos a cisplatina, acarboplatina, a auranofina e o glucantime (SALAS et al., 2013). O complexo metálico pode apresentar maior solubilidade em água, coeficiente de partição óleo-água mais adequado para permeação celular, aumento da biodisponibilidade e conferir proteção metabólica ao ligante ou ganho de afinidade pelo alvo terapêutico. Classicamente, o ligante utilizado é uma molécula de origem natural ou sintética que contenha ao menos um par de elétrons livres, tais como o átomo de nitrogênio, enxofre ou fósforo (HERNANDES et al., 2010; WANG et al., 2015).

De fato, um número expressivo de complexos metálicos contendo quinolinas como ligantes vêm sendo investigados como agentes antimaláricos (NAVARRO et al., 2011, 2014; DEDIJI et al., 2012; SALAS et al., 2013; EKENGARD et al., 2015). Nesta literatura, é

documentada um aumento da potência antiparasitária ou do índice de seletividade para os complexos metal-quinolina em comparação com os da quinolina. Considerando estes aspectos, visamos realizar o planejamento químico e triagem da atividade antimalárica de inéditos complexos metálicos com quinolinas.

Para alcançar esse objetivo, é necessária a seleção do metal de transição e também dos ligantes dos tipos quinolínicos. Tanto o rutênio quanto a platina são metais amplamente estudados no desenho de fármacos antiparasitários, sendo considerados os mais potentes e seletivos dentre as séries de metais de transição da tabela periódica (SALAS et al., 2013; WANG et al., 2015). Em relação à escolha do ligante quinolínico, a cloroquina apresenta vantagens para a composição de complexos metálicos, dentre tantos outros compostos quinolínicos, por apresentar efeitos farmacológicos em diversas doenças, exercer ação em múltiplos alvos terapêuticos e a possibilidade de ajustar o seu espectro de ação quando modificações estruturais são realizadas (KOVACS; KARPATI, 1989; ROCHA et al., 2013; RAINSFORD et al., 2015; HUTA et al., 2016).

É importante ressaltar que, embora um aumento da potência antiparasitária ou do índice de seletividade para diversos complexos metal-cloroquina em comparação com a cloroquina tenha sido descrita (NAVARRO et al., 2011, 2014; DEDIJI et al., 2012; SALAS et al., 2013; EKENGARD et al., 2015), pouco se sabe a respeito do mecanismo de ação antiparasitário e a eficácia desta classe de complexos metálicos na infecção *in vivo*. Além disso, a atividade antiparasitária no estágio hepático e nos gametócitos ainda é desconhecida para esta classe de complexos. Portanto, o objetivo deste trabalho é estudar se a incorporação da cloroquina em complexos de rutênio e platina altera a atividade antimalárica, avaliando também o espectro de ação e o mecanismo pelo qual tais complexos exercem atividade antiparasitária.

2 OBJETIVOS

2.1 OBJETIVO GERAL

Identificar potenciais fármacos antiparasitários para o tratamento da malária, com base em moléculas do tipo complexos metálicos com a cloroquina.

2.2 OBJETIVOS ESPECÍFICOS

- Determinar a citotoxicidade *in vitro* dos complexos metálicos de cloroquina em células de mamíferos;
- Avaliar a atividade antimalárica *in vitro* em formas eritrocíticas assexuada e sexuada de *P. falciparum* e em esporozoítos de *P. berghei*;
- Determinar *in vitro* a potência, seletividade e espectro de ação dos compostos testados em cepas do *P. falciparum,* sensível e resistente à cloroquina;
- Estudar a cinética e o mecanismo de ação pela qual os complexos metálicos de cloroquina e interferem na viabilidade do *P. falciparum;*
- Estudar a diferença entre cloroquina e seus complexos metálicos na interação e biossíntese da hemozoína;
- Determinar a eficácia dos compostos em reduzir parasitemia e mortalidade em modelo de infeção *in vivo* com *P. berghei*.

3 ARTIGO 1

Taís Soares Macedo, Legna C. Vegas, Marcelo da Paixão, Maribel Navarro, Breno Cardim Barreto, Poliana Cristina Mendes Oliveira, Simone Garcia Macambira, Marta Machado, Miguel Prudêncio, Sarah D'Alessandro, Nicoletta Basilico, Diogo Rodrigo M. Moreira, Alzir A. Batista, Milena Botelho P. Soares.

Chloroquine-containing organoruthenium complexes are fast-acting multistage antimalarial agents, publicado no periódico **Parasitology**.

O artigo descreve a ação antimalárica de complexos metálicos de rutênio contendo cloroquina, mostrando a atividade destes complexos em diferentes estágios do ciclo de vida do plasmódio, bem como o mecanismo de ação antiparasitária.

Chloroquine-containing organoruthenium complexes are fast-acting multistage antimalarial agents

TAÍS S. MACEDO[1]†, LEGNA COLINA-VEGAS[2]†, MARCELO DA PAIXÃO[1], MARIBEL NAVARRO[3], BRENO C. BARRETO[1,4], POLIANA C. M. OLIVEIRA[1,4], SIMONE G. MACAMBIRA[4,5], MARTA MACHADO[6], MIGUEL PRUDÊNCIO[6], SARAH D'ALESSANDRO[7], NICOLETTA BASILICO[8], DIOGO R. M. MOREIRA[1], ALZIR A. BATISTA[2] *and* MILENA B. P. SOARES[1,5]*

[1] *FIOCRUZ, Centro de Pesquisas Gonçalo Moniz, 40296-710, Salvador, BA, Brazil*
[2] *Departamento de Química, UFSCAR, 13565-905, São Carlos, SP, Brazil*
[3] *INMETRO, Xerém, 25250-020, Rio de Janeiro, RJ, Brazil*
[4] *Instituto de Ciências da Saúde, Universidade Federal da Bahia, CEP 40110-100, Salvador, BA, Brazil*
[5] *Centro de Biotecnologia e Terapia Celular, Hospital São Rafael, CEP 41253-190 Salvador, BA, Brazil*
[6] *Instituto de Medicina Molecular, Faculdade de Medicina, Universidade de Lisboa, 1649-028 Lisboa, Portugal*
[7] *Dipartimento di Scienze Farmacologiche e Biomolecolari, Università degli Studi di Milano, 20133 Milan, Italy*
[8] *Dipartimento di Scienze Biomediche, Chirurgiche e Odontoiatriche, Universitá degli Studi di Milano, 20133 Milan, Italy*

(*Received 24 March 2016; revised 13 May 2016; accepted 5 June 2016*)

SUMMARY

We report the pharmacological activity of organoruthenium complexes containing chloroquine (CQ) as a chelating ligand. The complexes displayed intraerythrocytic activity against CQ-sensitive 3D7 and CQ-resistant W2 strains of *Plasmodium falciparum,* with potency and selectivity indexes similar to those of CQ. Complexes displayed activity against all intraerythrocytic stages, but moderate activity against *Plasmodium berghei* liver stages. However, unlike CQ, organoruthenium complexes impaired gametocyte viability and exhibited fast parasiticidal activity against trophozoites for *P. falciparum*. This functional property results from the ability of complexes to quickly induce oxidative stress. The parasitaemia of *P. berghei*-infected mice was reduced by treatment with the complex. Our findings demonstrated that using chloroquine for the synthesis of organoruthenium complexes retains potency and selectivity while leading to an increase in the spectrum of action and parasite killing rate relative to CQ.

Key words: Malaria, *Plasmodium falciparum*, *Plasmodium berghei*, chloroquine, organoruthenium complexes, oxidative stress.

INTRODUCTION

Malaria remains a major health problem in the world. The latest survey published by the World Health Organization estimates that 3·2 billion people live in malaria-endemic areas, which accounts for 214 million cases each year and 438 000 deaths (WHO, 2015). Malaria is caused by *Plasmodium* parasites injected into the mammalian host through the bite of an infected female *Anopheles* mosquito. The life cycle of *Plasmodium* parasites oscillates between a mammalian host and an invertebrate vector. In the mammalian host, sporozoites injected by an infected mosquito home to the liver, where they undergo an asymptomatic, yet obligatory, phase of development inside hepatocytes (Prudêncio *et al*. 2006). This results in the formation of thousands of erythrocyte-infectious merozoites that invade red blood cells and cause the symptoms of malaria. The transmission of the human parasite to the mosquito is due to the gametocyte sexual form, which, when present in the bloodstream of the human host, can eventually be ingested by the mosquito vector during feeding (Nilsson *et al*. 2015). While *P. falciparum* is the deadliest human-infective malaria parasite, there are an additional four species of *Plasmodium, Plasmodium vivax, Plasmodium ovale, Plasmodium malariae* and *Plasmodium knowlesi*, capable of causing malaria in humans. Moreover, *P. vivax* and *P. ovale* are capable forming hypnozoites, dormant parasite forms that may lead to disease relapses long after the initial symptomatic infection has been treated.

Chemotherapy has long been a mainstay in the combat against malaria, but increasing emergence of drug resistance is limiting malarial control (Petersen *et al*. 2011; Price *et al*. 2014). Another problem regarding current therapies is that most available drugs have a narrow spectrum of action. The front-line antimalarial quinolines chloroquine (CQ), mefloquine and amodiaquine present long half-lives, affordable cost and safety profile, but lack strong activity against sexual and liver parasite forms, which are important stages for interrupting

* Corresponding author: FIOCRUZ, Centro de Pesquisas Gonçalo Moniz, CEP 40296-710, Salvador, BA, Brazil. Phone: (+55)71-31762292. E-mail: milena@bahia.fiocruz.br
† These authors share first authorship.

doi:10.1017/S0031182016001153

transmission and avoiding relapse, respectively (Prudêncio *et al*. 2015; Stone *et al*. 2015). Therefore, it is necessary to develop new antimalarial drugs with a multistage spectrum of action.

Compounds containing transition metals (i.e. metal complexes) are considered promising antimalarial agents (Scovill *et al*. 1982; Gabbiani *et al*. 2009; Khanye *et al*. 2010; Glans *et al*. 2011, 2012*a*, *b*; Adams *et al*. 2013; Barbosa *et al*. 2014; Chellan *et al*. 2014; Adams *et al*. 2015). A substantial number of metal complexes containing CQ as a ligand have been investigated as antimalarial agents, employing various metals, a variety of ligands and different numbers of chloroquine molecules. An improvement in the potency against intraerythrocytic stages of *P. falciparum* was observed in most cases, in comparison with metal-free CQ. An interesting finding is that the antiparasitic potency is not superior to complexes containing two CQ molecules in the structure, which indicates that metal complexes are not mere drug delivery systems that act by releasing CQ and that, instead, the entire chemical structure is involved in the antiparasitic activity (Sánchez-Delgado *et al*. 1996; Goldberg *et al*. 1997; Lewis *et al*. 1997; Navarro *et al*. 1997, 2004, 2011*a*, *b*, 2014; Rajapakse *et al*. 2009). Given this promising outlook, CQ analogs have been employed in the metal complex composition in the last years and given rise to many successful outcomes (Dubar *et al*. 2011, 2013; Glans *et al*. 2012*a*, *b*; Salas *et al*. 2013; Ekengard *et al*. 2015). Investigations of the mechanism of action demonstrated that CQ-metal complexes display different interactions with β-hematin, optimal oil-aqueous partition permeability and fast accumulation in the parasitic vacuoles (Martínez *et al*. 2009, 2011; Navarro *et al*. 2011*a*, *b*). Furthermore, it has been shown that the antimalarial activity of ferroquine, a CQ-derived iron organometallic compound, is superior to that of CQ, due to its ability to produce reactive oxygen species (ROS), which induce oxidative stress (Dubar *et al*. 2011, 2013). However, CQ-metal complexes other than ferroquine have not been fully examined against *P. falciparum*, especially when regarding their multistage spectrum of action and their *in vivo* efficacy.

From a pharmaceutical point of view, ruthenium is considered the most promising transition metal for drug development because of its safe and drugable profile (Meier *et al*. 2013; Maschke *et al*. 2014; Clavel *et al*. 2015). Regarding the use of CQ during composition of metal complexes, it presents a variety of advantages for drug development, especially pleiotropic effects and the possibility of tuning the spectrum of action by structural modification (Pérez *et al*. 2013; Lin *et al*. 2015; Huta *et al*. 2016). Bearing this in mind, we investigated here the activity of CQ-containing organoruthenium complexes. We found that, in addition to the classical activity of CQ against blood stages of *P. falciparum*, organoruthenium complexes presented a fast-action profile, promising activity against *P. berghei* liver stages and strong activity against gametocytes. Moreover, compounds presented *in vivo* efficacy and a mechanism of action involving toxic free heme accumulation in the parasite, which consequently induces oxidative stress.

MATERIALS AND METHODS

Drugs and dilutions

CQ-containing organoruthenium complexes (*BCQ*, *MCQ*, *FCQ* and *FFCQ*) and organoruthenium complex lacking CQ (*FCL*) were prepared as described in the literature (Colina-Vegas *et al*. 2015). All manipulations were carried out under argon using common Schlenk techniques. Solvents were purified by standard procedures immediately prior to use. Chloroquine, Mefloquine and Artesunate were supplied by FarManguinhos (Rio de Janeiro, Brazil). Primaquine was purchased from Sigma-Aldrich (St. Louis, MO). All drugs were dissolved in DMSO (PanReac, Barcelona, Spain) prior to use, and then diluted in culture medium. The final concentration of DMSO was less than 0·5% in all *in vitro* experiments.

Drug stability

The stability of the complexes in solution was monitored using the ^{1}H NMR technique. Approximately 15 mg of each complex was dissolved in DMSO-d_6 solution containing 20% of D_2O (CIL, Tewksbury, MA) and incubated up to 60 h. Aliquots were collected in the indicated time and analyzed on a 9·4 T Bruker Advance III (Billerica, MA) spectrometer with a 5 mm internal diameter indirect probe with Automatic Tuning Matching, holding the temperature stable at 300 K.

Animals

Male Swiss Webster mice (4–6 weeks), housed at Centro de Pesquisas Gonçalo Moniz (Fundação Oswaldo Cruz, Bahia, Brazil), were maintained in sterilized cages under a controlled environment, receiving a rodent balanced diet and water *ad libitum*. All experiments were carried out in accordance with the recommendations of Ethical Issues Guidelines and were approved by the local Animal Ethics Committee (protocol number 016/2013).

Cell culture

CQ-sensitive 3D7 and CQ-resistant W2 strains of *P. falciparum,* NK65 strain of *P. berghei* as well as transgenic *P. berghei* expressing green fluorescent

protein (GFP) and firefly luciferase (Luc), (*Pb*GFP-Luccon, parasite line 676m1cl1) and 3D7 strain *P. falciparum* 3D7*elo*1-*pfs*-16-CBG99 expressing the *Pyrophorus plagiophthalamus* CBG99 luciferase under the gametocyte specific promoter pfs16 (Cevenini *et al*. 2014) were used here. *P. falciparum* was cultivated in human O^+ erythrocytes (donated by HEMOBA, Salvador, Brazil) at 5% hematocrit with daily maintenance in Roswell Park Memorial Institute medium (RPMI-1640, Sigma-Aldrich) supplemented with 10% v/v human plasma (donated by HEMOBA, Salvador, Brazil), 25 mM HEPES (ChemCruz, Dallas, TX), 300 μM hypoxanthine (MP Biomedicals, Santa Ana, CA), 11 mM glucose (Sigma-Aldrich) and 20 μg mL^{-1} of gentamicin (Life, Carlsbad, CA). Five days prior to use, *P. falciparum* was cultivated without hypoxanthine and synchronized to rings by 5% D-sorbitol (USB, Santa Clara, CA). Gametocytes were obtained from cultures of asexual parasites as described elsewhere (D'Alessandro *et al*. 2013). J774 macrophages were cultured in Dulbecco's modified Eagle's medium (DMEM) (Sigma-Aldrich) supplemented with 10% heat-inactivated fetal bovine serum (FBS, Gibco, Gaithersburg, MD) and 50 μg mL^{-1} of gentamicin (Life). Hepatocellular carcinoma cells (HepG2) were cultivated in RPMI supplemented with 10% heat-inactivated FBS (Gibco) and 50 μg mL^{-1} of gentamicin (Life).

Mammalian cell toxicity

HepG2 or J774 cells were seeded in 100 μL of RPMI and DMEM, respectively, at 1×10^4 cells mL^{-1} in 96-well plates. Drugs were added 24 h later in a volume of 100 μL suspended in medium and the plates were incubated for 72 h at 37 °C and 5% CO_2. Drugs were tested in eight concentrations (150–0·78 μM), each one in triplicate. Gentian violet (Synth) was used as positive control, while untreated cells were employed as negative controls. Then, 25 μL of 10% AlamarBlue (Life) were added and incubated for 24 h. Colorimetric readings were performed at 570 and 600 nm using SpectraMAx 190 instrument (Molecular Devices, Sunnyvale, CA). CC_{50} values were calculated using data-points gathered from three independent experiments.

Drug-induced hemolysis

Fresh and uninfected human O^+ erythrocytes were washed three-times with sterile phosphate-buffered saline (PBS), adjusted for 1% hematocrit and 100 μL dispensed in a 96-well round bottom plate. Then, 100 μL of drugs previously in DMSO and suspended in PBS were dispensed in the respective wells. Each drug was tested in seven concentrations (100–0·1 μM) assayed in triplicate. Untreated cells received 100 μL of PBS containing 0·5% DMSO (negative control), while positive controls received saponin (Sigma-Aldrich) at 1% v/v. Plates were incubated for 1 h at 37 °C under 5% CO_2. Plates were centrifuged at 1500 rpm for 10 min and 100 μL of supernatant were transferred to another plate, in which absorbance at 540 nm was measured using a SpectraMax 190 instrument. The percentage of hemolysis was calculated in comparison with positive and negative controls, and plotted against drug concentration generated using GraphPad Prism 5·01. Three independent experiments were performed.

Cytostatic activity against intraerythrocytic P. falciparum

One hundred μL of rings at 1% parasitaemia and 2·5% hematocrit in RPMI were dispensed in a 96-well round bottom plate. Then, 100 μL of drugs (4·0–0·003 μM) previously suspended in RPMI were dispensed in the respective wells. Each drug was tested in triplicate, in seven different concentrations. Untreated parasite samples received 100 μL of medium containing 0·5% DMSO. Chloroquine and mefloquine were used as positive controls. Plates were incubated for 24 h at 37 °C under 3% O_2, 5% CO_2 and 91% N_2 atmosphere. Then, 25 μL of tritiated hypoxanthine (0·5 μCi well^{-1}, PerkinElmer, Shelton, CT) in RPMI was added to each well and incubated for 24 h. Plates were frozen at −20 °C and subsequently thawed and the contents transferred to UniFilter-96 GF/B PEI coated plates (PerkinElmer) using a cell harvester. After drying, 50 μL of scintillation cocktail (MaxiLight, Hidex, Turku, Finland) was added in each well, sealed and plate read in a liquid scintillation microplate counter (Chameleon, Turku, Finland). The per cent of inhibition was determined in comparison to untreated and inhibitory concentration for 50% (IC_{50}) values were determined by using non-linear regression with Logistic equation available at OriginPro 8·5. Three independent experiments were performed.

Cytocidal activity against intraerythrocytic P. falciparum

One hundred μL of trophozoites at 2% parasitaemia and 3·0% hematocrit in RPMI were dispensed in a 96-well round bottom plate. Then, 100 μL of drugs (10–0·07 μM) previously suspended in RPMI were added to the respective wells. Each drug was tested in seven concentrations, each one in triplicate. Untreated parasites received 100 μL of medium containing 0·5% DMSO, artesunate was used as positive control. Plates were incubated for 18 h at 37 °C under 3% O_2, 5% CO_2 and 91% N_2 atmosphere. The plate was centrifuged three times with 200 μL of drug-free medium at 1500 rpm for 5 min., then

200 μL of media containing tritiated hypoxanthine was added and plate incubated for 48 h. Plates were frozen at −20 °C and thawed and transferred to UniFilter-96 GF/B PEI coated plates (PerkinElmer) using of a cell harvester. After drying, 50 μL of scintillation cocktail was added in each well, sealed and plate read at liquid scintillation microplate counter. IC_{50} values were determined employing non-linear regression with Logistic equation available in the OriginPro 8·5 software. Minimal parasiticidal concentration (MPC) was determined as the concentration that reduces parasite growth by 99 ± 1·0%. At least three independent experiments were performed.

Activity in the intraerythrocytic P. falciparum *cycle*

A volume of 100 μL of rings of *P. falciparum* W2 strain at 2% parasitemia and 2·5% hematocrit in RPMI was dispensed per well in 96-well round bottom plates. Then, 100 μL of drugs previously suspended in RPMI were added to the respective wells. Each drug concentration was tested in triplicate. Untreated parasite received 100 μL of medium containing 0·5% DMSO. Plates were incubated for 48 h at 37 °C under 3% O_2, 5% CO_2, 91% N_2 atmosphere followed by centrifugation three times with 200 μL of drug-free medium at 1500 rpm for 5 min. A volume of 200 μL of media containing drugs were added and plates were incubated for additional 48 h. Thin blood smears were then prepared, fixed and stained with quick panoptic stain (Laborclin, Pinhais, Brazil). Slides were observed in an optical microscope (Olympus CX41, St. Louis, MO). The number of rings, trophozoites and schizonts were counted in at least 1500 cells per slide ($n = 4$) and plotted against drug concentration generated using GraphPad Prism 5·01. Two independent experiments were performed.

Activity against P. berghei *liver stages*

Inhibition of liver-stage infection by test compounds was determined by measuring the luminescence intensity in Huh-7 cells infected with a firefly luciferase-expressing *P. berghei* line as previously described (Ploemen *et al*. 2009). Briefly, Huh-7 cells, a human hepatoma cell line, were cultured in 1640 RPMI medium supplemented with 10% v/v FBS, 1% v/v non-essential amino acids, 1% v/v penicillin/streptomycin, 1% v/v glutamine and 10 mM 4-(2-hydroxyethyl)-1-piperazineethanesulfonic acid (HEPES), pH 7 and maintained at 37 °C with 5% CO_2. For infection assays, Huh-7 cells ($1{\cdot}0 \times 10^4$ per well) were seeded in 96-well plates the day before drug treatment and infection. The medium was replaced by medium containing the appropriate concentration of each compound approximately 1 h prior to infection with sporozoites freshly obtained through disruption of salivary glands of infected female *Anopheles stephensi* mosquitoes. An amount of the DMSO solvent equivalent to that present in the highest compound concentration was used as control. Sporozoite addition was followed by centrifugation at 1700 ***g*** for 5 min. Parasite infection load was measured 48 h after infection by a bioluminescence assay (Biotium, Hayward, CA). The effect of the compounds on the viability of Huh-7 cells was assessed by the AlamarBlue assay (Life) using the manufacturer's protocol.

Activity against P. falciparum *gametocytes*

Drugs were serially diluted in a 96-well round bottom plate (concentration range 29·0–0·22 μM) in 100 μL per well. Then, 100 μL of 3D7elo1-pfs16-CBG99 gametocytes at 0·5–1% parasitaemia and 2% hematocrit were dispensed. Each drug was tested in triplicate, in seven different concentrations. The DMSO concentration was not toxic for gametocytes. Methylene blue was used as positive control. Plates were incubated for 72 h at 37 °C under 3% O_2, 5% CO_2, 91% N_2 atmosphere. Luciferase activity was taken as measure of gametocytes viability, as previously described in the literature (Cevenini *et al*. 2014). Briefly, 100 μL of culture medium were removed from each well to increase hematocrit; 70 μL of resuspended culture were transferred to a black 96-well plate; 70 μL of D-luciferin (1 mM in citrate buffer 0·1 M, pH 5·5) were added. Luminescence measurements were performed after 10 min with 500 ms integration time. The IC_{50} was extrapolated from the non-linear regression analysis of the concentration–response curve. The percentage of gametocytes viability was calculated as 100 × [(OD treated sample − OD blank)/(OD untreated sample − μc-blank)] where 'blank' is the sample treated with 500 nM of methylene blue, which completely kills gametocytes.

Determination of the binding constant with ferriprotoporphyrin IX

The association constant of organoruthenium complexes to ferriprotoporphyrin IX (Sigma-Aldrich) was measured as described previously (Egan *et al*. 1997). Titration of a 2 mL solution (7·5 μM of ferriprotoporphyrin IX in 40% of DMSO, pH 7·5) in presence of compound (500 μM in 40% of DMSO, pH 7·5) was performed by UV absorbance at λ = 402 nm using Hewlett Packard spectrophotometer, diode array model 8452 (Santa Clara, CA). The volume of each titration was 5 μL and the relative molar ratio varied from 0 to 10 with regard to [Fe^{III}-PPIX]. Spectra were recorded about 1 min after each addition. The absorption of all compounds was subtracted by adding the same

amounts to the blank (40% of DMSO, pH 7·5). Fitting model with a 1:1 association using the equation described by Egan (Egan *et al*. 1997):

$$A = \frac{A_0 + A_\infty K[C]}{1 + K[C]}$$

where, A_0 is the absorbance of hemin before addition of complex or free chloroquine, A_∞ is the absorbance for the drug-hemin adduct at saturation, A is the absorbance at each point of the titration, and K is the conditional association constant. Three independent experiments were performed.

Assessment of inhibition of β*-hematin formation by infrared spectroscopy*

Polymerization of hemin into β-hematin in acid acetate buffer was studied using the method previously described in the literature (Egan *et al*. 1994). Briefly, 12 mg of hemin (Sigma-Aldrich) dissolved in 3 mL of NaOH 0·1 M were added in 0·3 mL of HCl 0·1 M and 1·7 mL of acetate buffer 10 M (pH 5), keeping the temperature at 60 °C during reaction. Primaquine and chloroquine were used as positive and negative controls, respectively. In a control test, after 0, 10, 30 and 60 min, 1 mL of each solution was collected, cooled on ice for 10 min, and then filtered over cellulose acetate (0·22 μm). The effect of the compounds was studied by performing the reaction as described above, adding three equivalents of each compound to the reaction mixture, where the reaction was stopped after 30 min. prior acidification. Pellets were thoroughly washed with water in order to remove acetate salts. Each solid was dried in silica gel and P_2O_5 for 48 h. Disks were mounted in KBr pellets and infrared spectra were analyzed in a Bomem–Michelson FT MB-102 instrument in the 4000–200 cm^{-1} region. Three independent experiments were performed.

Assessment of inhibition of β*-hematin formation by UV-Vis spectroscopy*

The assay was performed according to the method previously described in the literature (Parapini *et al*. 2000). A solution of hemin chloride (50 μL, 4 mM) dissolved in DMSO was distributed in 96-well plates. Different concentrations (1–100 mM) of each complex was dissolved in DMSO and added in triplicate (50 μL) to a final concentration of 1·25–25 mM $well^{-1}$. Control contained water or DMSO. The formation of β-hematin was initiated by addition of acetate buffer (100 μL, 0·2 M, pH 4·4). The plates were incubated at 37 °C for 48 h and then centrifuged. After removing the supernatant, the solid was washed twice with DMSO and finally dissolved in NaOH (200 μL, 0·2 N). After diluting with NaOH (0·1 N), absorbance was measured at 405 nm in a spectrophotometer. The inhibition of β-hematin was calculated in comparison with negative control, plotted against drug concentration generated using GraphPad Prism 5·01. Three independent experiments were performed.

SYTO 61 staining of P. falciparum

100 μL of rings of *P. falciparum* 3D7 strain at 2% parasitemia and 2·0% hematocrit in RPMI were dispensed in a 96-well round bottom plate. Then, 100 μL of drugs previously suspended in RPMI were added to the respective wells. Each drug concentration was tested in triplicate. Untreated parasite received 100 μL of medium containing 0·5% DMSO. Plates were incubated for 48 h at 37 °C under 3% O_2, 5% CO_2, 91% N_2 atmosphere. Plate was centrifuged with 200 μL of drug-free medium at 1500 rpm for 5 min. and 100 μL of SYTO 61 (Life) at 0·5 μM suspended in medium was added to each well and incubated in the dark for 30 min. After washing and adding 400 μL of isoton diluent, samples were analyzed in a flow cytometer (LSRFortessa, BD, Franklin Lakes, NJ). Gate of infected cells was determined in comparison with uninfected control. At least 200·000 events were acquired in the allophycocyanin channel (633, 660 nm). The analysis was performed using FlowJo (LLC, Ashland, Covington, LA). Three independent experiments were recorded.

CM-H2-DCFDA and SYTO 61 staining of P. falciparum

A volume of 100 μL of rings of *P. falciparum* 3D7 strain at 3·0% parasitaemia and 1·0% hematocrit in RPMI were dispensed per well in a 96-well round bottom plate. A volume of 25 μL of CM-H2-DCFDA (Life) at 15 μM suspended in media was added to each well and incubated in the dark for 20 min. Then, 100 μL of drugs previously suspended in RPMI were added to the respective wells. Each drug concentration was tested in triplicate. Untreated parasite received 100 μL of medium containing 0·5% DMSO. Plates were incubated for 3·5 h at 37 °C under 3% O_2, 5% CO_2, 91% N_2 atmosphere. A volume of 25 μL of SYTO 61 (Life) at 0·5 μM suspended in media was added to each well and incubated in the dark for 30 min. Plates were centrifuged at 1500 rpm for 5 min, supernatant was discarded and 200 μL of isoton diluent was added and samples were analyzed in a flow cytometer (LSRFortessa, BD). Gate of infected cells was determined in comparison with uninfected control. At least 200·000 events were acquired in the fluorescein isothiocyanate channel (488, 585 nm) for CM-H2-DCFDA and allophycocyanin channel (633, 660 nm) for SYTO 61. The analysis was performed using FlowJo (LLC), in three independent experiments.

In vivo *blood schizontocidal activity*

Male Swiss Webster mice (4–6 weeks) were infected by intraperitoneal injection of 10^6 NK65 strain *P. berghei*-infected erythrocytes and randomly divided into groups of $n = 5$. Each drug was solubilized in DMSO/saline (20:80 v/v) prior administration. Treatment was initiated within 3 h post-infection and given daily for 4 consecutive days orally by gavage or by intraperitoneal injection of 100 μL. Chloroquine treated mice were used as positive control group, while untreated infected mice were used as negative control group. The following parameters were evaluated: parasitaemia counted at 4, 5, 6, 7 and 8 days post-infection and 30 days post-infection animal survival. The per cent of parasitaemia reduction was calculated as follows ([mean vehicle group – mean treated group)/mean vehicle group] × 100%). Two independent experiments were performed.

Ex vivo *drug-induced cardiotoxicity in rat hearts using Langendorff system*

Male Wistar rats of 6–8 weeks-old were heparinized (800 IU kg^{-1}, i.p.) and following 20 min anaesthetized with ketamine (90 mg kg^{-1}, i.p.) and xylazine (10 mg kg^{-1}, i.p.). Heart was quickly excised via thoracotomy and immediately cannulated through the aorta to retrograde perfusion on the Langendorff system apparatus with peristaltic pump Minipuls 3 (Peristaltic Pump, ADInstruments, Sydney, Australia) under constant flow 6·5 mL min^{-1}. The heart was immersed in Krebs-Henseleit buffer (KHB) solution containing (in mM): 4·7 KCl, 1·2 KH_2PO_4, 118 NaCl, 25 Na_2HCO_3, 1·2 $MgSO_4$, 1·75 $CaCl_2$, 0·5 EDTA and 8·0 D-glucose, pH7·4; 37 °C; 5% CO_2, warmed to 37 °C. Two electrodes were then positioned at atrium and ventricle to obtain optimal electrocardiographic recordings. These electrodes were connected to the differential inputs of a Bioamplifier (PowerLab 8/35, AD Instrument) and a third was connected to ground. Recordings were displayed on a computer. Experimental protocol consisted of taking control records for 20 min in Krebs' solution, 10-min, perfusion period with MCQ or FCQ drugs (0·1; 1·0 and 10 μg mL^{-1}) dissolved in DMSO and suspended in KHB solution and a return to Krebs' solution for 20 min. Each drug was tested in triplicate at the three different concentrations. Electrocardiography recordings were registered as the presence of arrhythmias, heart rate, ventricular activation time, PR intervals, amplitude and time intervals of QT waves. Each drug was tested in at least three isolated hearts, LabChart Pro software including blood pressure and ECG analysis was used.

Statistical analyses

Non-linear regression analysis was used to calculate CC_{50} and IC_{50} values by using GraphPad Prism version 5.01 (Graph Pad Software, San Diego, USA), OriginPro version 8.5 (OriginLab, Northampton, USA) or Gen5 1·10 software provided with the Synergy4 plate reader (Biotek, Winooski, USA). One-way ANOVA analysis and Bonferroni multiple comparison tests were used. Results were considered statistically significant when $P < 0{\cdot}05$ as analysed by GraphPad Prism version 5.01.

RESULTS

Chemical structure and stability of organoruthenium complexes

The structures of organoruthenium complexes with general formula $[RuCQ(\eta^6\text{-}C_{10}H_{14})(N\text{-}N)]^{2+}$ studied in this work are shown in Fig. 1, where $\eta^6\text{-}C_{10}H_{14}$ is α-phellandrene and N-N is 2′-bipyridine (*BCQ*), 5,5′-dimethyl-2,2′-bipyridine (*MCQ*), 1,10-phenanthroline (*FCQ*), 4,7-diphenyl-1,10-phenanthroline (*FFCQ*). An organoruthenium complex lacking CQ in its composition, named *FCL*, was used during pharmacological evaluation. All these complexes were previously characterized by usual chemical tools (Colina-Vegas *et al*. 2015). To assess whether these organoruthenium complexes are dissociating in cell culture media and releasing CQ, stability in 80% DMSO-d_6 and 20% D_2O solution was monitored by ^{1}H NMR at different times up to 60 h. Spectra of *FCQ* samples are shown in Fig. 2. Any modification in intensity and chemical shifts were observed in the spectra up 60 h of incubation time. The same profile was observed after the monitoring of *MCQ* samples (data not shown).

Organoruthenium complexes are active against asexual blood stages and display low toxicity against mammalian cells

The mean IC_{50} values of the compounds were determined against CQ-sensitive and CQ-resistant strains of *P. falciparum*, while the CC_{50} values in mammalian cells were determined against J774 macrophages and HepG2 hepatocellular cells (Table 1). In the CQ-sensitive strain, all complexes were 2-fold less active than CQ. In the CQ-resistant strain, with the exception of compound *FFCQ*, the activity of complexes was similar to that of CQ. Apart from the *FFCQ* complex, susceptibility to drugs tested was in general similar for CQ–sensitive and CQ –resistant strains. Complexes did not either cause hemolysis in concentration up 100 μM (Fig. S1, supporting information) or cardiotoxicity in *ex vivo* isolated rat hearts (Table S1, supporting information). Regarding mammalian cytotoxicity, CC_{50}s for complexes were 5- to 10-fold higher than for the reference drug gentian violet. The only exception was observed for the *FFCQ* compound, which was cytotoxic in low micromolar concentrations. The cytotoxicity of complexes

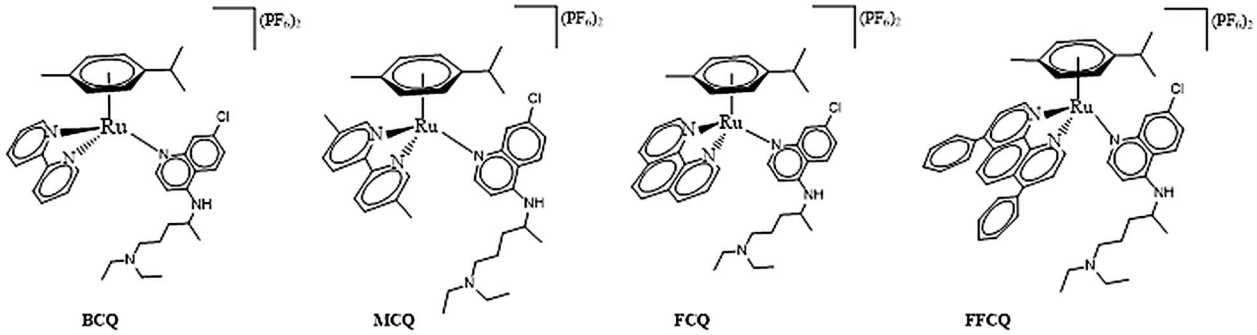

Fig. 1. Chemical structures of organoruthenium complexes.

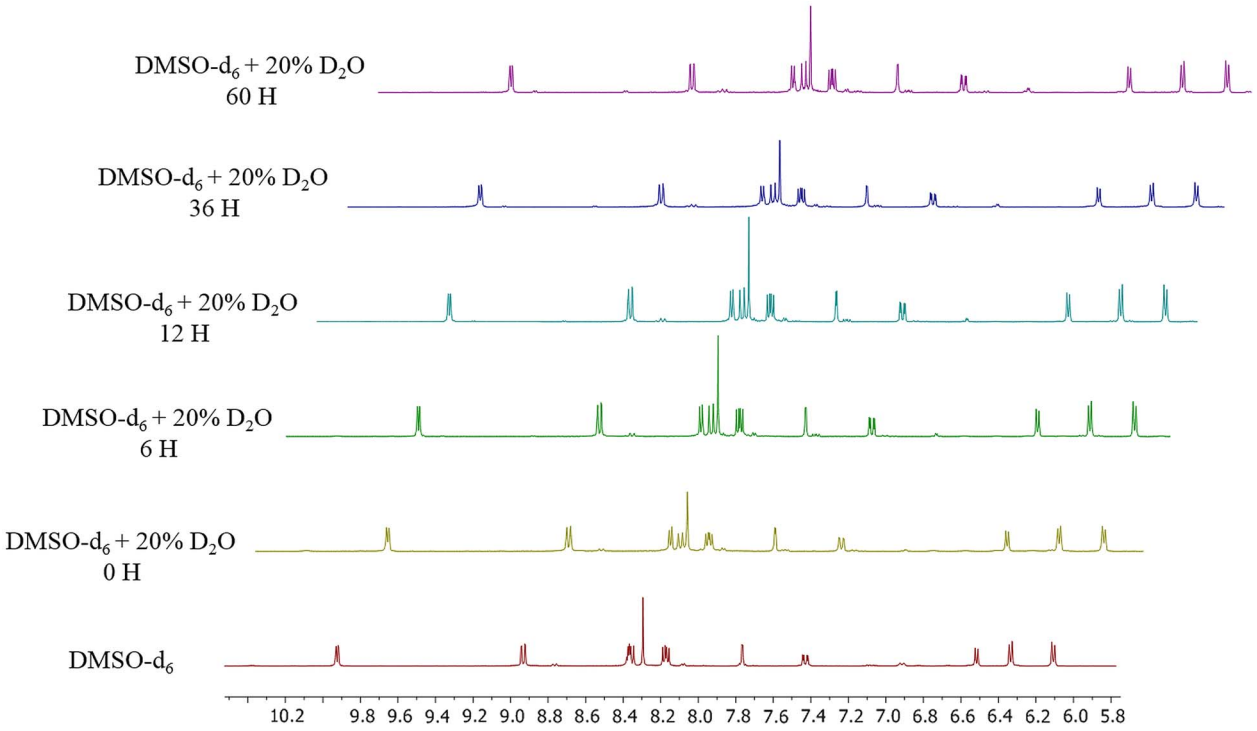

Fig. 2. Organoruthenium complexes stability in aqueous solution in incubation up to 60 h. ^{1}H-NMR spectra of *FCQ* complex in DMSO-d_6 containing 20% of D_2O. The incubation times are displayed in the left side. At least two independent experiments were performed.

was similar or lower than that of CQ. Calculated selectivity index (SI) values of 513 and 450 were obtained for *FCQ* and *BCQ*, respectively, which are similar or higher than that of CQ. Of note, the *FCL* complex showed low antiparasitic activity and SI values several folds lower than CQ-ruthenium complexes.

Organoruthenium complexes impair asexual parasite differentiation

Once antiparasitic activity had been observed, the onset of action and the activity against erythrocytic parasite cycle was investigated for *MCQ* and *FCQ* complexes (Fig. 3). Treatment with an IC_{50} concentration of *MCQ* decreased parasitaemia at the onset of drug exposure, while an accumulation of parasites in the trophozoite stage and consequent impairment to schizont progression were observed 96 h post exposure. In the presence of approximately 2-fold the IC_{50} of *MCQ*, substantial accumulation of trophozoites was achieved 48 h post exposure, while progression in parasite growth and differentiation was abrogated 96 h post exposure. Similar treatments with *FCQ* led to a similar impairment on parasite cycle at the IC_{50} values of the drugs and complete blockage of the parasite cycle twice that concentration. A morphological examination of stained blood smears revealed that during treatment with the IC_{50} concentration of *MCQ* and *FCQ*, digestive vacuoles containing hemozoin crystals were absent in trophozoites (data not shown). This is typically observed for CQ, a well-known hemozoin inhibitor. At higher concentration of complexes, most parasites appeared as a picnotic mass.

Table 1. Cytostatic activity against intraerythrocytic *P. falciparum*, mammalian cell cytotoxicity and selectivity indexes of organoruthenium complexes

	P. falciparum, IC_{50} ± S.E.M. (μM)[a]		Cells, CC_{50} ± S.E.M. (μM)[b]		Selectivity index[c]	
Compounds	CQ-sensitive 3D7	CQ-resistant W2	J774	HepG2	3D7	W2
FCL	3·4 ± 0·75	4·6 ± 0·54	111·3 ± 51	29·7 ± 2·6	32	23
BCQ	0·34 ± 0·13	0·52 ± 0·04	153·9 ± 6·3	>300	450	307
MCQ	0·30 ± 0·007	0·30 ± 0·1	42·6. ± 1·6	77·7 ± 1·4	142	142
FCQ	0·30 ± 0·03	0·31 ± 0·01	154·0 ± 6·9	84·9 ± 2·2	513	513
FFCQ	0·21 ± 0·039	2·1 ± 0·3	2·4 ± 0·2	21·2 ± 0·8	11	1
CQ	0·11 ± 0·035	0·43 ± 0·09	37·6 ± 3·6	76·1 ± 3·1	690	190
Mefloquine	–	0·0035 ± 0·0004	–	–	–	–
Gentian violet	–	–	4·3 ± 0·8	14·2 ± 0·3	–	–

[a] Determined 48 h after incubation with compounds.
[b] Determined 72 h after incubation with compounds. Values were calculated as mean of three independent experiments.
[c] Determined as CC_{50} (J774 cells)/IC_{50}. IC_{50}, inhibitory concentration at 50%. CC_{50}, cytotoxic concentration at 50%. S.E.M., standard error of the mean.

Organoruthenium complexes are fast-acting parasiticidal agents against asexual blood stages

To assess the parasiticidal activity of complexes, time- and concentration-dependent effects were studied in synchronized *P. falciparum* trophozoites. Growth inhibition by drug exposure for 6, 18, 24 or 48 h was monitored by microscopy examination. At 2 × the IC_{50} values of the *FCQ* and *MCQ*, parasite inhibition was detected after 18 h of compound exposure (data not shown). This incubation time was selected for the parasiticidal activity study. After 18 h of exposure to different drug concentrations, followed by extensive washing to remove drugs, the culture was maintained for 48 h and growth was quantified by hypoxanthine incorporation relative to untreated control. Artesunate was used as a positive control. Parasite clearance was estimated as 99 ± 1·0% parasite growth and expressed as MPC. Table 2 shows mean LC_{50} and MPC values. Complexes show parasiticidal activity, with LC_{50} values comparable with CQ. MPC values show that *MCQ* was more potent than *FCQ*. The parasiticidal potency of the complexes was lower than artesunate but higher than CQ, which did not lead to parasite clearance in concentrations up 10 μM.

Antiparasitic activity is not governed by inhibition of β*-hematin formation*

Given their potent *in vitro* growth inhibition against trophozoites, the effects of organoruthenium complexes within hemin polymerization as well as their interaction to ferriprotoporphyrin IX (α-hematin) were investigated. Firstly, we determined the binding constant to ferriprotoporphyrin IX by analyzing the absorption spectra at various concentrations of complexes. As shown in Fig. 4, increasing the concentration of complex caused a reduction in the absorption intensity, ranging from 60 to 70%. These titration curves were further fitted to a 1:1 association model to give the binding constant values expressed as logK (Table 3). LogK values for organoruthenium complexes were lower than the observed for CQ and in general, there was no great difference when the complexes were compared with each other.

After measuring the interaction with hematin, the compounds' ability to inhibit hemin aggregation into β-hematin was evaluated by UV-Vis spectroscopy analysis (Soret's porphyrin band). This experiment was performed in acetate buffer at pH 4·9 and determined 48 h after incubation (Table 3). Comparison of IC_{50} values revealed that *FFCQ* complex was unable to inhibit hemin aggregation process in concentration up 2·0 mM. In contrast, other organoruthenium complexes inhibited hemin aggregation with potency similar to CQ. Additionally, the hemin aggregation process was evaluated by infrared spectra. Figure S2 illustrates the infrared spectrum of hemin in the absence or presence of CQ, primaquine and organoruthenium complexes. Over time, hemin aggregates into β-hematin, leading to the formation of iron-carboxylate bonds observed as bands at 1·660 and 1·210 cm^{-1}. Adding primaquine did not impair β-hematin formation, while adding CQ or its ruthenium complexes inhibited β-hematin formation.

Oxidative stress induced by organoruthenium treatment

Firstly, we determined parasite viability in 3D7 strain trophozoites by staining with SYTO 61 accordingly to a previously described protocol (Fu *et al.* 2010) and analyzing by flow cytometry.

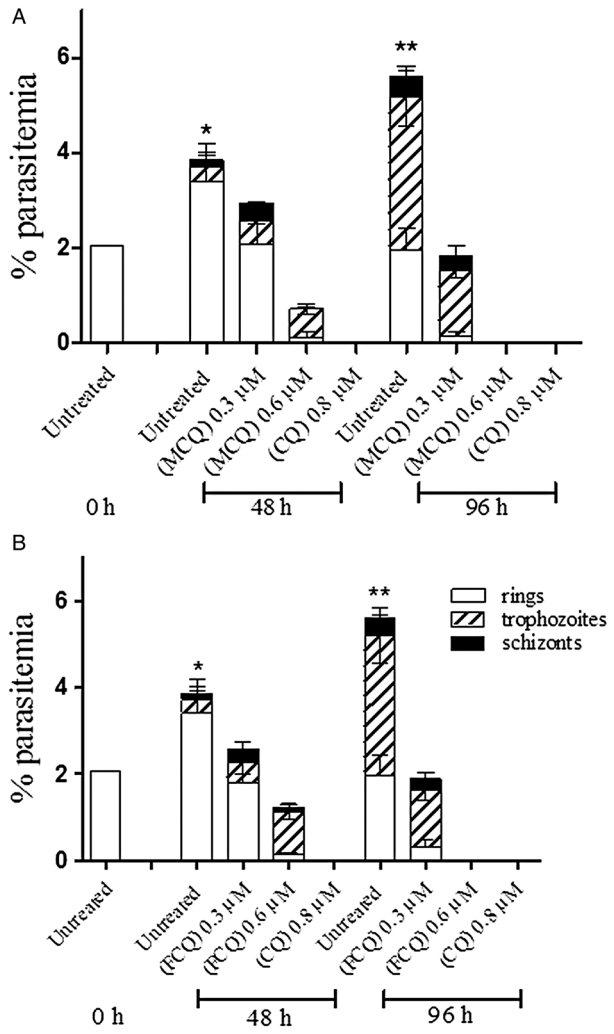

Fig. 3. Drug-susceptibility testing against blood stage W2 strain *P. falciparum*. Ring stage parasites (2% parasitaemia, 2·5% hematocrit) were incubated with vehicle (DMSO 0·5%) as a untreated control, CQ, *MCQ* (panel A) and *FCQ* (panel B) at 0 and 48 h. Quantification of intraerythrocytic stages at 48 and 96 after addition of the compounds are shown. Values are shown from one of two independent experiments. Error bars represent standard deviation. *$p < 0·05$ for quantification of rings *vs* untreated 0 h. **$p < 0·05$ for quantification of trophozoites *vs* untreated 48 h. CQ, chloroquine.

Treatment at 1·25 μM of CQ, *MCQ* and *FCQ* for 48 h incubation time led a population of non-viable parasites, while at 0·31 μM we observed two populations: a non-viable population and another that is viable but with decreased SYTO 61 staining, possible due to delay in parasite growth (Fig. S3, supporting information). Trophozoites were treated with CQ or complexes and incubated for 4 h and co-labelled with ROS probe CM-H2DCFDA and SYTO 61 (Fig. S4, supporting information). Parasite viability following treatment at 0·15 μM and monitored by SYTO 61 staining was not altered in comparison to untreated parasites (Fig. 5). In contrast, at the same incubation and treatment, *MCQ* and *FCQ* increased DCF fluorescence levels in approximately 2-fold in comparison with untreated parasites. CQ treatment at same concentration increased in approximately 50% DCF fluorescence, while the complex lacking CQ in its composition (*FCL*) did not increase DCF when compared with untreated parasites.

Multistage action of organoruthenium complexes

We next examined whether ruthenium complexes possess multistage activity. Firstly, the ability to inhibit *Plasmodium* hepatic infection was assessed in a well-established *in vitro* infection model, employing *P. berghei*-infected Huh7 cells, a human hepatoma cell line (Prudêncio *et al*. 2011). Huh7 cells were cultured in the presence of each complex followed by addition of luciferase-expressing *P. berghei* sporozoites. Infection load and host cell cytotoxicity were analyzed 48 h post-infection. Primaquine, the only licensed drug against *Plasmodium* liver stages (Rodrigues *et al*. 2012), was used as the reference drug. As shown in Fig. 6, the *FCQ* compound did not decrease infection in comparison to the untreated control. The *MCQ* compound inhibited approximately 50% infection at a 10 μM concentration, without affecting host cell confluency. A similar concentration of primaquine inhibited infection by 50%. For comparison, CQ

Table 2. *In vitro* parasiticidal property of organoruthenium complexes against intraerythrocytic *P. falciparum*

	CQ-sensitive 3D7[a]		CQ-resistant W2[a]	
Compounds	LC_{50} ± S.E.M. (μM)[b]	MPC (μM)[c]	LC_{50} ± S.E.M. (μM)[b]	MPC (μM)[c]
MCQ	0·81 ± 0·073	5·0	0·37 ± 0·017	2·5
FCQ	1·05 ± 0·078	5·0	0·87 ± 0·04	5·0
CQ	0·64 ± 0·04	>10	0·43 ± 0·03	>10
Artesunate	0·0053 ± 0·00032	0·12	0·0049 ± 0·0009	0·19

[a] Activity determined in trophozoites incubated for 18 h with drugs then for 48 h in drug-free conditions.
[b] LC_{50}, lethal concentration at 50%.
[c] MPC, minimal parasiticidal concentration.

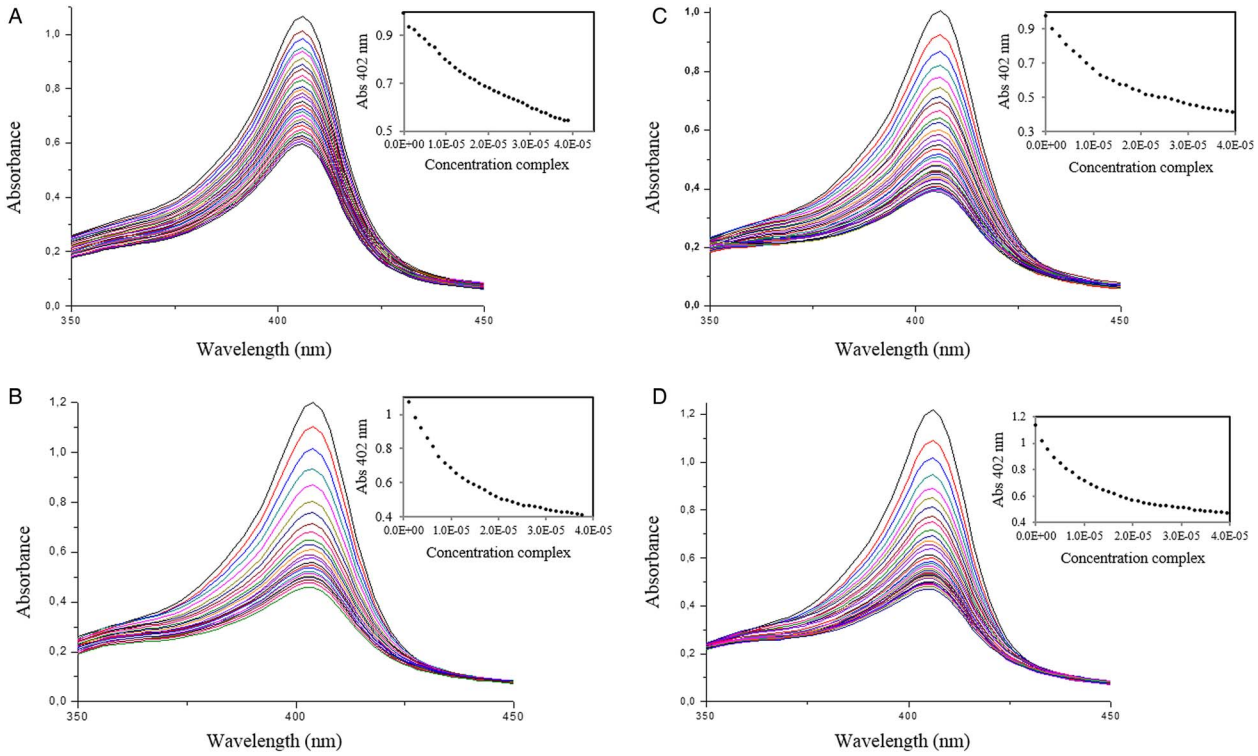

Fig. 4. Spectroscopic titration of Fe(III)PPIX at pH 7·4 with organoruthenium complexes. Panel A, *FCQ* complex; Panel B, *FFCQ* complex; Panel C, *BCQ* complex; Panel 4, *MCQ* complex.

Table 3. Binding constant for hematin and inhibition of hemin polymerization for organoruthenium complexes

	Hematin		Hemin	
	UV–vis titration			
Compounds	logK[a]	% hypochromism[b]	$IC_{50} \pm$ S.D. (mM)[c]	Presence of peaks at 1660 and 1210 cm^{-1}[d]
BCQ	4·77 ± 0·04	58	0·30 ± 0·11	–
MCQ	4·98 ± 0·05	60	0·43 ± 0·03	–
FCQ	4·44 ± 0·03	57	0·50 ± 0·01	–
FFCQ	5·02 ± 0·01	62	>2·0	–
CQ	5·09 ± 0·02	55	0·40 ± 0·11	–
PQ	–	–	–	+

[a] Binding constant expressed as logK.
[b] Determined in comparison with untreated (no drug).
[c] Determined 48 h after drug incubation.
[d] Determined by infrared spectrum.

reduces hepatic infection by 50% at a 15 μM concentration (Rodrigues *et al*. 2012). We then assessed the transmission-blocking potential of each compound against stage V *P. falciparum* gametocytes. Inhibition of viability of stage V *P. falciparum* 3D7 gametocytes was evaluated and the compounds' IC_{50} values were determined. Methylene blue was used as positive control (Table 4). In concentrations up 14 μM, the *MCQ* complex did not inhibit gametocytes, while the *FCQ* and *FFCQ* complexes presented inhibitory activity. The *BCQ* complex was the most potent, exhibiting an IC_{50} value in the low micromolar range. Although less potent than methylene blue, this compound was active, while CQ is inactive in impairing gametocyte viability.

Organoruthenium complexes reduce parasitaemia in infected mice

Before evaluating efficacy, compounds were examined regarding lethal doses in Swiss Webster mice ($n = 3$). A single intraperitoneal injection of *MCQ* or *BCQ* was not lethal at a dose of 50 mg kg^{-1} $weight^{-1}$. *FCQ* was lethal at 50 mg kg^{-1}, but safer

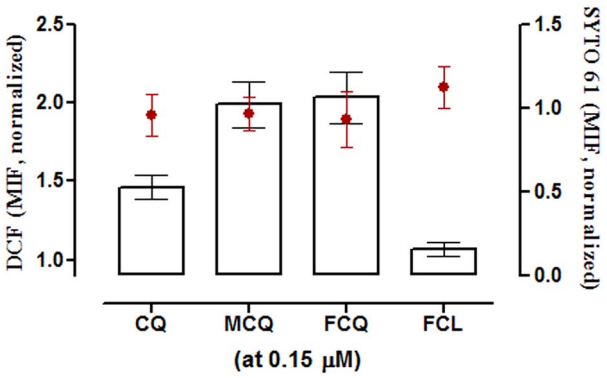

Fig. 5. 3D7 strain *P. falciparum* trophozoites (3·0% parasitaemia, 1% hematocrit) double stained with CM-H2-DCFDA (probe for reactive oxygen species) and SYTO 61 (probe for cell viability). Drugs were incubated for 4 h and analysed by flow cytometry. Bars represent DCF signal and red dots represent SYTO 61 signal. MIF were normalized from untreated control and obtained from pooling data gathered of two independent experiments. MIF, median intensity fluorescence. Error bars represent standard deviation.

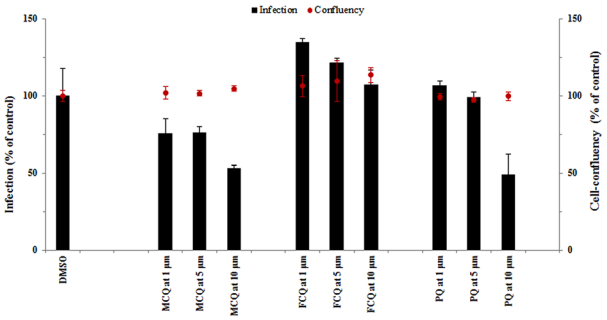

Fig. 6. Drug-susceptibility testing against *P. berghei* sporozoites. Seeded Huh7 cells were treated with drugs and infected with sporozoites. Bioluminescence intensity was measured 48 h post-infection. Bars represent infection and red dots represent Huh7 cell confluency. Untreated control received only DMSO. PQ, Primaquine. Error bars represent standard deviation from each concentration in triplicate. Results of two independent experiments.

at 5·0 mg kg^{-1}. Due to its low SI, *FFCQ* was not tested in mice. By following 4-day treatment test in *P. berghei*-infected mice, parasitaemia suppression and survival rate were evaluated in comparison with untreated infected mice (vehicle). CQ was used as the reference drug (Table 5, Fig. S5). On day 8 post-infection, 50 mg kg^{-1} of *MCQ* caused a 95·1% reduction in parasitaemia in comparison with untreated group, with 40% of animal survival observed 30 days post-infection. When *MCQ* was used at 10 mg kg^{-1}, a 46·2% reduction in parasitaemia was observed and no survival was achieved. In infected mice treated with *FCQ*, parasitaemia was reduced by 76·9% *vs* untreated group. Treatment with 10 mg kg^{-1} *BCQ* led to a 62·3% reduction in parasitaemia and 40% protection in animal survival *vs* untreated group. In comparison, treatment with CQ at same dose reduced in 100% the parasitaemia and conferred 80% protection in animal survival.

Table 4. *In vitro* activity of organoruthenium complexes against stage V gametocytes of 3D7 *P. falciparum*

Compounds	$IC_{50} \pm$ S.D. (μM)[a]
CQ	>20
MCQ	>14·5
FCQ	4·28 ± 1·05
BCQ	0·78 ± 0·24
FFCQ	1·43 ± 0·24
Methylene blue	0·047 ± 0·015

[a] Activity determined in gametocytes incubated for 72 h with drugs. Three independents experiments performed, each concentration in duplicate.

Table 5. Summary of activities of organoruthenium complexes against blood stage *in vivo* infection

Compounds	Doses (mg kg^{-1})[a]	% infection reduction[b]	Survival[c]
Vehicle	0	–	0/5
MCQ	50	95·1	2/5
	10	46·2	0/5
	5·0	48·7	0/5
FCQ	5·0	76·9	0/5
BCQ	10	62·3	2/5
CQ	50 (oral)	100	5/5
	10	100	4/5
	5·0 (oral)	59·6	0/5

[a] Given for 4 days, by intraperitoneal route, with the exception for CQ at 50 and 5·0 mg kg^{-1}, which were given orally. Vehicle = DMSO:saline (20:80 v/v).
[b] Determined on day 8 post infection.
[c] Number of mice alive 30 days post infection/(n = 5).

DISCUSSION

The insertion of CQ into organoruthenium complex resulted in compounds with antiparasitic activity, while a ruthenium complex lacking CQ did not present such property. Most complexes displayed potency and selectivity against the *Plasmodium* blood asexual stage with a magnitude similar to that of free CQ. Unspecific cytotoxicity was only observed for the *FFCQ* complex, possibly due to the presence of 4,7-diphenyl-1,10-phenanthroline ligand in its composition. Like CQ, complexes presented activity against all forms of blood asexual stages (rings, trophozoites and schizonts), which is an important characteristic to reduce a mixed parasite population during infection. A common feature of metal complexes is dissociation in

solution, with concomitant ligand exchange (Peacock and Sadler, 2008). Here we showed that these organoruthenium complexes do not release CQ upon solution in the same incubation time in the pharmacological evaluation, indicating that the entire organoruthenium complex is responsible for activity.

CQ-complexes present advantages in terms of pharmacological profile. Firstly, complexes inhibited the growth of all tested *P. falciparum* strains, irrespective of their drug resistance background. Secondly, they exhibited an onset of action detectable after 18 h drug exposure, which is faster than what is observed for CQ treatment. The LC_{50} values for complexes fall in the same micromolar range of IC_{50} values, indicating that compounds act as a cytotoxic rather than as a cytostatic drug. The MPC values revealed that complexes were able to clear parasites after 18 h drug exposure. Although these properties were not as potent as those of the fast-acting artesunate, they were superior to those observed for CQ. These findings show that ruthenium complexes induce parasite killing and this is achieved in short time. The fast parasite killing rate displayed by these complexes is attractive, especially because this can shorten treatment time as well as prevent parasite escape.

We further observed that ruthenium complexes present activity in the liver and in the blood sexual stages. In the liver-stage *Plasmodium, MCQ* complex displayed antiparasitic activity comparable with Primaquine and superior to CQ. Regarding the action in the sexual stage, we observed reduction of gametocyte viability in response to ruthenium complex treatment. Therefore, unlike CQ, which is classically an effective drug during blood schizogony, the ruthenium complexes show a multistage antiplasmodial profile. In fact, the effective concentrations of ruthenium complexes against sporozoites and gametocytes stages are higher than in the blood asexual stages. However, to the best of our knowledge, this is the first time that a multistage activity profile is demonstrated for metal complexes. This is desirable since drugs targeting different stages of the parasite vertebrate life cycle can work effectively in the prevention and against the relapse of malaria.

The strong activity of the complexes against trophozoites, where hemozoin formation takes place, led us to investigate whether organoruthenium complexes inhibit β-hematin formation. Except *FFCQ*, which was inactive, other complexes inhibited polymerization of hemin into β-hematin with potency similar to CQ. In contrast, all complexes presented lower binding constant to ferriprotoporphyrin IX (α-hematin) than CQ. These results argued that complexes are more potent in interaction with hemin rather than β-hematin, which is a finding also observed for other CQ-metal complexes (Martínez *et al*. 2009). CQ binds to free heme through its quinoline nitrogen, while in the CQ-ruthenium complexes this nitrogen is bound to ruthenium, indicating that these complexes interact with heme in a binding process different to CQ.

We demonstrated that the organoruthenium treatment increased ROS levels in trophozoites, where β-hematin formation is most active. Their effects on inducing oxidative stress were more pronounced than CQ-treatment and absence under treatment with CQ-lacking complex *FCL*. Importantly, these properties were observed in viable parasites, which reflect a primary mechanism of action of organoruthenium complexes rather than secondary consequences of cell death. Therefore, organoruthenium complexes achieved antiparasitic activity against asexual forms because they inhibit β-hematin formation, which cause an insult in parasites since it raises toxic free heme and consequently produces oxidative stress.

MCQ complex exhibited a dose-dependent effect and presented an optimal efficacy when treatment was given at 50 mg kg^{-1}. This reduced blood parasitaemia and increased survival, showing that organometallic complexes are efficacious and kill parasites. A similar property was observed for *BCQ* treatment, while the *FCQ* complex presented narrow therapeutic window, restricting its evaluation. As a limitation, the efficacy of organoruthenium complexes is inferior to CQ treatment. Apart from *FFCQ* complex, unspecific cytotoxicity was not a concern since complexes were not toxic for two different cell linages (macrophages and hepatocellular cells). Absence of hemolysis of uninfected erythrocytes and of cardiotoxicity in isolated hearts suggests low toxicity for these organoruthenium complexes. Therefore, a major challenge that remains is to optimize the efficacy of this class of compounds to enable effective reduction of parasitaemia *in vivo*.

CONCLUSION

We have evaluated the antimalarial activity of organoruthenium complexes containing CQ. We showed that this class of compounds is stable in mixed DMSO-aqueous media without releasing CQ, and presented potency against blood asexual forms similar to CQ. Organoruthenium complexes exhibited moderate activity against liver stage and potent activity against sexual stage, while CQ is devoid of such properties. They operate by a mechanism of action that is distinct from that of CQ, by causing oxidative stress. Importantly, we demonstrated that organoruthenium complex treatment presented efficacy in inhibiting parasitaemia in mice, pointing out that further pharmacological investigation, as well as chemical modification are relevant to strengthen antimalarial drug development based on inorganic compounds.

SUPPLEMENTARY MATERIAL

The supplementary material for this article can be found at http://dx.doi.org/10.1017/S0031182016001153.

ACKNOWLEDGEMENTS

We are thankful to the flow cytometry facility of CPqGM (Brazil) and AVIS Comunale Milano (Italy) for providing blood samples for gametocyte culture.

FINANCIAL SUPPORT

This research was funded by FAPESB (grant PET0042/2013, Brazil) to M.B.P.S, FAPESP (grant 14/10516-7, Brazil) to A.A.B. and Fundação para a Ciência e Tecnologia (grant PTDC/SAU-MIC/117060/2010 Portugal) to M.P. A.A.B. and M.B.P.S. are recipients of senior fellowships by CNPq (Brazil).

TRANSPARENCY DECLARATIONS

The authors declare no competing financial interest.

CONTRIBUTING AUTHORS

A.A.B., D.R.M.M. and M.B.P.S. initiated the project and provided guidance for experimental design and interpretation of data. T.S.M. performed *in vitro* and *in vivo* drug susceptibility studies; M.D.P. assisted with cell culture; L.C.V. and M.N. synthesized and validated drugs, performed hematin assays; M.P. and M.M. performed liver stage drug activity assays; S.D. and NB performed drug susceptibility assays in gametocytes; P.C.M.O., B.C.B. and S.G.M. performed cardiotoxicity evaluation; D.R.M.M. initiated manuscript preparation. All authors have read and approved the final manuscript.

REFERENCES

Adams, M., Li, Y., Khot, H., De Kock, C., Smith, P. J., Land, K., Chibale, K. and Smith, G. S. (2013). The synthesis and antiparasitic activity of aryl- and ferrocenyl-derived thiosemicarbazone ruthenium(II)-arene complexes. *Dalton Transactions* **42**, 4677–4685.

Adams, M., de Kock, C., Smith, P. J., Land, K. M., Liu, N., Hopper, M., Hsiao, A., Burgoyne, A. R., Stringer, T., Meyer, M., Wiesner, L., Chibale, K. and Smith, G. S. (2015). Improved antiparasitic activity by incorporation of organosilane entities into half-sandwich ruthenium(II) and rhodium(III) thiosemicarbazone complexes. *Dalton Transactions* **44**, 2456–2468.

Barbosa, M. I., Corrêa, R. S., de Oliveira, K. M., Rodrigues, C., Ellena, J., Nascimento, O. R., Rocha, V. P., Nonato, F. R., Macedo, T. S., Barbosa-Filho, J. M., Soares, M. B. and Batista, A. A. (2014). Antiparasitic activities of novel ruthenium/lapachol complexes. *Journal of Inorganic Biochemistry* **136**, 33–39.

Cevenini, L., Camarda, G., Michelini, E., Siciliano, G., Calabretta, M. M., Bona, R., Kumar, T. R., Cara, A., Branchini, B. R., Fidock, D. A., Roda, A. and Alano, P. (2014). Multicolor bioluminescence boosts malaria research: quantitative dual-color assay and single-cell imaging in *Plasmodium falciparum* parasites. *Analytical Chemistry* **86**, 8814–8821.

Chellan, P., Land, K. M., Shokar, A., Au, A., An, S. H., Taylor, D., Smith, P. J., Riedel, T., Dyson, P. J., Chibale, K. and Smith, G. S. (2014). Synthesis and evaluation of new polynuclear organometallic Ru (II), Rh(III) and Ir(III) pyridyl ester complexes as *in vitro* antiparasitic and antitumor agents. *Dalton Transactions* **43**, 513–526.

Clavel, C. M., Păunescu, E., Nowak-Sliwinska, P., Griffioen, A. W., Scopelliti, R. and Dyson, P. J. (2015). Modulating the anticancer activity of ruthenium(II)-arene complexes. *Journal of Medicinal Chemistry* **58**, 3356–3365.

Colina-Vegas, L., Villarreal, W., Navarro, M., de Oliveira, C. R., Graminha, A. E., Maia, P. I., Deflon, V. M., Ferreira, A. G., Cominetti, M. R. and Batista, A. A. (2015). Cytotoxicity of Ru(II) piano-stool complexes with chloroquine and chelating ligands against breast and lung tumor cells: interactions with DNA and BSA. *Journal of Inorganic Biochemistry* **153**, 150–161.

D'Alessandro, S., Silvestrini, F., Dechering, K., Corbett, Y., Parapini, S., Timmerman, M., Galastri, L., Basilico, N., Sauerwein, R., Alano, P. and Taramelli, D. (2013). A *Plasmodium falciparum* screening assay for anti-gametocyte drugs based on parasite lactate dehydrogenase detection. *Journal of Antimicrobial Chemotherapy* **68**, 2048–2058.

Dubar, F., Egan, T. J., Pradines, B., Kuter, D., Ncokazi, K. K., Forge, D., Paul, J. F., Pierrot, C., Kalamou, H., Khalife, J., Buisine, E., Rogier, C., Vezin, H., Forfar, I., Slomianny, C., Trivelli, X., Kapishnikov, S., Leiserowitz, L., Dive, D. and Biot, C. (2011). The antimalarial ferroquine: role of the metal and intramolecular hydrogen bond in activity and resistance. *ACS Chemical Biology* **6**, 275–287.

Dubar, F., Slomianny, C., Khalife, J., Dive, D., Kalamou, H., Guérardel, Y., Grellier, P. and Biot, C. (2013). The ferroquine antimalarial conundrum: redox activation and reinvasion inhibition. *Angewandte Chemie International Edition in English* **52**, 7690–7693.

Egan, T. J., Ross, D. C. and Adams, P. A. (1994). Quinoline anti-malarial drugs inhibit spontaneous formation of beta-haematin (malaria pigment). *FEBS Letters* **352**, 54–57.

Egan, T. J., Mavuso, W. W., Ross, D. C. and Marques, H. M. (1997). Thermodynamic factors controlling the interaction of quinoline antimalarial drugs with ferriprotoporphyrin IX. *Journal of Inorganic Biochemistry* **68**, 137–145.

Ekengard, E., Glans, L., Cassells, I., Fogeron, T., Govender, P., Stringer, T., Chellan, P., Lisensky, G. C., Hersh, W. H., Doverbratt, I., Lidin, S., de Kock, C., Smith, P. J., Smith, G. S. and Nordlander, E. (2015). Antimalarial activity of ruthenium(ii) and osmium(ii) arene complexes with mono- and bidentate chloroquine analogue ligands. *Dalton Transactions* **44**, 19314–19329.

Fu, Y., Tilley, L., Kenny, S. and Klonis, N. (2010). Dual labeling with a far red probe permits analysis of growth and oxidative stress in *P. falciparum*-infected erythrocytes. *Cytometry Part A*. **77**, 253–263.

Gabbiani, C., Messori, L., Cinellu, M. A., Casini, A., Mura, P., Sannella, A. R., Severini, C., Majori, G., Bilia, A. R. and Vincieri, F. F. (2009). Outstanding plasmodicidal properties within a small panel of metallic compounds: hints for the development of new metal-based antimalarials. *Journal of Inorganic Biochemistry* **103**, 310–312.

Glans, L., Taylor, D., de Kock, C., Smith, P. J., Haukka, M., Moss, J. R. and Nordlander, E. (2011). Synthesis, characterization and antimalarial activity of new chromium arene-quinoline half sandwich complexes. *Journal of Inorganic Biochemistry* **105**, 985–990.

Glans, L., Ehnbom, A., de Kock, C., Martínez, A., Estrada, J., Smith, P. J., Haukka, M., Sánchez-Delgado, R. A. and Nordlander, E. (2012*a*). Ruthenium(II) arene complexes with chelating chloroquine analogue ligands: synthesis, characterization and *in vitro* antimalarial activity. *Dalton Transactions* **41**, 2764–2773.

Glans, L., Hu, W., Jöst, C., de Kock, C., Smith, P. J., Haukka, M., Bruhn, H., Schatzschneider, U. and Nordlander, E. (2012*b*). Synthesis and biological activity of cymantrene and cyrhetrene 4-aminoquinoline conjugates against malaria, leishmaniasis, and trypanosomiasis. *Dalton Transactions* **41**, 6443–6450.

Goldberg, D. E., Sharma, V., Oksman, A., Gluzman, I. Y., Wellems, T. E. and Piwnica-Worms, D. (1997). Probing the chloroquine resistance locus of *Plasmodium falciparum* with a novel class of multidentate metal(III) coordination complexes. *Journal of Biological Chemistry* **272**, 6567–6572.

Huta, B. P., Mehlenbacher, M. R., Nie, Y., Lai, X., Zubieta, C., Bou-Abdallah, F. and Doyle, R. P. (2016). The lysosomal protein saposin B binds chloroquine. *ChemMedChem* **11**, 277–282.

Khanye, S. D., Smith, G. S., Lategan, C., Smith, P. J., Gut, J, Rosenthal, P. J. and Chibale, K. (2010). Synthesis and *in vitro* evaluation of gold(I) thiosemicarbazone complexes for antimalarial activity. *Journal of Inorganic Biochemistry* **104**, 1079–1083.

Lewis, M. D., Behrends, J., Sá, E., Cunha, C., Mendes, A. M., Lasitschka, F., Sattler, J. M., Heiss, K., Kooij, T. W., Navarro, M., Pérez, H. and Sánchez-Delgado, R. A. (1997). Toward a novel

metal-based chemotherapy against tropical diseases. 3. Synthesis and antimalarial activity *in vitro* and *in vivo* of the new gold-chloroquine complex [Au(PPh3)(CQ)]PF6. *Journal of Medicinal Chemistry* **40**, 1937–1939.

Lin, J. W., Spaccapelo, R., Schwarzer, E., Sajid, M., Annoura, T., Deroost, K., Ravelli, R. B., Aime, E., Capuccini, B., Mommaas-Kienhuis, A. M., O'Toole, T., Prins, F., Franke-Fayard, B. M., Ramesar, J., Chevalley-Maurel, S., Kroeze, H., Koster, A. J., Tanke, H. J., Crisanti, A., Langhorne, J., Arese, P., Van den Steen, P. E., Janse, C. J. and Khan, S. M. (2015). Replication of *Plasmodium* in reticulocytes can occur without hemozoin formation, resulting in chloroquine resistance. *Journal of Experimental Medicine* **212**, 893–903.

Martínez, A., Rajapakse, C. S., Jalloh, D., Dautriche, C. and Sánchez-Delgado, R. A. (2009). The antimalarial activity of Ru-chloroquine complexes against resistant *Plasmodium falciparum* is related to lipophilicity, basicity, and heme aggregation inhibition ability near water/n-octanol interfaces. *Journal of Biological Inorganic Chemistry* **14**, 863–871.

Martínez, A., Suárez, J., Shand, T., Magliozzo, R. S. and Sánchez-Delgado, R. A. (2011). Interactions of arene-Ru(II)-chloroquine complexes of known antimalarial and antitumor activity with human serum albumin (HSA) and transferrin. *Journal of Inorganic Biochemistry* **105**, 39–45.

Maschke, M., Alborzinia, H., Lieb, M., Wölfl, S. and Metzler-Nolte, N. (2014). Structure-activity relationship of trifluoromethyl-containing metallocenes: electrochemistry, lipophilicity, cytotoxicity, and ROS production. *ChemMedChem* **9**, 1188–1194.

Meier, S. M., Novak, M., Kandioller, W., Jakupec, M. A., Arion, V. B., Metzler-Nolte, N., Keppler, B. K. and Hartinger, C. G. (2013). Identification of the structural determinants for anticancer activity of a ruthenium arene peptide conjugate. *Chemistry* **19**, 9297–9307.

Navarro, M., Vásquez, F., Sánchez-Delgado, R. A., Pérez, H., Sinou, V. and Schrével, J. (2004). Toward a novel metal-based chemotherapy against tropical diseases. 7. Synthesis and *in vitro* antimalarial activity of new gold-chloroquine complexes. *Journal of Medicinal Chemistry* **47**, 5204–209.

Navarro, M., Castro, W., Higuera-Padilla, A. R., Sierraalta, A., Abad, M. J., Taylor, P. and Sánchez-Delgado, R. A. (2011*a*). Synthesis, characterization and biological activity of trans-platinum(II) complexes with chloroquine. *Journal of Inorganic Biochemistry* **105**, 1684–1691.

Navarro, M., Castro, W., Martínez, A. and Sánchez Delgado, R. A. (2011*b*). The mechanism of antimalarial action of [Au(CQ)(PPh(3))] PF(6): structural effects and increased drug lipophilicity enhance heme aggregation inhibition at lipid/water interfaces. *Journal of Inorganic Biochemistry* **105**, 276–282.

Navarro, M., Castro, W., Madamet, M., Amalvict, R., Benoit, N. and Pradines, B. (2014). Metal-chloroquine derivatives as possible anti-malarial drugs: evaluation of anti-malarial activity and mode of action. *Malaria Journal* **13**, 471.

Nilsson, S. K., Childs, L. M., Buckee, C. and Marti, M. (2015). Targeting human transmission biology for malaria elimination. *PLoS Pathogens* **11**, e1004871.

Parapini, S., Basilico, N., Pasini, E., Egan, T. J., Olliaro, P., Taramelli, D. and Monti, D. (2000). Standardization of the physicochemical parameters to assess *in vitro* the beta-hematin inhibitory activity of antimalarial drugs. *Experimental Parasitology* **96**, 249–256.

Peacock, A. F. and Sadler, P. J. (2008). Medicinal organometallic chemistry: designing metal arene complexes as anticancer agents. *Chemistry Asian Journal* **3**, 1890–1189.

Pérez, B. C., Teixeira, C., Albuquerque, I. S., Gut, J., Rosenthal, P. J., Gomes, J. R., Prudêncio, M. and Gomes, P. (2013). *N*-cinnamoylated chloroquine analogues as dual-stage antimalarial leads. *Journal of Medicinal Chemistry* **56**, 556–567.

Petersen, I., Eastman, R. and Lanzer, M. (2011). Drug-resistant malaria: molecular mechanisms and implications for public health. *FEBS Letters* **585**, 1551–1562.

Ploemen, I. H., Prudêncio, M., Douradinha, B. G., Ramesar, J., Fonager, J., van Gemert, G. J., Luty, A. J., Hermsen, C. C., Sauerwein, R. W., Baptista, F. G., Mota, M. M., Waters, A. P., Que, I., Lowik, C. W., Khan, S. M., Janse, C. J. and Franke-Fayard, B. M. (2009). Visualisation and quantitative analysis of the rodent malaria liver stage by real time imaging. *Plos ONE* **4**, e7881.

Price, R. N., von Seidlein, L., Valecha, N., Nosten, F., Baird, J. K. and White, N. J. (2014). Global extent of chloroquine-resistant *Plasmodium vivax*: a systematic review and meta-analysis. *Lancet Infectious Diseases* **14**, 982–991.

Prudêncio, M., Rodriguez, A. and Mota, M. M. (2006). The silent path to thousands of merozoites: the *Plasmodium* liver stage. *Nature Reviews Microbiology* **4**, 849–856.

Prudêncio, M., Mota, M. M. and Mendes, A. M. (2011). A toolbox to study liver stage malaria. *Trends in Parasitology* **27**, 565–574.

Prudêncio, M., Bringmann, G., Frischknecht, F. and Mueller, A. K. (2015). Chemical attenuation of Plasmodium in the liver modulates severe malaria disease progression. *Journal of Immunology*. **194**, 4860–4870.

Rajapakse, C. S., Martínez, A., Naoulou, B., Jarzecki, A. A., Suárez, L., Deregnaucourt, C., Sinou, V., Schrével, J., Musi, E., Ambrosini, G., Schwartz, G. K. and Sánchez-Delgado, R. A. (2009). Synthesis, characterization, and *in vitro* antimalarial and antitumor activity of new ruthenium(II) complexes of chloroquine. *Inorganic Chemistry* **48**, 1122–1131.

Rodrigues, T., Prudêncio, M., Moreira, R., Mota, M. M. and Lopes, L. (2012). Targeting the liver stage of malaria parasites: a yet unmet goal. *Journal of Medicinal Chemistry* **55**, 995–1012.

Salas, P. F., Herrmann, C., Cawthray, J. F., Nimphius, C., Kenkel, A., Chen, J., de Kock, C., Smith, P. J., Patrick, B. O., Adam, M. J. and Orvig, C. (2013). Structural characteristics of chloroquine-bridged ferrocenophane analogues of ferroquine may obviate malaria drug-resistance mechanisms. *Journal of Medicinal Chemistry* **56**, 1596–1613.

Sánchez-Delgado, R. A., Navarro, M., Pérez, H. and Urbina, J. A. (1996). Toward a novel metal-based chemotherapy against tropical diseases. 2. Synthesis and antimalarial activity *in vitro* and *in vivo* of new ruthenium- and rhodium-chloroquine complexes. *Journal of Medicinal Chemistry* **39**, 1095–1099.

Scovill, J. P., Klayman, D. L. and Franchino, C. F. (1982). 2-Acetylpyridine thiosemicarbazones. 4. Complexes with transition metals as antimalarial and antileukemic agents. *Journal of Medicinal Chemistry* **25**, 1261–1264.

Stone, W., Gonçalves, B. P., Bousema, T. and Drakeley, C. (2015). Assessing the infectious reservoir of falciparum malaria: past and future. *Trends in Parasitology* **31**, 287–296.

WHO Global Malaria Programme. *World Malaria Report (2015)*, World Health Organization, Geneva, 2015. http://apps.who.int/iris/bitstream/10665/200018/1/9789241565158_eng.pdf?ua=1

Supporting information

Table S1. Effects of ruthenium complexes on ECG parameters on *ex vivo* isolated rat hearts.

Compounds/ concentration (μg/mL)	Heart rate (bpm)	RR intervals (ms)	QT (ms)	sinus rhythm
Untreated	287±27	194	70±3	regular
(**MCQ**) 10	294±7	204	90±5	regular
(**MCQ**) 1.0	275±11	217	70±1	regular
(**MCQ**) 0.1	263±5	227	70±2	regular
(**FCQ**) 10	323±9	185	69±1	regular
(**FCQ**) 1.0	316±11	189	70±3	regular
(**FCQ**) 0.1	308±15	194	69±2	regular

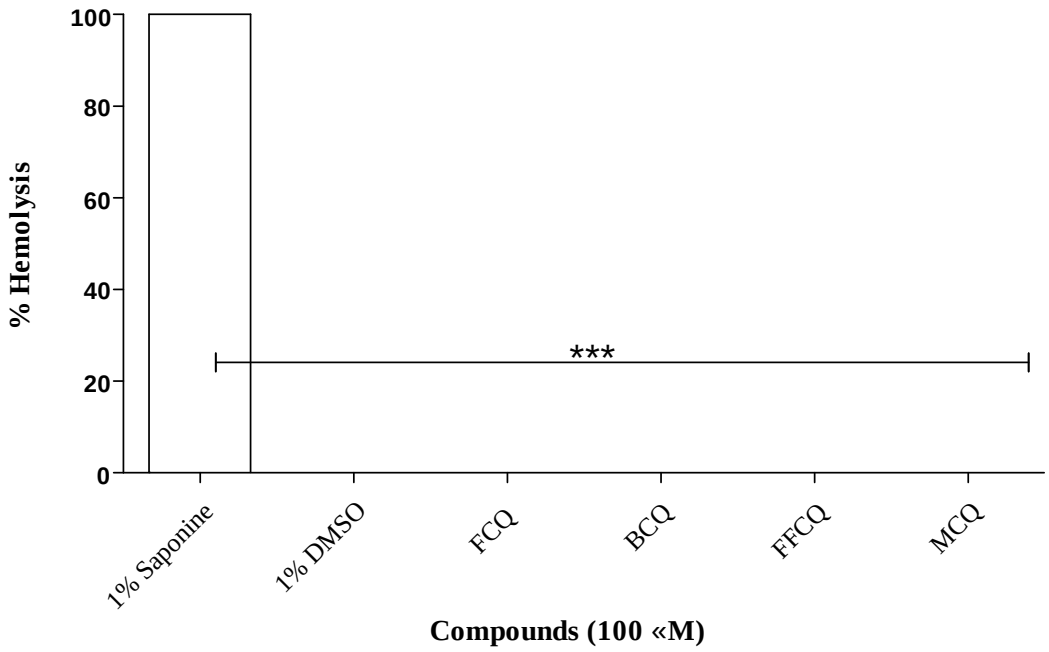

Figure S1: Percentage of hemolysis in uninfected erythrocytes after 1 h incubation with the compounds. ****p*<0.001 in comparison to Saponine.

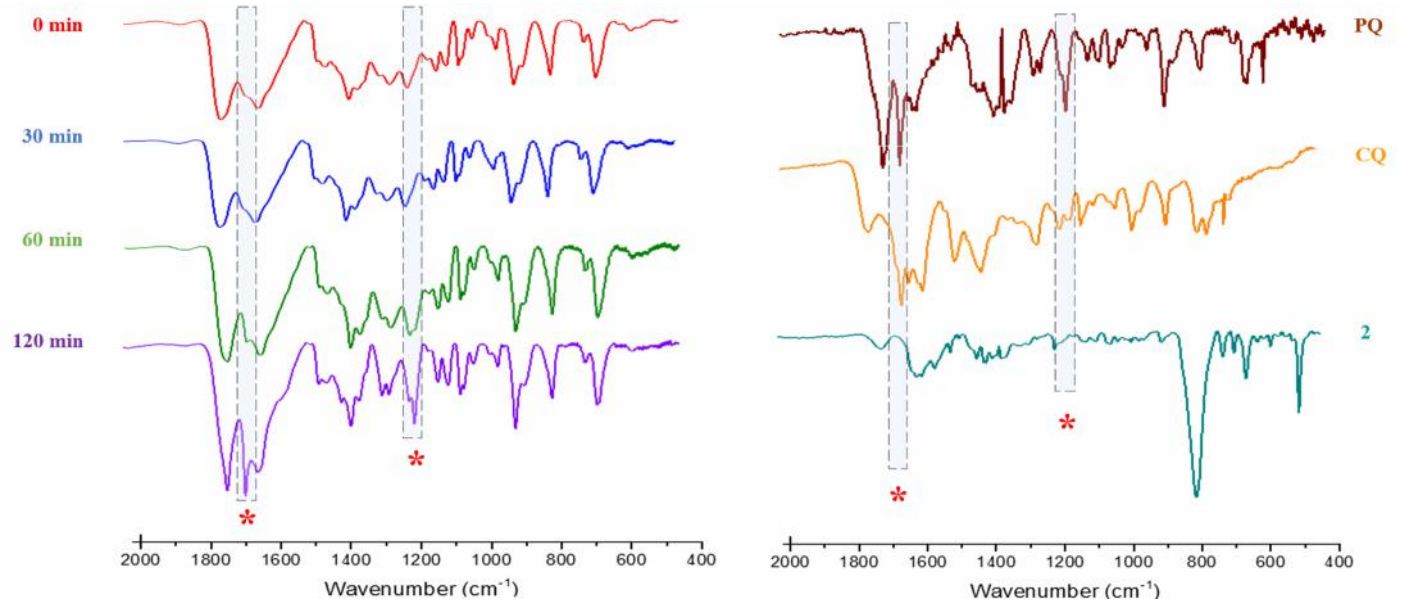

Figure S2. Fourier transform infrared spectroscopy of β-hematin formation. Left: solutions extracted in different times of formation without drug. Right: formation in presence of Primaquine (PQ), CQ or **FFCQ** complex (**2**). The characteristic peaks for iron-carboxylate bonds at 1.660 cm^{-1} and 1.210 cm^{-1} are highlighted with asterisks. Heme:Primaquine ratio 1:10; heme:CQ ratio 1:2; heme:**FFCQ** 1:2.

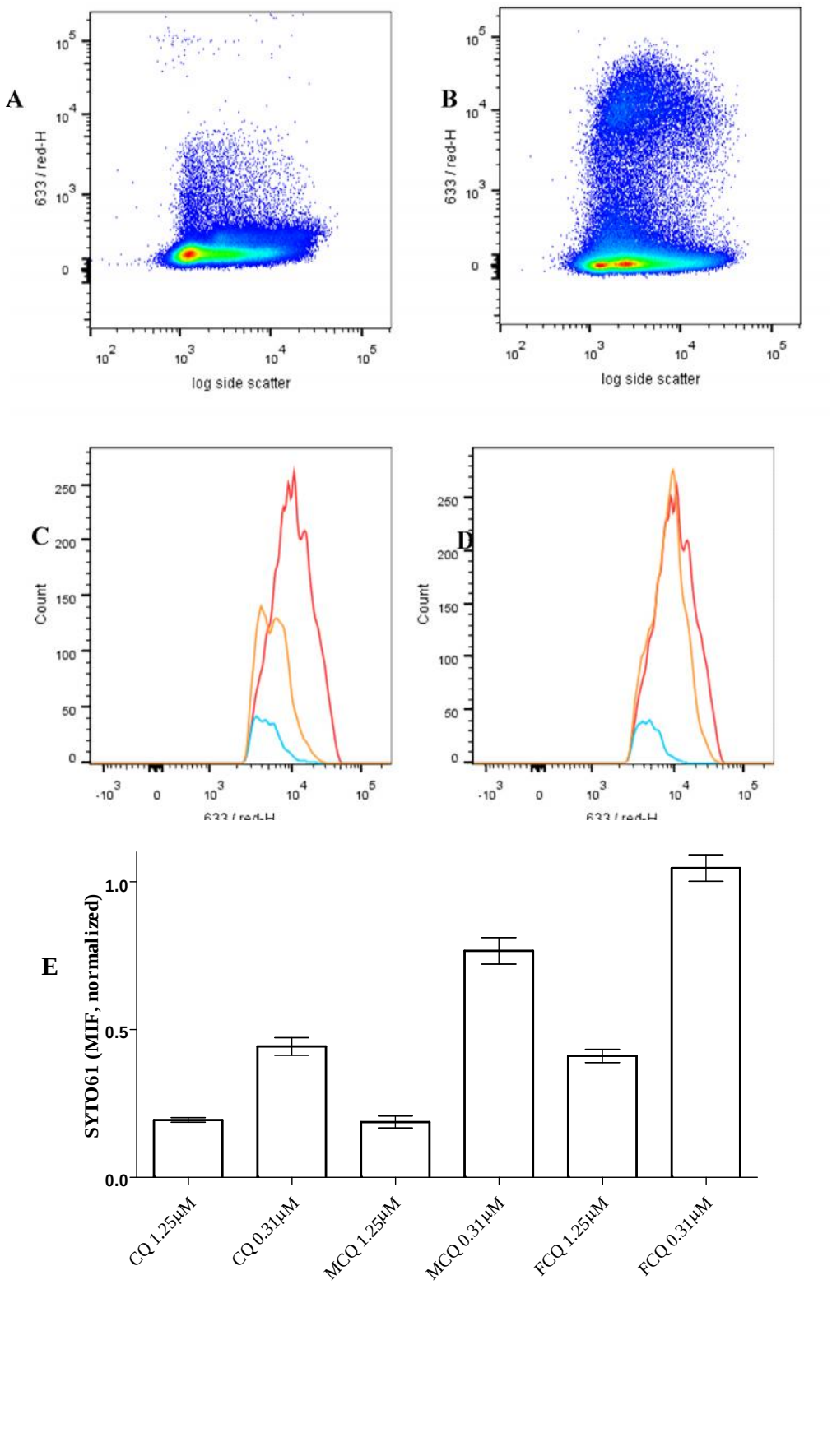
A
B
633 / red-H
log side scatter
C
D
Count
633 / red-H
E
SYTO61 (MIF, normalized)
1.0
0.5
0.0
CQ 1.25μM
CQ 0.31μM
MCQ 1.25μM
MCQ 0.31μM
FCQ 1.25μM
FCQ 0.31μM

Figure S3: 3D7 strain *P. falciparum* culture (2.5 % hematocrit, 2.0% parasitemia, ring stage) was labeled with SYTO 61 at 37ºC for 30 min. and analyzed by flow cytometry. Panel A: Uninfected erythrocytes. Panel B: Infected erythrocytes. Dot plots showing side scatter versus SYTO 61 staining (red fluorescence). Panel C: *P. falciparum* culture after 42 h incubation in absence (red curve) or presence of lethal (1.25 μM, blue) and sublethal (0.31 μM, orange) concentrations of Chloroquine. Panel D: *P. falciparum* culture after 48 h incubation in absence (red curve) or presence of lethal (1.25 μM, blue) and sublethal (0.31 μM, orange) concentrations of organoruthenium complex **MCQ**. Panel E: Median fluorescence intensity (MFI) obtained in *P. falciparum* culture after 48 h incubation in presence of compounds. MFI was normalized to untreated. Data correspond to mean ± standard deviation.

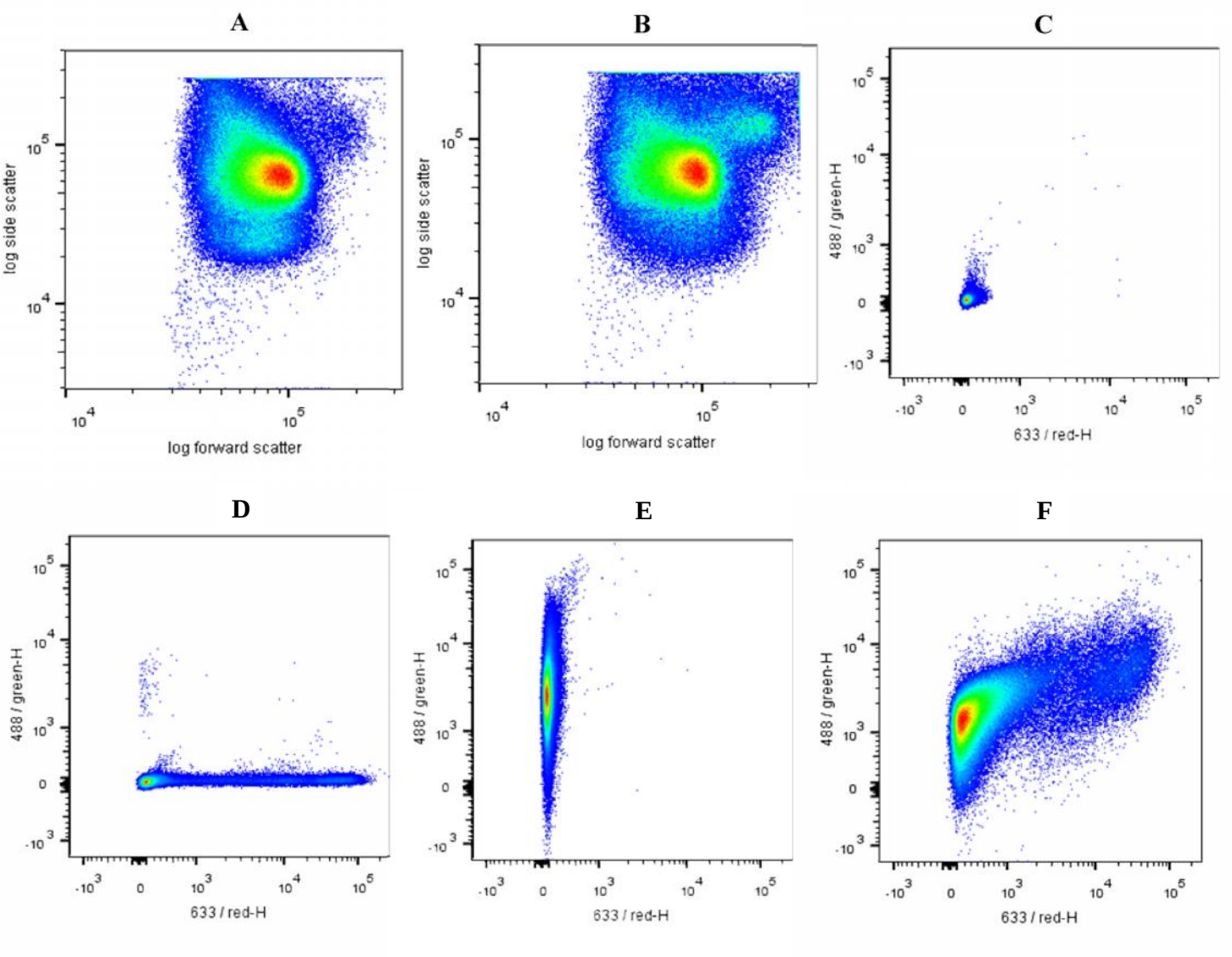

Figure S4: 3D7 strain *P. falciparum* trophozoites (3.0 % parasitemia, 1 % hematocrit) staining with CM-H2-DCFDA and analyzed by flow cytometry. Panel A: Uninfected erythrocytes. Panel B: infected erythrocytes. Ordinate shows side scatter and the abscissa displays forward scatter. Panels C-F: infected erythrocytes. Panel C: Unlabeled. Panel D: single labeling with SYTO 61. Panel E: single labeling with CM-H2-DCFDA. Panel F: double labeling SYTO 61 and CM-H2-DCFDA.

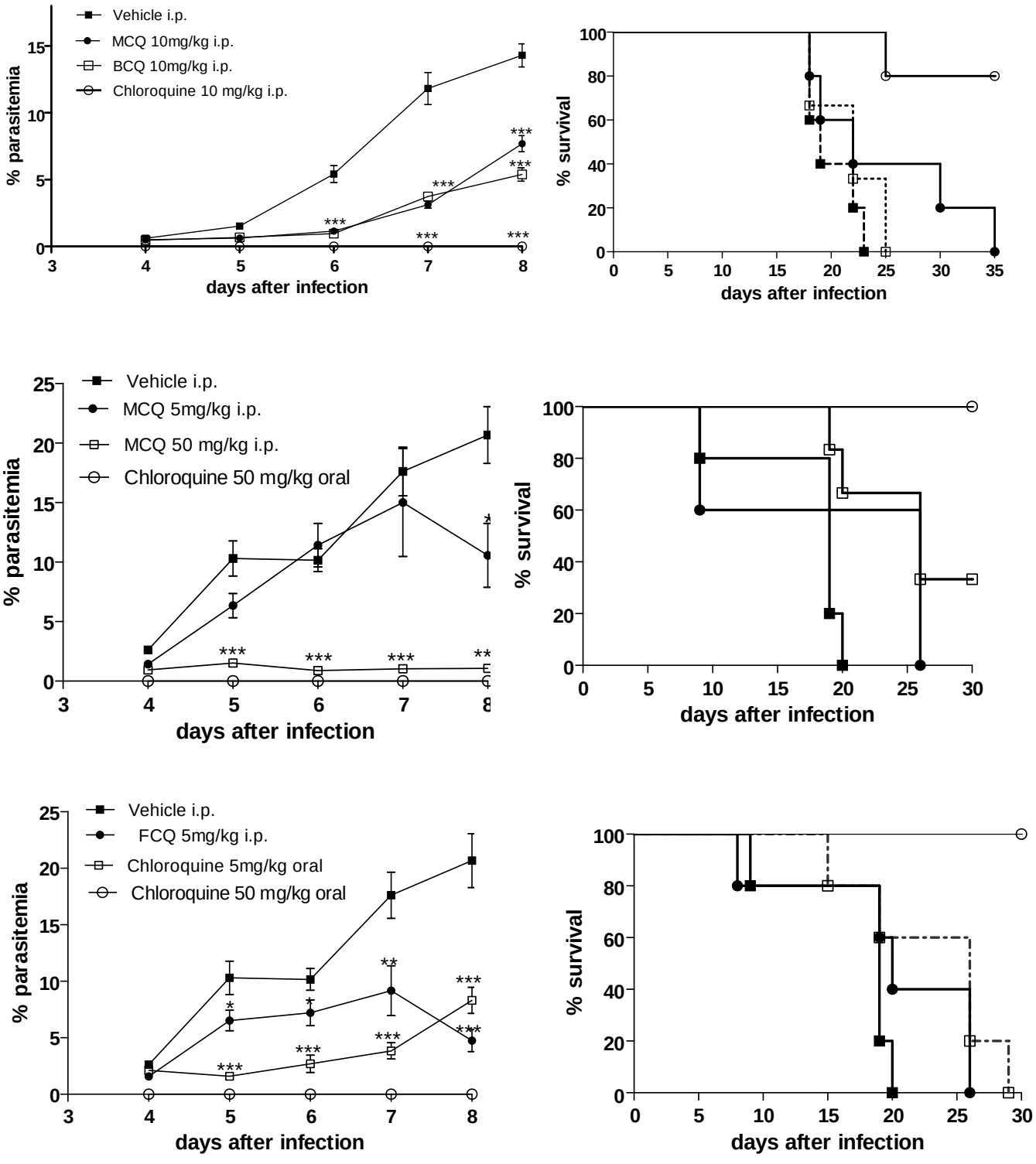

Figure S5: (*Left*) Blood parasitemia and (*Right*) survival in *P. berghei*-infected mice. Swiss Webster mice (n=5/group) were infected with *P. berghei* and treated daily for four consecutive days. Values represent the mean±S.E.M. of one experiment. *p<0.05; **p<0.01; ***p<0.001 in comparison to vehicle group.

4 ARTIGO 2

Taís S. Macedo, Wilmer J. V. Peña, Diogo R. M. Moreira, Camila C. Couto, Maribel Navarro, Marta Machado, Miguel Prudêncio, Alzir A. Batista, Milena B. P. Soares

Platinum(II)-chloroquine complexes are antimalarial agents against blood and liver stages by impairing with mitochondrial function, artigo a ser submetido ao periódico **Molecular and Biochemical Parasitology**.

O manuscrito descreve a atividade antimalárica de complexos metálicos de platina contendo cloroquina, em diferentes fases do parasita, bem como a análise do mecanismo de ação antiparasitária.

Platinum(II)-chloroquine complexes are antimalarial agents against blood and liver stages by impairing with mitochondrial function

Taís S. Macedo,[a‡] Wilmer J. V. Peña,[b‡] Diogo R. M. Moreira,[a] Camila C. Couto,[a] Maribel Navarro,[c] Marta Machado,[d] Miguel Prudêncio,[d] Alzir A. Batista,[b] Milena B. P. Soares[a,e*]

[a]*FIOCRUZ, Centro de Pesquisas Gonçalo Moniz, 40296-710, Salvador, BA, Brazil.*
[b]*UFSCAR, Departamento de Química, 13565-905, São Carlos, SP, Brazil.*
[c]*INMETRO, Xerém, 25250-020, Rio de Janeiro, RJ, Brazil.*
[d]*Instituto de Medicina Molecular, Faculdade de Medicina, Universidade de Lisboa, 1649-028 Lisboa, Portugal.*
[e]*Centro de Biotecnologia e Terapia Celular, Hospital São Rafael, 41253-190, Salvador, BA, Brazil.*

*Corresponding author: FIOCRUZ, Centro de Pesquisas Gonçalo Moniz, CEP 40296-710, Salvador, BA, Brazil. (+55)71-31762292; email: milena@bahia.fiocruz.br

[‡]Footnote: Taís S. Macedo and Wilmer J. V. Peña share first authorship.

SUMMARY

The identification of new antimalarial compounds presenting multistage activity is urgently needed. Chloroquine is a potent antimalarial agent against blood stage, but has no activity activity for the liver stage. In addition, the presence of parasite stains resistant to chloroquine has limited its clinical use. Previously, it was shown that platinum complexes composed of chloroquine and phosphine displayed stronger affinity to DNA and albumin than chloroquine. To investigate whether this class of platinum complexes has improved antimalarial activity, we examined the *in vitro* antimalarial activity of four platinum complexes containing chloroquine. The platinum complexes WV-90, WV-92, WV-93, WV-94 presented activity similar to chloroquine against the blood stage of two strains of *Plasmodium falciparum*. In addition, the selectivity index of these complexes was also of similar range, being WV-90 and WV-93 those of higher indexes. Regarding the mechanism of action against blood stages, complexes incubated for 4 h did not elevate the production of reactive oxygen species. However, when incubated for 24 h, we observed that complexes inhibited mitochondrial viability, while 48 h after incubation, loss of mitochondrial viability and an initial reduction of parasite integrity were observed. In addition, complexes inhibited the polymerization of hemin into β-hematin at the same order of potency when compared to chloroquine. In agreement to this, we showed that platinum complexes are able to interrupt the intraerythrocytic parasite cycle as well as exert parasiticidal property against trophozoites. Against liver stage of *P. berghei*, complex WV-93 presented activity, while chloroquine is inactive at the same concentration range. Importantly, WV-90 given intraperitoneally at 25 mg/kg has reduced parasitemia in *P. berghei*-infected mice. In conclusion, we demonstrated that platinum complexes containing chloroquine are endowed with *in vitro* and *in vivo* antiparasitic activities, which are achieved by inhibiting β-hematin formation and mitochondrial function.

Keywords: Malaria, *Plasmodium falciparum, Plasmodium berghei,* chloroquine, platinum, mitochondria.

1.0 INTRODUCTION

Malaria is a widespread infectious disease caused by five *Plasmodium* parasite species, which affect in special the Sub-Saharan Africa, Southeast Asia and Latin America populations [1]. The employment of insecticide-treated bed nets in epidemic areas [2,3], along with a rapid diagnosis [4] and the implementation of artemisinin-based combination therapies [5,6] have substantially decreased the spread of disease in the last three decades. However, reports of decreasing parasite sensitivity to artemisinin- therapy, mainly in the Southeast Asia [7], support the urgency to the development of novel antimalarial drugs.

In the antimalarial drug discovery, two well-established therapeutic targets are the hemoglobin-derived Fe(III)-protoporphyrin IX (heme) [8-10] and the mitochondrial electron transport chain [11]. Crystallization of heme into the insoluble pigment hemozoin takes place in the digestive vacuole of trophozoites [8-10]. Chloroquine and other 4-aminoquinolines, such as mefloquine and amodiaquine, achieve antiparasitic activity by impairing the hemozoin biosynthesis. An important advantage of this target is its absence in humans. Given the fact that hemozoin formation is restricted to the blood stage, antimalarial drug discovery based on hemozoin inhibitors result in compounds with a limited spectrum of action [9].

The mitochondrial electron transport chain of *Plasmodium* sp. is its only way to regenerate ubiquinone (coenzyme Q10), making this pathway crucial for parasite survival [11] not only in the blood but also against liver and sexual parasite stages [12]. Electron transport chain is mainly composed of cytochrome *bc*1 complex III and dihydroorotate dehydrogenase [11]. The naphthoquinone atovaquone, an approved antimalarial drug, achieves activity by blocking *bc*1 complex of the mitochondrial electron transport chain of *Plasmodium* sp. [13,14].

In recent years, the discovery of novel antimalarial agents endowed with multiple-stages activity has been possible, in part by approaching these two therapeutic targets [15,16]. Regarding the chemical structure, quinolones and quinones are very often employed within drug design, giving successful antimalarial drug candidates with multiple-stages properties [15,16]. In fact, drug design of aminoquinoline derivatives, including chloroquine, has shown the possibility of modifying the structure of this class of compounds seeking improvement of action spectrum [17-22]. In this line of research, we recently showed that organoruthenium complexes containing chloroquine in their composition presented *in vitro* and *in vivo* antimalarial activity. These organoruthenium complexes affected trophozoites by inhibiting hemozoin formation and producing reactive oxygen species but,

unlike chloroquine, they exhibited fast parasiticidal activity against blood stage and reduced gametocytes viability [23]. To advance the knowledge of antiparasitic metal complexes, here we examined a new class of platinum complexes composed of chloroquine and phosphine in their composition. We demonstrate that these platinum complexes are antiparasitic agents, inhibit β-hematin formation and mitochondrial function. Importantly, complexes presented superior activity against liver parasites than chloroquine.

2.0 MATERIALS AND METHODS

2.1 Drugs and dilutions: Platinum complexes containing chloroquine (**WV-90, WV-92, WV-93, WV-94**) and a complex lacking chloroquine (**WV-48**) were prepared as described in the literature [24]. All manipulations were carried out under argon using common Schlenk techniques. Solvents were purified by standard procedures immediately prior to use. Chloroquine, mefloquine and artesunate were supplied by FarManguinhos (Rio de Janeiro, Brazil). Primaquine was purchased from Sigma-Aldrich (St. Louis, MO). All drugs were dissolved in DMSO (PanReac, Barcelona, Spain) prior to use, and then diluted in culture medium. The final concentration of DMSO was less than 0.5 % in all *in vitro* experiments.

2.2 Animals: Male Swiss Webster mice (4–6 weeks), housed at Centro de Pesquisas Gonçalo Moniz (Fundação Oswaldo Cruz, Bahia, Brazil), were maintained in sterilized cages under a controlled environment, receiving a rodent balanced diet and water *ad libitum*. All experiments were carried out in accordance with the recommendations of Ethical Issues Guidelines and were approved by the local Animal Ethics Committee (protocol number 016/2013).

2.3 Cell culture: CQ-sensitive 3D7 and CQ-resistant W2 strains of *P. falciparum,* NK65 strain of *P. berghei* as well as transgenic *P. berghei* sporozoites expressing green fluorescent protein (GFP) and firefly luciferase (Luc), (*Pb*GFP-Luccon, parasite line 676m1cl1) were used here. *P. falciparum* was cultivated in human O^+ erythrocytes (donated by HEMOBA, Salvador, Brazil) at 5 % hematocrit with daily maintenance in Roswell Park Memorial Institute medium (RPMI-1640, Sigma-Aldrich) supplemented with 10 % v/v human plasma (donated by HEMOBA, Salvador, Brazil), 25 mM HEPES (ChemCruz, Dallas, TX), 300 μM hypoxanthine (MP Biomedicals, Santa Ana, CA), 11 mM glucose (Sigma-Aldrich) and 20 μg/mL of gentamicin (Life, Carlsbad, CA). Five days prior to use,

P. falciparum was cultivated without hypoxanthine and synchronized to rings by 5 % D-sorbitol (USB, Santa Clara, CA). J774 macrophages were cultured in Dulbecco′s modified Eagle′s medium (DMEM) (Sigma-Aldrich) supplemented with 10 % heat-inactivated fetal bovine serum (FBS, Gibco, Gaithersburg, MD) and 50 µg/mL of gentamicin (Life). Hepatocellular carcinoma cells (HepG2 and Huh7) were cultivated in RPMI supplemented with 10 % heat-inactivated FBS (Gibco) and 50 µg/mL of gentamicin (Life).

2.4 Mammalian cell toxicity: HepG2 or J774 cells were seeded in 100 µL of RPMI and DMEM, respectively, at 1×10^4 cells/mL in 96-well plates. Drugs were added 24 h later in a volume of 100 µL suspended in medium and the plates were incubated for 72 h at 37 ^oC and 5 % CO_2. Drugs were tested in eight concentrations (150-0.78 µM), each one in triplicate. Gentian violet (Synth) was used as positive control, while untreated cells were employed as negative controls. Then, 20 µL of AlamarBlue (Life) were added and incubated for 24 h. Colorimetric readings were performed at 570 and 600 nm using SpectraMAx 190 instrument (Molecular Devices, Sunnyvale, CA). CC_{50} values were calculated using data-points gathered from three independent experiments.

2.5 Hemolysis assay: fresh uninfected human O^+ erythrocytes were washed three-times with sterile phosphate-buffered saline (PBS), adjusted for 1 % hematocrit and 100 µL dispensed in a 96-well round bottom plate. Then, 100 µL of drugs previously in DMSO and suspended in PBS were dispensed in the respective wells. Each drug was tested in four concentrations (100-0.1 µM) assayed in triplicate. Untreated cells received 100 µL of PBS containing 0.5 % DMSO (negative control), while positive controls received saponin (Sigma-Aldrich) at 1 % v/v. Plates were incubated for 1 h at 37 ^oC under 5 % CO_2. Plates were centrifuged at 1500 rpm for 10 min and 100 µL of supernatant were transferred to another plate, in which absorbance at 540 nm was measured using a SpectraMax 190 instrument. The percentage of hemolysis was calculated in comparison to positive and negative controls, and plotted against drug concentration generated using GraphPad Prism 5.01. One experiment was performed.

2.6 Cytostatic activity against intraerythrocytic *P. falciparum*: One hundred µL of rings at 1 % parasitemia and 2.5 % hematocrit in RPMI were dispensed in a 96-well round bottom plate. Then, 100 µL of drugs (4.0-0.003 µM) previously suspended in RPMI were dispensed in the respective wells. Each drug was tested in triplicate, in seven different concentrations. Untreated parasite samples

received 100 µL of medium containing 0.5 % DMSO. Chloroquine and mefloquine were used as positive controls. Plates were incubated for 24 h at 37 ^{o}C under 3 % O_2, 5 % CO_2 and 91 % N_2 atmosphere. Then, 25 µL of tritiated hypoxanthine (0.5 µCi/well, PerkinElmer, Shelton, CT) in RPMI was added to each well and incubated for 24 h. Plates were frozen at -20 ^{o}C and subsequently thawed and the contents transferred to UniFilter-96 GF/B PEI coated plates (PerkinElmer) using a cell harvester. After drying, 50 µL of scintillation cocktail (MaxiLight, Hidex, Turku, Finland) was added in each well, sealed and plate read in a liquid scintillation microplate counter (Chameleon, Turku, Finland). The % of inhibition was determined in comparison to untreated and inhibitory concentration for 50 % (IC_{50}) values were determined by using non-linear regression with Logistic equation available at OriginPro 8.5. Three independent experiments were performed.

2.7 Cytocidal activity against intraerythrocytic *P. falciparum*: One hundred µL of trophozoites at 2 % parasitemia and 3.0 % hematocrit in RPMI were dispensed in a 96-well round bottom plate. Then, 100 µL of drugs (10-0.07 µM) previously suspended in RPMI were added to the respective wells. Each drug was tested in seven concentrations, each one in triplicate. Untreated parasites received 100 µL of medium containing 0.5 % DMSO, artesunate was used as positive control. Plates were incubated for 18 h at 37 ^{o}C under 3 % O_2, 5 % CO_2 and 91 % N_2 atmosphere. The plate was centrifuged three times with 200 µL of drug-free medium at 1500 rpm for 5 min, then 200 µL of media containing tritiated hypoxanthine was added and plate incubated for 48 h. Plates were frozen at -20 ^{o}C and thawed and transferred to UniFilter-96 GF/B PEI coated plates (PerkinElmer) using of a cell harvester. After drying, 50 µL of scintillation cocktail was added in each well, sealed and plate read at liquid scintillation microplate counter. IC_{50} values were determined employing non-linear regression with Logistic equation available in the OriginPro 8.5 software. Minimal parasiticidal concentration (MPC) was determined as the concentration that reduces parasite growth by 99±1.0 %. At least three independent experiments were performed.

2.8 Activity in the intraerythrocytic *P. falciparum* cycle: A volume of 100 µL of trophozoites of *P. falciparum* W2 strain at 2 % parasitemia and 2.5 % hematocrit in RPMI was dispensed per well in 96-well round bottom plates. Then, 100 µL of drugs previously suspended in RPMI were added to the respective wells. Each drug concentration was tested in triplicate. Untreated parasite received 100 µL of medium containing 0.5 % DMSO. Plates were incubated for 48 h at 37 ^{o}C under 3 % O_2, 5 % CO_2, 91 % N_2 atmosphere followed by centrifugation three times with 200 µL of drug-free medium

at 1500 rpm for 5 min. A volume of 200 µL of media containing drugs were added and plates were incubated for additional 48 h. Thin blood smears were then prepared, fixed and stained with quick panoptic stain (Laborclin, Pinhais, Brazil). Slides were observed in an optical microscope (CX41, Olympus, St. Louis, MO). The number of rings, trophozoites and schizonts were counted in at least 1500 cells per slide (*n*=4) and plotted against drug concentration generated using GraphPad Prism 5.01. Two independent experiments were performed.

2.9 Activity against *P. berghei* liver stages: inhibition of liver-stage infection by test compounds was determined by measuring the luminescence intensity in Huh-7 cells infected with a firefly luciferase-expressing *P. berghei* line as previously described [25]. For infection assays, Huh-7 cells (1.0×10^4 per well) were seeded in 96-well plates the day before drug treatment and infection. The medium was replaced by medium containing the appropriate concentration of each compound approximately 1 h prior to infection with sporozoites freshly obtained through disruption of salivary glands of infected female *Anopheles stephensi* mosquitoes. An amount of the DMSO solvent equivalent to that present in the highest compound concentration was used as control. Sporozoite addition was followed by centrifugation at 1700 g for 5 min. Parasite infection load was measured 48 h after infection by a bioluminescence assay (Biotium, Hayward, CA). The effect of the compounds on the viability of Huh-7 cells was assessed by the AlamarBlue assay (Life) using the manufacturer's protocol.

2.10 Assessment of inhibition of -hematin formation by UV-Vis spectroscopy: The assay was performed according to the method previously described in the literature [26]. A solution of hemin chloride (50 µl, 0.5 mg/mL) dissolved in NaOH 0.2 M was distributed in 96-well plates. Each complex was dissolved in DMSO and added in triplicate (50 µL) to a final concentration of 2 mM. Control contained water or DMSO. The formation of β-hematin was initiated by addition of acetic acid (25 µL, 17.4 M, pH 4.4). The plates were incubated at 37 ° C for 24 h and then centrifuged. After removing the supernatant, the solid was washed twice with DMSO and finally dissolved in NaOH (150 µl, 0.1 M). After diluting, absorbance was measured at 405 nm in a spectrophotometer. The inhibition of β-hematin was calculated in comparison to negative control, plotted against drug concentration generated using GraphPad Prism 5.01. Three independent experiments were performed.

2.11 CM-H2-DCFDA staining of *P. falciparum*: A volume of 100 µL of trophozoites of *P. falciparum* 3D7 strain at 3.0 % parasitemia and 1.0 % hematocrit in RPMI were dispensed per well in a 96-well round bottom plate. A volume of 25 µL of CM-H2-DCFDA (Life) at 15 µM suspended in media was added to each well and incubated in the dark for 20 min. Then, 100 µL of drugs previously suspended in RPMI were added to the respective wells. Each drug concentration was tested in triplicate. Untreated parasites received 100 µL of medium containing 0.5 % DMSO. Plates were incubated for 3.5 h at 37 ^{o}C under 3 % O_2, 5 % CO_2, 91 % N_2 atmosphere. Plates were centrifuged at 1500 rpm for 5 min, supernatant was discarded and 200 µL of isoton diluent was added and samples were analyzed in a flow cytometer (LSRFortessa, BD). Gate of infected cells was determined in comparison to uninfected control. At least 200.000 events were acquired in the fluorescein isothiocyanate channel (488, 585 nm) for CM-H2-DCFDA. The analysis was performed using FlowJo (LLC), in three independent experiments.

2.12 Double mitotracker and SYBR staining of *P. falciparum*: 100 µL of trophozoites of *P. falciparum* 3D7 strain at 2 % parasitemia and 1.0 % hematocrit in RPMI were dispensed in a 96-well round bottom plate. Then, 100 µL of drugs previously suspended in RPMI were added to the respective wells. Each drug concentration was tested in triplicate. Untreated parasite received 100 µL of medium containing 0.5 % DMSO. Plates were incubated for 24 h and 48 h at 37 ^{o}C under 3 % O_2, 5 % CO_2, 91 % N_2 atmosphere. Plate was centrifuged with 200 µL of drug-free medium at 1500 rpm for 5 min and then 150 µL of mitotracker deep red FM (Life) at 5.0 µM and SYBRgreenI (at 2.5x suspended in medium) were added to each well and incubated in the dark for 30 min. After washing and adding 400 µL of isoton diluent, samples were analyzed in a flow cytometer (LSRFortessa, BD, Franklin Lakes, NJ). The gate of infected cells was determined in comparison to uninfected control. At least 200.000 events were acquired in the allophycocyanin channel (633, 660 nm) for mitotracker and fluorescein isothiocyanate channel (488, 585 nm) for SYBR. The analysis was performed using FlowJo (LLC, Ashland, Covington, LA). Three independent experiments were recorded.

2.13 *In vivo* blood schizontocidal activity: Male Swiss Webster mice (4-6 weeks) were infected by intraperitoneal injection of 10^6 NK65 strain *P. berghei*-infected erythrocytes and randomly divided into groups of n=5. Each drug was solubilized in DMSO/saline (20:80 v/v) prior to administration. Treatment was initiated within 1-3 h post infection and given daily for four consecutive days by intraperitoneal injection of 100 µL. Chloroquine-treated mice were used as positive control group,

while untreated infected mice were used as negative control group. The following parameters were evaluated: parasitemia counted at 4, 5, 6, 7 and 8 days post-infection and 30 days post-infection animal survival. The % of parasitemia reduction was calculated as follows: [mean vehicle group − mean treated group/mean vehicle group] × 100%. One experiment was performed.

2.14 Statistical analyses: Nonlinear regression analysis was used to calculate CC_{50} and IC_{50} values by using GraphPad Prism version 5.01 (Graph Pad Software, San Diego, USA), OriginPro version 8.5 (OriginLab, Northampton, USA). One-way ANOVA analysis and Bonferroni multiple comparison tests were used. Results were considered statistically significant when $p < 0.05$ as analyzed by GraphPad Prism version 5.01. Log-rank (Mantel-Cox) test was employed for survival analysis.

3.0 RESULTS

The structures of platinum complexes containing chloroquine are shown in **Figure 1**. Complex **WV48** is the chemical precursor of complex **WV90** but without chloroquine in its composition. *In vitro* antiparasitic activity was firstly performed against blood stage of 3D7 and W2 strains of *P. falciparum* and activity was expressed as mean IC_{50} values. In parallel, *in vitro* cytotoxicity was performed in J774 and HepG2 linages, and activity was expressed as mean CC_{50} values. Selectivity indexes were calculated for both parasite strains versus J774 lineage. All these values are summarized in **Table 1**.

Chloroquine had an IC_{50} value of 0.11±0.035 μM against sensitive 3D7 strain. In comparison to chloroquine, platinum complexes WV-90 and WV-93 were twice less active, while WV92 and WV94 were four times less active. In contrast, WV48 did not inhibit parasite growth up to 2.0 μM. Against resistant W2 strain, chloroquine had an IC_{50} value of 0.43±0.09 μM. Platinum complexes WV-90 and WV-94 were as active as chloroquine, while WV-92 and WV-93 were twice less active. WV48 also did not inhibit parasite growth up to 2.0 μM against W2 strain. Regarding cytotoxicity, gentian violet displayed CC_{50} values of 14.2±0.3 and 4.3 ±0.8 μM. Platinum complexes and chloroquine were less cytotoxic than gentian violet. In comparison to Chloroquine, platinum complex WV-93 was equally cytotoxic to J774 lineage, while other platinum complexes were approximately twice more cytotoxic. Selectivity indexes revealed that none platinum complexes were as selective

as chloroquine. Among the platinum complexes, WV90 and WV93 were the most selective ones and were further investigated.

To examine the activity of platinum complexes on intraerythrocytic cell cycle, synchronous cultures of *P. falciparum* 3D7 was incubated for 48 and 96 h in presence of approximately twice the IC_{50} of the compound. Growth of all three asexual erythrocytic forms (rings, trophozoites and schizonts) was quantified by microscopy and results were compared to untreated controls. **Figure 2** shows that untreated parasites developed from rings to trophozoites and to schizonts, while mefloquine inhibited development of ring into trophozoites. After 48 h incubation, treatment with WV90 did not inhibit parasite cell cycle, while in contrast treatment with WV93 or chloroquine delayed parasite development. Treatment with WV90 for 96 h caused a delay in parasite cycle, remaining only few viable parasites at ring stage. In contrast, WV93 or chloroquine treatment completely abrogated cell cycle.

Next, the *in vitro* parasiticidal activity was determined in parasites synchronized into trophozoites stage and incubated for 18 h in the presence of drugs. After this period of exposure, the compound was removed by extensive washing and was quantified by hypoxanthine incorporation relative to untreated controls. Activity was expressed as mean LC_{50} and MPC values. Artesunate presented LC_{50} values of 0.0053±0.00032 and 0.0049±0.0009 μM against 3D7 and W2 strains, respectively. In comparison to artesunate, chloroquine and platinum complexes WV90 and WV93 were less potent parasiticidal agents. Chloroquine was more active than platinum complexes, and presented similar parasiticidal activity for both strains. However, platinum complex WV90 at concentration range of 5.0-8.0 μM was able in eliminate parasitemia, while chloroquine did not (**Table 2**). Importantly, platinum complex WV90 did not induce hemolysis in concentration below 12.5 μM (**Figure 3**), showing a parasite clearance activity without affecting host cells.

Given that platinum complexes exhibited parasiticidal activity against trophozoites, where hemozoin formation takes place, we investigated whether platinum complexes inhibit polymerization of heme into hemin. **Table 3** shows that chloroquine inhibits hemin formation with an IC_{50} of 0.6±0.2 mM, while WV48 did not inhibit hemin formation in concentrations up to 2.0 mM. All chloroquine-platinum complexes inhibited polymerization of heme with potency similar to that of chloroquine. Considering that there was no difference of hemin inhibitory activity among complexes, this led us to think that other mechanisms are involved in the antiparasitic activity.

The ability of platinum complexes in inducing oxidative stress in trophozoites was studied by flow cytometry using CM-H2-DCFDA, a general probe for reactive oxygen species. **Figure 4** shows

that, in comparison to untreated trophozoites, chloroquine at 0.6 μM increased the content of reactive oxygen species. At the same concentration, neither WV90 nor WV93 increased reactive oxygen species. Therefore, in contrast to chloroquine, which inhibits hemozoin formation leading to accumulation of toxic heme and generating an oxidative stress insult, platinum complexes inhibit hemozoin formation, but heme accumulation was not followed by oxidative stress. It has been reported that heme can be decomposed by glutathione present in the host cells [27], which may explain the escape of the parasite to the heme toxic insult. Interestingly, previous investigated ruthenium complexes presenting chloroquine induced oxidative stress in similar conditions. This shows us that the nature of transition metal result in different pharmacological profile [23], which is also a similar finding observed in the literature [28,29]

Based on the fact that chloroquine also acts on lysosomal enzymes and coenzyme Q, involved in mitochondrial function [30,31], we studied the effect of platinum complexes on parasite mitochondrial viability. To this end, untreated and treated trophozoites were co-stained with MitoTracker deep red (probe for mitochondria) and SYTO 61 (DNA staining) and analyzed by flow cytometry (**Figure 5**). In comparison to untreated parasites, treatment with 2.5 μM of chloroquine or WV90 for 24 h incubation reduced in approximately 50 % mitochondria staining. This effect was not followed by reduction of parasitemia, as observed by SYTO 61 staining. When parasites were incubated for 48 h, reduction in both mitochondria viability and parasitemia were observed under treatment with 2.5 μM of chloroquine or WV90. At 0.6 μM concentration of chloroquine or WV90, the reduction of mitochondria staining was greater than the reduction in parasitemia. These effects were not observed under treatment with WV48 complex. These results suggest that the initial action of platinum complexes is by affecting mitochondrial function inducing mitophagy and interfering on the mitochondrial electron transport chain of the parasite.

After ascertaining activity against blood stage, the activity of platinum complexes on liver stage was studied in Huh-7 cells infected by sporozoites of *P. berghei* (**Figure 6**). In comparison to untreated control, treatment with WV90 complex did not inhibit parasite load at the concentrations tested. In contrast, WV93 reduced in 50 % parasite load at 10 μM without affecting viability of Huh-7 cells. In regard to parasite load, calculated IC_{50} for WV93 complex was of 10.88 ± 0.68 μM. For comparison, primaquine and chloroquine presented IC_{50} of 10 and 15 μM, respectively.

Finally, we studied the efficacy of complex WV90 in *P. berghei*-infected mice. By using a 4-day treatment test in *P. berghei*-infected mice, parasitemia suppression and survival rate were evaluated in comparison to untreated infected mice (vehicle). Chloroquine was used as the reference

drug (**Figure 7**). On day 8 post-infection, chloroquine at 10 mg /kg of animal weight reduced in 100 % the parasitemia and conferred 80 % protection in animal survival. Treatment with 25 mg/kg **WV90** caused a 46 % reduction in parasitemia in comparison to untreated group, but did not protect against mortality, as observed 30 days post-infection, therefore having an inferior *in vivo* efficacy than chloroquine.

4.0 CONCLUSION

The incorporation of chloroquine into platinum compounds produced antiparasitic agents against *Plasmodium*. These complexes presented classical properties like chloroquine, such as activity against blood stage and inhibitory activity in β-hematin. However, unlike chloroquine, platinum complexes did not induce oxidative stress but they reduced parasite load in the liver stage. Both chloroquine and WV90 impaired mitochondrial activity, although a more pronounced effect was observed under platinum complex treatment. Complex WV90 had in vivo efficacy in mice but lower than Chloroquine. Further experiments are under progress to full investigate the efficacy and underlying mechanism of action of this class of compounds.

5.0 ACKNOWLEDGEMENTS

We are thankful to the flow cytometry facility of CPqGM (Brazil).

6.0 FINANCIAL SUPPORT

This research was funded by FAPESB (grant PET0042/2013, Brazil), FAPESP (grant 14/10516-7, Brazil) and Fundação para a Ciência e Tecnologia (grant PTDC/SAU-MIC/117060/2010 Portugal). A.A.B. and M.B.P.S. are recipients of senior fellowships by CNPq (Brazil).

7.0 REFERENCES

[1] Cibulskis RE, Alonso P, Aponte J, Aregawi M, Barrette A, Bergeron L, Fergus CA, Knox T, Lynch M, Patouillard E, Schwarte S, Stewart S, Williams R. Malaria: Global progress 2000 - 2015 and future challenges. Infect. Dis. Poverty. 2016; 5:61. Doi: 10.1186/s40249-016-0151-8.

[2] Willey BA, Paintain LS, Mangham L, Car J, Schellenberg JA. Strategies for delivering insecticide-treated nets at scale for malaria control: a systematic review. Bull. World Health Organ. 2012; 90:672-684E. Doi: 10.2471/BLT.11.094771.

[3] Wilson AL, Dhiman RC, Kitron U, Scott TW, van den Berg H, Lindsay SW. Benefit of insecticide-treated nets, curtains and screening on vector borne diseases, excluding malaria: a systematic review and meta-analysis. PLoS Negl. Trop. Dis. 2014; 8:e3228. Doi: 10.1371/journal.pntd.0003228.

[4] Kyabayinze DJ1, Asiimwe C, Nakanjako D, Nabakooza J, Counihan H, Tibenderana JK. Use of RDTs to improve malaria diagnosis and fever case management at primary health care facilities in Uganda. Malar. J. 2010; 9:200. Doi: 10.1186/1475-2875-9-200.

[5] Tilley L, Straimer J, Gnädig NF, Ralph SA, Fidock DA. Artemisinin action and resistance in *Plasmodium falciparum*. Trends Parasitol. 2016; in press. Doi: 10.1016/j.pt.2016.05.010.

[6] Lucchi NW, Komino F, Okoth SA, Goldman I, Onyona P, Wiegand RE, Juma E, Shi YP, Barnwell JW, Udhayakumar V, Kariuki S. In vitro and molecular surveillance for antimalarial drug resistance in *Plasmodium falciparum* parasites in western Kenya reveals sustained artemisinin sensitivity and increased chloroquine sensitivity. Antimicrob. Agents Chemother. 2015; 59:7540-7. Doi: 10.1128/AAC.01894-15.

[7] Pyae Phyo A, Ashley EA, Anderson TJ, Bozdech Z, Carrara VI, Sriprawat K, Nair S, White MM, Dziekan J, Ling C, Proux S, Konghahong K, Jeeyapant A, Woodrow CJ, Imwong M, McGready R, Lwin KM, Day NP, White NJ, Nosten F. Declining efficacy of artemisinin combination therapy against *P. falciparum* malaria on the Thai-Myanmar border (2003-2013): the role of parasite genetic factors. Clin. Infect. Dis. 2016, in press.

[8] Egan TJ, Ross DC, Adams PA. Quinoline anti-malarial drugs inhibit spontaneous formation of beta-haematin (malaria pigment). FEBS Lett. 1994; 352:54-57. Doi: 10.1016/0014-5793(94)00921-X

[9] Weissbuch I, Leiserowitz L. Interplay between malaria, crystalline hemozoin formation, and antimalarial drug action and design. Chem. Rev. 2008; 108:4899-4914. Doi: 10.1021/cr078274t.

[10] Egan TJ. Recent advances in understanding the mechanism of hemozoin (malaria pigment) formation. J. Inorg. Biochem. 2008; 102:1288-1299. Doi: 10.1016/j.jinorgbio.2007

[11] Krungkrai J. The multiple roles of the mitochondrion of the malarial parasite. Parasitology 2004; 129:511-524. Doi: 10.1017/S0031182004005888

[12] Stickles AM, Ting LM, Morrisey JM, Li Y, Mather MW, Meermeier E, Pershing AM, Forquer IP, Miley GP, Pou S, Winter RW, Hinrichs DJ, Kelly JX, Kim K, Vaidya AB, Riscoe MK, Nilsen A. Inhibition of cytochrome bc1 as a strategy for single-dose, multi-stage antimalarial therapy. Am. J. Trop. Med. Hyg. 2015; 92:1195-1201. Doi: 10.4269/ajtmh.14-0553.

[13] Fry M1, Pudney M. Site of action of the antimalarial hydroxynaphthoquinone, 2-[trans-4-(4'-chlorophenyl) cyclohexyl]-3-hydroxy-1,4-naphthoquinone (566C80). Biochem Pharmacol. 1992; 43:1545-1553.

[14] Siregar JE, Kurisu G, Kobayashi T, Matsuzaki M, Sakamoto K, Mi-ichi F, Watanabe Y, Hirai M, Matsuoka H, Syafruddin D, Marzuki S, Kita K. Direct evidence for the atovaquone action on the *Plasmodium* cytochrome bc1 complex. Parasitol. Int. 2015; 64:295-300. Doi: 10.1016/j.parint.2014.09.011.

[15] Hovlid ML, Winzeler EA. Phenotypic screens in antimalarial drug discovery. Trends Parasitol. 2016, in press, Doi: 10.1016/j.pt.2016.04.014.

[16] Birkholtz LM, Coetzer TL, Mancama D, Leroy D, Alano P. Discovering new transmission-blocking antimalarial compounds: challenges and opportunities. Trends Parasitol. 2016, in press. doi: 10.1016/j.pt.2016.04.017.

[17] Ressurreição AS, Gonçalves D, Sitoe AR, Albuquerque IS, Gut J, Góis A, Gonçalves LM, Bronze MR, Hanscheid T, Biagini GA, Rosenthal PJ, Prudêncio M, O'Neill P, Mota MM, Lopes F, Moreira R. Structural optimization of quinolon-4(1H)-imines as dual-stage antimalarials: toward increased potency and metabolic stability. J. Med. Chem. 2013; 56:7679-7690. Doi: 10.1021/jm4011466.

[18] Gomes A, Pérez B, Albuquerque I, Machado M, Prudêncio M, Nogueira F, Teixeira C, Gomes P. N-cinnamoylation of antimalarial classics: quinacrine analogues with decreased toxicity and dual-stage activity. ChemMedChem. 2014; 9:305-310. Doi: 10.1002/cmdc.201300459.

[19] Gomes A, Machado M, Lobo L, Nogueira F, Prudêncio M, Teixeira C, Gomes P. *N*-Cinnamoylation of antimalarial classics: effects of using acyl groups other than cinnamoyl toward dual-stage antimalarials. ChemMedChem. 2015; 10:1344-1349. Doi: 10.1002/cmdc.201500164.

[20] Kaur H, Machado M, de Kock C, Smith P, Chibale K, Prudêncio M, Singh K. Primaquine-pyrimidine hybrids: synthesis and dual-stage antiplasmodial activity. Eur. J. Med. Chem. 2015; 101:266-273. Doi: 10.1016/j.ejmech.2015.06.045

[21] Mushtaque M, Shahjahan. Reemergence of chloroquine (CQ) analogs as multi-targeting antimalarial agents: a review. Eur. J. Med. Chem. 2015; 90:280-295. Doi: 10.1016/j.ejmech.2014.11.022.

[22] Penna-Coutinho J, Almela MJ, Miguel-Blanco C, Herreros E, Sá PM, Boechat N, Krettli AU. Transmission-blocking potential of MEFAS, a hybrid compound derived from artesunate and mefloquine. Antimicrob Agents Chemother. 2016; 60:3145-3147. Doi: 10.1128/AAC.02216-15.

[23] Macedo TS, Vegas LC, Paixão M, Navarro M, Barreto BC, Oliveira PCM, Macambira SG, Machado M, Prudêncio M, D'Alessandro S, Basilico N, Moreira DRM, Batista AA, Soares MBP. Chloroquine-containing organoruthenium complexes are fast-acting multistage antimalarial agents. Parasitology; 2016, in press.

[24] Villarreal W, Colina-Vegas L, Rodrigues de Oliveira C, Tenorio JC, Ellena J, Gozzo FC, Cominetti MR, Ferreira AG, Ferreira MA, Navarro M, Batista AA. Chiral platinum(II) complexes featuring phosphine and chloroquine ligands as cytotoxic and monofunctional DNA-binding agents. Inorg. Chem. 2015; 54:11709-11720. Doi: 10.1021/acs.inorgchem.5b01647

[25] Ploemen IH, Prudêncio M, Douradinha BG, Ramesar J, Fonager J, van Gemert GJ, Luty AJ, Hermsen CC, Sauerwein RW, Baptista FG, Mota MM, Waters AP, Que I, Lowik CW, Khan SM, Janse CJ, Franke-Fayard BM.. Visualisation and quantitative analysis of the rodent malaria liver stage by real time imaging. Plos One 2009; 4: e7881. Doi: 10.1371/journal.pone.0007881

[26] Parapini S1, Basilico N, Pasini E, Egan TJ, Olliaro P, Taramelli D, Monti D. Standardization of the physicochemical parameters to assess in vitro the beta-hematin inhibitory activity of antimalarial drugs. Exp. Parasitol. 2000; 96:249-256. Doi: 10.1006/expr.2000.4583

[27] Huy NT1, Kamei K, Yamamoto T, Kondo Y, Kanaori K, Takano R, Tajima K, Hara S. Clotrimazole binds to heme and enhances heme-dependent hemolysis: proposed antimalarial mechanism of clotrimazole. J. Biol. Chem. 2002; 277:4152-4158.

[28] Souza NB, Aguiar AC, Oliveira AC, Top S, Pigeon P, Jaouen G, Goulart MO, Krettli AU. Antiplasmodial activity of iron(II) and ruthenium(II) organometallic complexes against *Plasmodium falciparum* blood parasites. Mem Inst Oswaldo Cruz. 2015;110:981-988. Doi: 10.1590/0074-02760150163.

[29] Ekengard E, Glans L, Cassells I, Fogeron T, Govender P, Stringer T, Chellan P, Lisensky GC, Hersh WH, Doverbratt I, Lidin S, de Kock C, Smith PJ, Smith GS, Nordlander E. Antimalarial activity of ruthenium(II) and osmium(II) arene complexes with mono- and bidentate chloroquine analogue ligands. Dalton Trans. 2015;44:19314-19329. Doi: 10.1039/c5dt02410b.

[30] Huta BP, Mehlenbacher MR, Nie Y, Lai X, Zubieta C, Bou-Abdallah F, Doyle RP. The lysosomal protein saposin B binds chloroquine. ChemMedChem. 2016; 11:277-282. Doi: 10.1002/cmdc.201500494.

[31] Teguh SC, Klonis N, Duffy S, Lucantoni L, Avery VM, Hutton CA, Baell JB, Tilley L. Novel conjugated quinoline-indoles compromise *Plasmodium falciparum* mitochondrial function and show promising antimalarial activity. J. Med. Chem. 2013; 56:6200-6215. Doi: 10.1021/jm400656s.

List of Figures and Tables

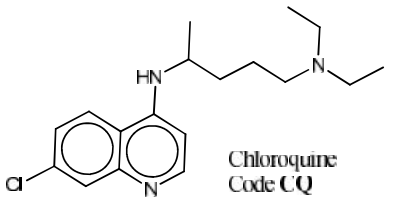

Chloroquine
Code **CQ**

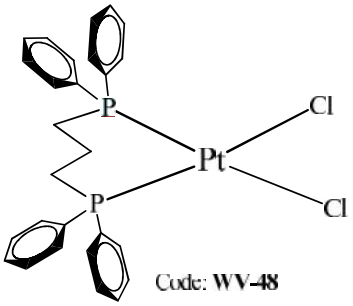

Code: **WV-48**

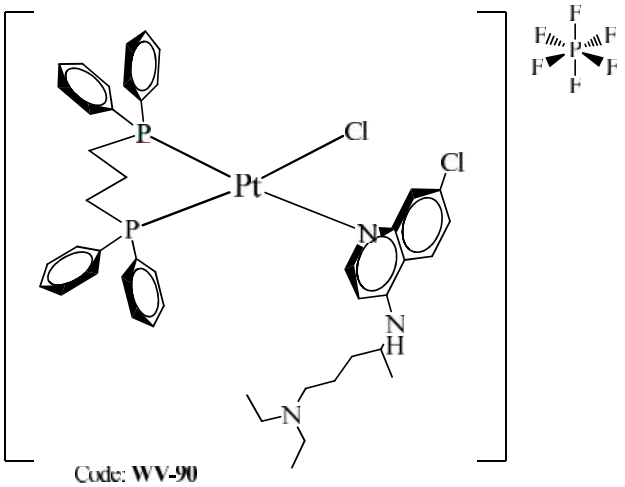

Code: **WV-90**

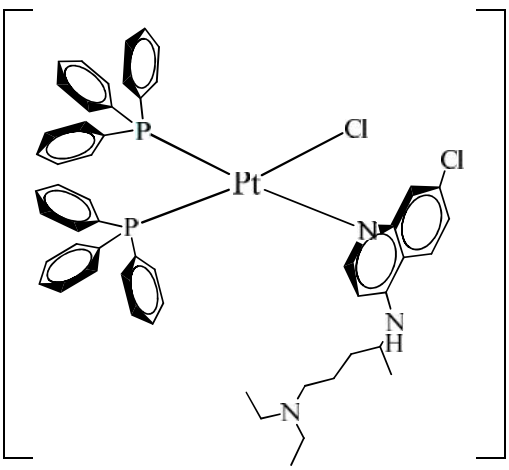

Code: **WV-92**

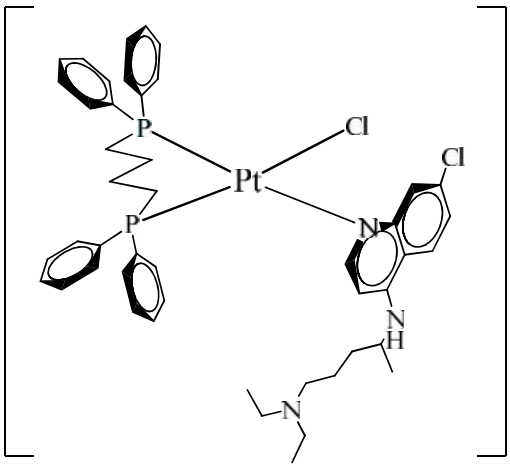

Code: **WV-93**

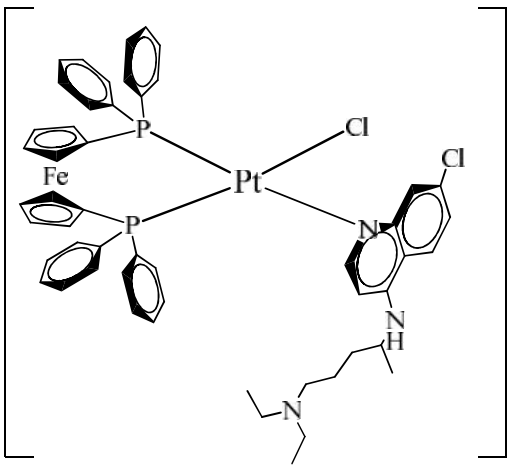

Code: **WV-94**

Figure 1. Chemical structures of chloroquine and its platinum complexes.

Table 1. Cytostatic activity of platinum complexes against intraerythrocytic *P. falciparum*, mammalian cell cytotoxicity and selectivity indexes.

Comp.	*P. falciparum*, IC_{50} ±S.E.M.(μM)[a]		Cells, CC_{50}±S.E.M.(μM)[b]		Selectivity index[c]	
	CQ-sensitive 3D7	CQ-resistant W2	J774	HepG2	3D7	W2
(WV48)	> 2.0	3.6±0.3	94.4±6.4	37.5±4.0	N.D.	26
(**WV90**)	0.38±0.06	0.5±0.07	39.6.±4.3	87.4±1.2	104	79
(**WV92**)	0.6±0.01	0.7±0.2	17.9.±2.4	35.5±1.7	29	25
(**WV93**)	0.32±0.02	0.76±0.10	78.1±1.7	58.5±2.8	244	102
(**WV94**)	0.41±0.1	0.5±0.06	21.5±1.0	29.3±0.4	52	43
CQ	0.11±0.035	0.43±0.09	76.1±3.1	37.6 ±3.6	690	190
Gentian violet	-	-	14.2±0.3	4.3±0.8	-	-

[a] Determined 48 h after incubation with compounds. [b] Determined 72 h after incubation with compounds. [c] Determined as CC_{50} (J774 cells) /IC_{50}. IC_{50} = inhibitory concentration at 50 %. Values were calculated as mean of three independent experiments. CC_{50} = cytotoxic concentration at 50 %. S.E.M. = standard error of the mean.

Table 2. Parasiticidal activity of platinum complexes against intraerythrocytic *P. falciparum*.

Compounds	CQ-sensitive 3D7[a]		CQ-resistant W2[a]	
	LC_{50} ±S.E.M.(μM)[b]	MPC (μM)[c]	LC_{50} ±S.E.M.(μM)[b]	MPC (μM)[c]
(**WV90**)	1.03±0.038	8.0	0.84±0.03	5.0
(**WV93**)	1.8±0.16	10	1.0±0.2	10
CQ	0.64±0.04	>10	0.43±0.03	>10
Artesunate	0.0053±0.00032	0.12	0.0049±0.0009	0.19

[a]Activity determined in trophozoites incubated for 18 h with drugs then for 48 h in drug-free conditions. [b]LC_{50} = lethal concentration at 50 %. MPC = minimal parasiticidal concentration.

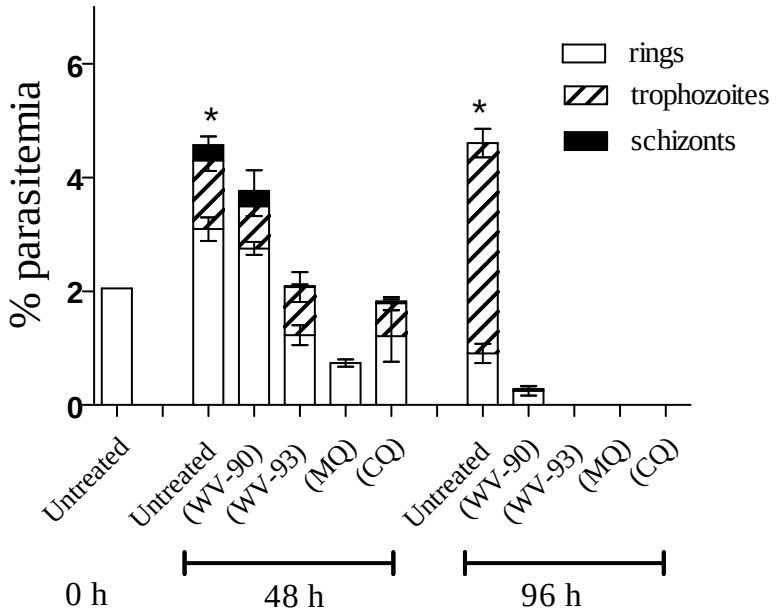

Figure 2: Drug-susceptibility testing against blood stage 3D7 strain *P. falciparum*. Ring stage parasites (2 % parasitemia, 2.5 % hematocrit) were incubated with vehicle (DMSO 0.5 %) as a untreated control or 0.65 μM of each compounds at 0 and 48 h. Mefloquine was used at concentration of 0.1 μM. Quantification of intraerythrocytic stages at 48 and 96 after addition of the compounds are shown. Two independent experiments were determined. Error bars represent standard deviation from pooling triplicate values of one experiment. CQ = chloroquine. MQ = mefloquine. * $p < 0.05$ for quantification of parasitemia versus untreated 0 h.

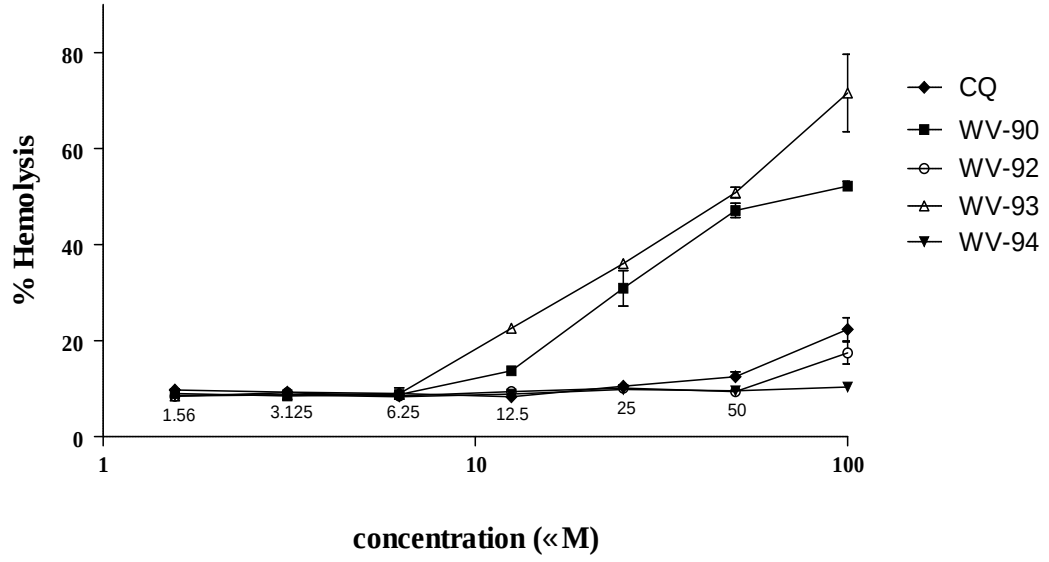

Figure 3: Percent of hemolysis in uninfected erythrocytes after 1 h incubation of compounds at indicated concentration. Two independent experiments were performed. Error bars represent standard deviation from pooling triplicate values of one experiment.

Table 3. Inhibitory activity of platinum complexes against polymerization of hemin into β-hematin.

Comp.	β-hematin, IC_{50} ±S.D.(mM)[a]
WV48	N.D.
(**WV90**)	0.6±0.4
(**WV92**)	0.5±0.1
(**WV93**)	0.8±0.2
(**WV94**)	0.8±0.2
CQ	0.6±0.2

[a] Determined 24 h after incubation with compounds. S.D. = standard deviation from triplicate values of one experiment. N.D. = not determined.

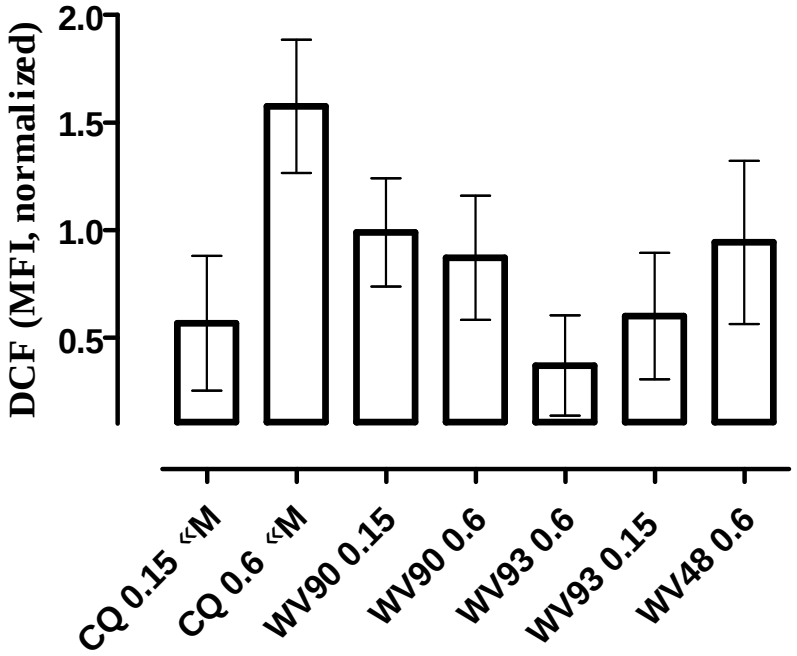

Figure 4: 3D7 strain *P. falciparum* trophozoites (3.0 % parasitemia, 1 % hematocrit) stained with CM-H2-DCFDA, a probe for reactive oxygen species. Drugs were incubated for 4 h and analyzed by flow cytometry. Bars represent DCF signal. Median fluorescence intensity (MFI) were normalized from untreated control and obtained from pooling data gathered of two independent experiments. Error bars represent standard error of the mean (S.E.M.).

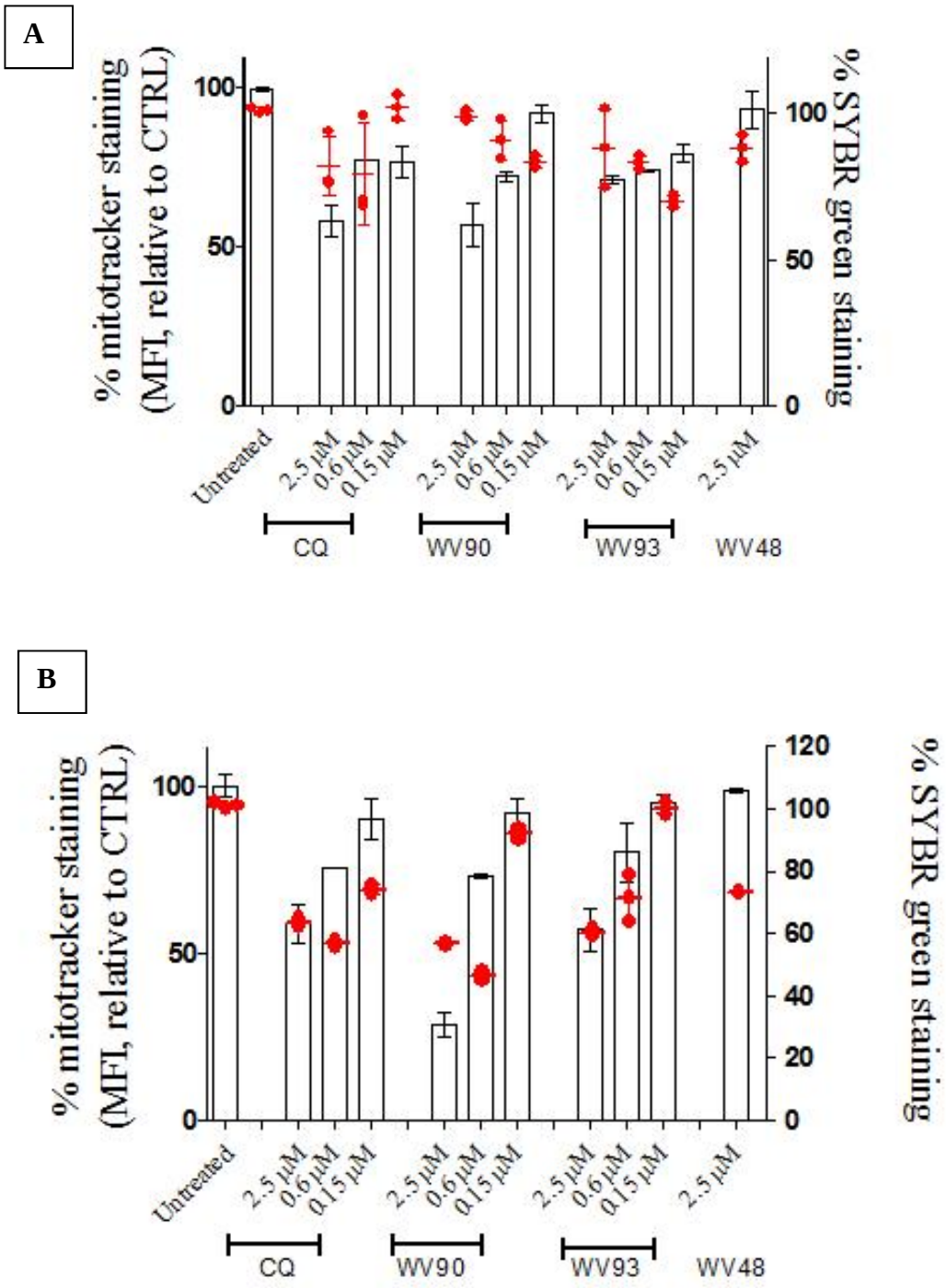

Figure 5: 3D7 strain *P. falciparum* trophozoites (2.0 % parasitemia, 1 % hematocrit) double stained with mitotracker deep red FM (probe for mitochondria) and SYBRgreenI (nucleic acid stain). Panel A) Drugs were incubated for 24 h and analyzed by flow cytometry. Panel B) Drugs were incubated for 48 h and analyzed by flow cytometry Bars represent mitotracker signal and red dots represent SYBR signal. Median fluorescence intensity (MFI) were normalized from untreated control and obtained from pooling data gathered of two independent experiments. Error bars represent S.E.M.

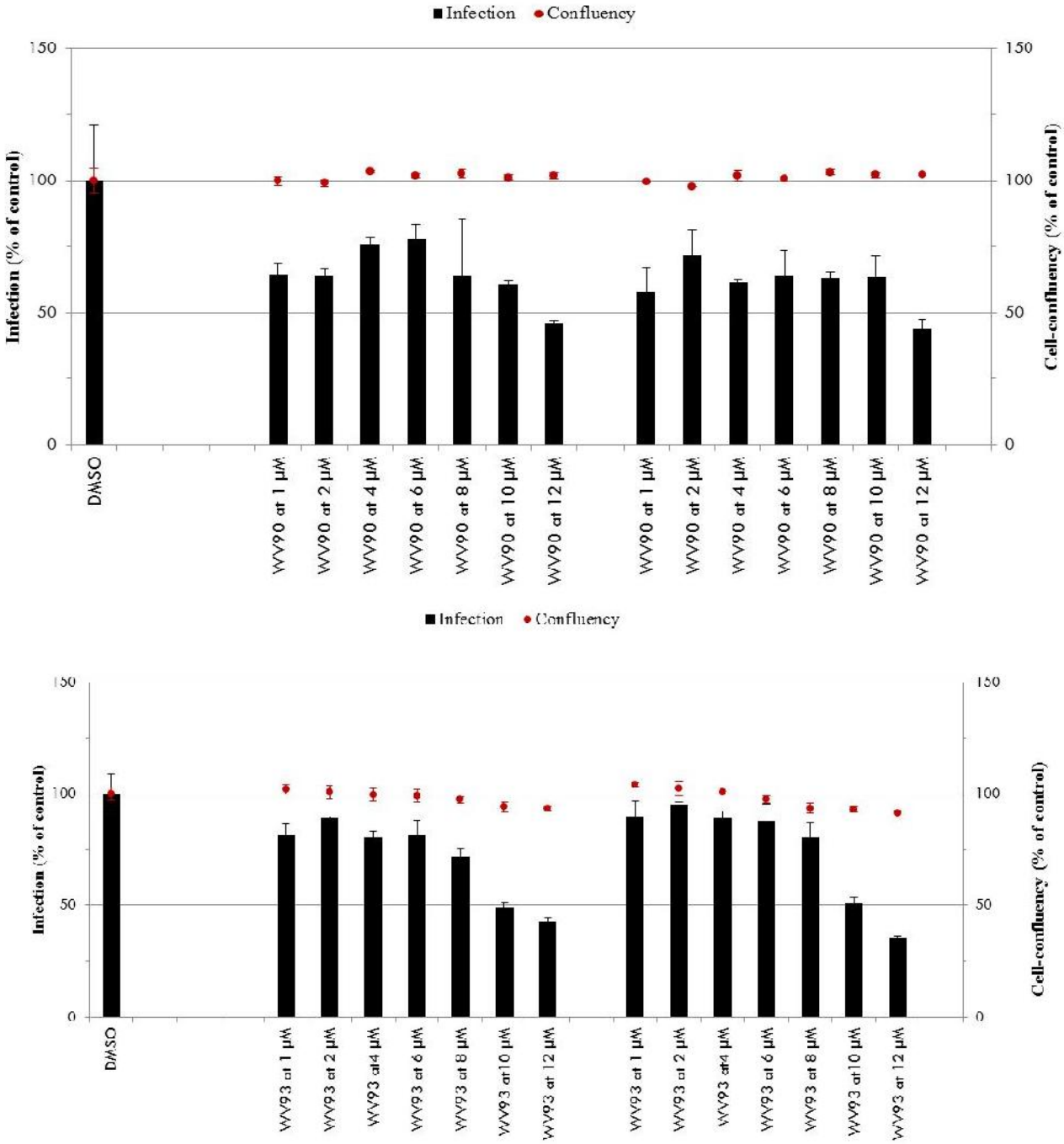

Figure 6: Drug-susceptibility testing against *P. berghei* sporozoites. Seeded Huh7 cells were treated with drugs and infected with sporozoites. Bioluminescence intensity was measured 48 h post-infection. Bars represent infection and red dots represent Huh7 cell confluency. Untreated control received only DMSO. Compound WV-93 presented IC_{50} = 10.8±0.68 µM. Error bars represent standard deviation from each concentration in triplicate. Results of two independent experiments are shown.

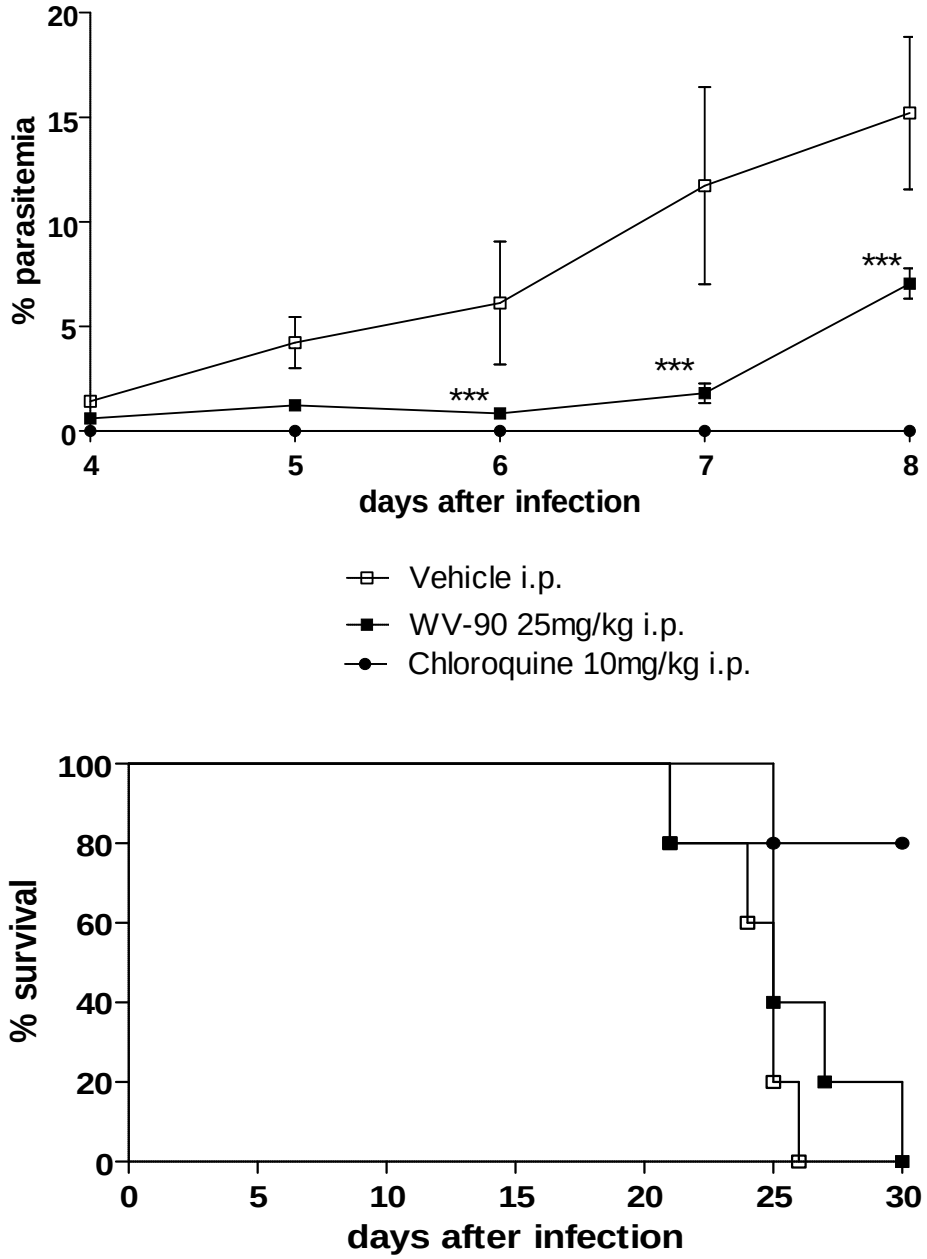

Figure 7: Blood parasitemia (top) and survival (bottom) in *P. berghei*-infected mice. Swiss Webster mice (n=5/group) were infected with *P. berghei* and treated daily for four consecutive days. Values represent the mean±S.E.M. of one experiment. i.p. = intraperitoneal. (Top): ***p<0.001 in comparison to vehicle group. (Bottom): p<0.05 for vehicle *versus* Chloroquine group (Log-rank and Mantel-Cox).

5 DISCUSSÃO

A cloroquina é um fármaco antimalárico com amplo uso em áreas endêmicas mesmo diante da existência de cepas resistentes. Algumas características da cloroquina, tais como a sua baixa toxicidadade, perfil farmacocinético adequado e baixo custo de produção tem tornado este composto um protótipo para a descoberta de novos fármacos antimaláricos. Além disso, a cloroquina é considerada um fármaco com propriedades farmacológicas pleiotrópicas, exercendo inclusive ação imunossupressora e como potencial fármaco na terapia combinada anticâncer (KOVACS et al. 1989; HUTA et al. 2016). Sendo assim, neste trabalho utilizamos a cloroquina como principal componente na produção de complexos metálicos antimaláricos.

Os complexos de platina ou rutênio sem cloroquina na composição foram destituídos de ação antiparasitária *in vitro* frente ao *P. falciparum*. Entretanto, a incorporação da cloroquina na composição de complexos com platina ou rutênio resultou em compostos com atividade antiparasitária. Em muitos casos, os complexos metálicos podem ser instáveis em solução, sofrendo dissociação e liberando as moléculas orgânicas ligadas ao metal (PEACOCK; SADLER, 2008; SALAS et al., 2013). Porém, a análise de estabilidade dos complexos metálicos com cloroquina por ressonância magnética nuclear revelou que não houve dissociação da cloroquina mesmo após incubação em solução mantida por 60 horas. Portanto, foi possível estabelecer que a ação antiparasitária dos complexos metálicos da cloroquina se deve ao conjunto da estrutura química ao invés de ser um sistema de liberação de cloroquina.

Em relação à atividade no ciclo eritrocítico assexuado do *P. falciparum*, tanto os complexos com platina como os de rutênio apresentaram potência inferior ou igual à cloroquina. Ao se comparar as duas classes de complexos metálicos (platina *versus* rutênio), não se observou diferença na magnitude da potência antiparasitária. Além disso, os complexos metálicos apresentaram índice de seletividade similar ao observado com a cloroquina. Um aspecto importante é o grau de resistência das cepas de *P. falciparum* utilizadas. Não observamos diferença de atividade antiparasitária dos complexos metálicos frente a cepa sensível e resistente à cloroquina. Estes resultados sugerem que os complexos metálicos são capazes de contornar o mecanismo de resistência à cloroquina.

A avaliação da velocidade de ação em trofozoítos do *P. falciparum* tratados com 2.5 a 5.0 μM dos complexos de rutênio MCQ e FCQ, um efeito parasiticida foi observado após 18 h de incubação, enquanto que a cloroquina não apresentou ação mesmo testada na concentração de 10 μM, revelando assim que os complexos de rutênio possuem uma ação antiparasitária mais rápida que a cloroquina.

Os complexos de platina apresentaram velocidade de ação mais lenta que os de rutênio, apresentando perfil mais similar a cloroquina. A efetividade rápida contra todos os estágios eritrocíticos assexuados do plasmódio (anéis, trofozoítos e esquizontes) é um critério essencial para o desenvolvimento de um novo antimalárico. De fato, este critério se baseia na premissa de que uma redução rápida em população misturada de parasitos pode diminuir a recrudescência. Mais importante ainda é o fato que uma eficácia rápida pode ser crucial no uso da terapia combinada, eliminando a fração de parasitos que não foram afetados pelo outro fármaco da combinação. Outrossim, o começo da ação antiparasitária rápida pode reduzir o tempo do tratamento (SANZ et al., 2012; LE MANACH et al., 2013).

Exceto a primaquina, a maioria dos compostos 4-aminoquinolinicos interagem no sentido de evitar a formação da hemozoína presente nos trofozoítos. Este mecanismo é importante para o desenvolvimento de novos antimaláricos, pois é ausente em células humanas. Como limitante, a biossíntese da hemozoína ocorre somente no ciclo sanguíneo da doença, sendo então necessário desenvolver fármacos que atuem por mais de um mecanismo de ação (EGAN; ROSS; ADAMS, 1994; EGAN et al., 1997). Neste trabalho, verificamos que, tal como a cloroquina, os complexos de platina e de rutênio foram capazes de inibir a polimerização da hemina em β-hematina. Em geral, a potência, expressa com os valores de CI_{50}, mostrou que os complexos tão potentes ou menos do que a cloroquina. Sendo assim, a interação dos complexos metálicos com β-hematina não explica as diferenças das propriedades antiparasitárias observadas entre cloroquina e seus complexos metálicos.

Uma vez que a biossíntese da hemozoína é interrompida, o acúlumo de heme no interior do parasito é tóxico, pois leva a uma sequencia de eventos que interferem na cadeia respitatória, síntese de proteínas e balanço homeostático (OLAFSON et al., 2015). De fato, desvendou-se aqui que os complexos de rutênio exercem ação parasiticida em trofozoítos através da produção de espécies reativas de oxigênio, enquanto que os complexos de platina não induzem a sua produção de maneira significativa. Esta observação nos pareceu intrigante ao primeiro momento, pois a principal diferença entre estas duas classes dos complexos metálicos é o tipo de metal usado. Porém, analisando a literatura, verificamos que complexos de platina são descritos classicamente como moléculas que atuam ao nível do DNA, enquanto que complexos de rutênio interagem com proteínas citosólicas (SALAS; HERRMANN; ORVIG, 2013). De fato, nós observamos uma propriedade farmacológica para os complexos de platina que não foram observados para os complexos de rutênio. Os complexos de platina reduziram a viabilidade da mitocôndria em trofozoítos, possivelmente por exercerem ação

mitofágica. Estas observações indicam a necessidade de estudar se os complexos de platina interferem com a cadeia transportadora de elétrons do plasmódio.

Outro importante achado refere-se ao espectro de ação frente aos estágios do ciclo de vida do *P. falciparum*. Um novo fármaco antimalárico para ser aprovado, necessita apresentar um espectro de ação multiestágio, atuando na infecção, progressão e transmissão da doença. Anterior ao nosso trabalho, não havia nenhuma literatura de compostos inorgânicos com ação frente ao estágio não-sanguíneo da malária.

Em nosso trabalho demonstramos que, ao contrário da cloroquina, que apresenta um espectro de ação basicamente restrita ao ciclo eritrocítico assexuado do *P. falciparum*, tanto os complexos de rutênio quanto os complexos de platina apresentaram um espectro de ação mais amplo. Os complexos de rutênio, em especial o composto BCQ, inibiu a viabilidade celular de gametócitos da cepa 3D7 do *P. falciparum*, enquanto que a cloroquina é destituída de tal efeito. Além do ciclo assexuado, os complexos de rutênio foram capazes de reduzir a carga parasitária em células infectadas com esporozoítos do *P. berguei*, embora com potência inferior quando comparado com a primaquina. Por outro lado, o complexo de platina WV-93 inibiu a proliferação de esporozoítos do *P. berguei* com potência igual à primaquina, enquanto que a cloroquina não apresentou atividade frente aos esporozoítos. Embora nós tenhamos investigado alguns dos mecanismos envolvidos na ação antiparasitária no estágio sanguíneo, ainda não sabemos qual o mecanismo de ação dos complexos de rutênio na redução da viabilidade dos gametócitos nem a ação dos complexos de platina na redução da carga parasitária na fase hepática.

Exceto o complexo de rutênio FCCQ, os demais complexos de rutênio foram capazes de reduzir a parasitemia em camundongos Suíços infectados com a cepa NK65 do *P. berghei*. Dentre estes, o complexo MCQ foi o que apresentou maior eficácia, reduzindo em 95.1 % a parasitemia e em 40 % a taxa de mortalidade quando administrado na dose de 50 mg/kg por via intraperitoneal. A cloroquina na mesma dose por via oral resultou na cura e reduziu em 100 % a taxa de mortalidade. Portanto, os complexos de rutênio apresentaram eficácia inferior à da cloroquina. Em relação aos complexos de platina, nós verificamos que o complexo WV90 na dose 25 mg/kg por via intraperitoneal foi capaz de reduzir a parasitemia *in vivo*. Este estudo ainda precisa ser concluído, verificando o efeito dose-resposta, todavia é aparente que os complexos de platina são menos eficazes que os de rutênio, que apresentaram eficácia similar numa dose de 10 mg/kg.

A demonstração que os complexos metálicos com cloroquina possuem eficácia *in vivo* representa uma etapa importante na consolidação de compostos inorgânicos no desenvolvimento de

um novo antimalárico. É importante frisar que, embora a literatura seja abundante na investigação de compostos inorgânicos como antimaláricos, somente um único trabalho descrito em 1996 investigou um complexo metálico da cloroquina em modelo murino de infecção pelo *P. berghei,* sem todavia ter estudado o efeito dose dependente nem ter apresentado dados de sobrevivência (LEWIS et al., 1997).

Nosso trabalho avançou na compreensão de compostos inorgânicos como potenciais candidatos à fármacos antimaláricos em desenvolvimento, principalmente por ter apresentado um estudo mais completo da eficácia *in vivo* e por ter demonstrado pela primeira vez a ação frente estágios de transmissão e hepático. No entanto, ainda existem barreiras no desenvolvimento farmacológico desta classe de compostos candidatos a fármacos. Uma das principais barreiras é a ausência de informações sobre a farmacocinética de compostos inorgânicos. Considerando que os complexos de rutênio apresentaram atividade antiparasitária *in vitro* similar à da cloroquina, porém com eficácia *in vivo* inferior, conclui-se que os complexos de rutênio possuam um perfil farmacocinético inadequado. Tendo em vista que os complexos foram estáveis em solução aquosa por 60 horas de incubação e que os mesmos foram administrados por via intraperitoneal, no qual a metabolização hepática de primeira passagem é menos intensa, é plausível que esta classe de compostos apresente um perfil de distribuição nos fluídos biológicos inadequado.

Por fim, são necessários experimentos futuros visando avaliar a eficácia dos outros complexos de platina em reduzir a parasitemia em camundongos Suíços infectados com a cepa NK65 do *P. berghei*. Além disso, avaliar também a atividade de tais complexos na viabilidade de gametócitos da cepa 3D7 do *P. falciparum*. Diante da atividade antiparasitária observada com o complexo de platina WV-93 em esporozoítos do *P. berguei*, é importante investigar se este composto apresenta ação antiparasitária no *P. vivax*, onde o estágio hepático tem um papel importante no quadro clínico da doença. Outra perspectiva importante é a investigação da atividade e do espectro de ação quando outra quinolina antimalárica é utilizada na composição de complexos metálicos no lugar da cloroquina, a exemplo da amodiaquina e mefloquina.

6 CONCLUSÃO

No presente trabalho foi possível observar que o desenvolvimento de complexos metálicos contendo quinolinas como ligantes pode resultar em agentes antiparasitários com amplo espectro de ação. Neste estudo a incorporação de cloroquina em compostos de rutênio ou platina produziu agentes antimaláricos com as propriedades clássicas da cloroquina, mas também com ação em outros estágios do ciclo do plasmódio. Além disso, foi observado que o mecanismo pelo qual tais complexos exercem atividade antiparasitária parece ser distinto da cloroquina.

No estudo *in vivo* os complexos testados reduziram a parasitemia de camundongos infectados, mas com eficácia inferior à cloroquina, sugerindo um perfil farmacocinético inadequado. Fica evidenciado a importância de uma investigação farmacológica mais aprofundada, bem como a modificação química, visando fortalecer o desenvolvimento de medicamentos contra a malária.

Os dados aqui apresentados são de extrema relevância na compreensão de compostos inorgânicos, em especial complexos metálicos, como candidatos a agentes antimaláricos.

REFERÊNCIAS

ACHAN, J. et al. Quinine, an old anti-malarial drug in a modern world: role in the treatment of malaria. **Malaria Journal**, v. 10, p.144, 2011.

ADEDIJI, J. F.; OBALEYE, J. A.; AKINREMI, C. A. Ni(II) complex of mefloquine-pyrimethamine: Synthesis, toxicological and antimalarial activities against *Plasmodium berghei*. **Journal of Chemical and Pharmaceutical Research**, v. 4, n.8, p. 4066-4072, 2012.

ADEDIJI, J. F.; OBALEYE, J. A. Co(II) complex of mefloquine hydrochloride: Synthesis, antimicrobial potential, antimalaria and toxicological activities. **Journal of Chemistry**, v. 9, n.4, p. 2245-2254, 2012.

AGUIAR, A. C. C.; ROCHA, E. M. M.; SOUZA, N. B.; FRANÇA, T. C. C.; KRETTLI, A. U. New approaches in antimalarial drug discovery and development - A Review. **Memórias do Instituto Oswaldo Cruz,** v. 107, n.7, p. 831-845, 2012.

AMINO, R.; MARTIN, B.; THIBERGE, S.; CELLI, S.; SHORTE, S.; FRISCHKNECHT, F.; MENARD, R. Quantitative imaging of *Plasmodium* transmission from mosquito to mammal. **Nature Medicine**, v. 12, n.2, p. 220–224, 2006.

ANTINORI, S.; GALIMBERTI, L.; MILAZZO, L.; CORBELLINO, M. *Plasmodium knowlesi*: The emerging zoonotic malaria parasite. **Acta Tropica**, v.125, n.2, p. 191– 201, 2013.

ASKLING, H. H. et al. Management of imported malaria in Europe. **Malaria Journal,** v. 11, p.328, 2012.

BARAGAÑA, B. et al. A novel multiple-stage antimalarial agent that inhibits protein synthesis. **Nature,** v. 522, n. 7556, p.315-20, 2015.

BLOLAND, P. B. **Drug resistence in malaria.** Malaria Epidemiology Branch. World Health Organization/ Centers for Disease Control and Prevention. Chamblee, GA: United States of America, 2001.

BRASIL. Ministério da Saúde. Secretaria de vigilância em saúde. Departamento de vigilância epidemiológica. **Ações de controle da malária: manual para profissionais de saúde na atenção básica.** Brasília: Editora do Ministério da Saúde, 2006. 52p Il.

BRASIL. Ministério da Saúde. Secretaria de Vigilância em Saúde. Departamento de Vigilância Epidemiológica. **Guia prático de tratamento da malária no Brasil.** Brasília: Editora do Ministério da Saúde, 2010. 30p Il.

BRASIL. Ministério da Saúde. Secretaria de Vigilância em Saúde. **Boletim Epidemiológico: Situação epidemiológica da malária no Brasil, 2012 e 2013**. v. 46, n. 43. 2015. Disponível em: < http://portalsaude.saude.gov.br/images/pdf/2015/dezembro/16/2015-003---Mal--ria.pdf> Acesso em 14 maio 2016.

BRUCE-CHWATT, L. J.; ZULETA, J. **The rise and fall of malaria in Europe**. Oxford: Oxford University Press, 1980.

BUSTAMANTE, C.; BATISTA, C. N.; ZALIS, M. Molecular and biological aspects of antimalarial resistance in *Plasmodium falciparum* and *Plasmodium vivax*. **Current Drug Targets,** v. 10, n. 3, p. 279-290, 2009.

CABRERA, M.; CUI, L. In vitro Activities of primaquine-schizonticide combinations on asexual blood stages and gametocytes of *Plasmodium falciparum*. **Antimicrobial Agents Chemotherapy**, v. 59, n.12, p.7650-766, 2015.

CARTER, R.; MENDIS, K. N. Evolutionary and historical aspects of the burden of malaria. **Clinical microbiology review**, 15: 564-594. 2002. REY, L. **Parasitologia**. 3º ed. Rio de Janeiro: Guanabara Koogan, 2001.

CEVENINI, L. et al. Multicolor bioluminescence boosts malaria research: quantitative dual-color assay and single-cell imaging in *Plasmodium falciparum* parasites. **Journal of Antimicrobial Chemotherapy**, v. 68, n.9, p. 2048-2058, 2013.

CHERUIYO, T. J. et al. Polymorphisms in Pfmdr1, Pfcrt, and Pfnhe1 genes are associated with reduced *in vitro* activities of quinine in *Plasmodium falciparum* isolates from western Kenya. **Antimicrobial Agents and Chemotherapy**, v. 58, n.7, p. 3737-3743, 2014.

CRAWLEY, J.; CHU, C.; MTOVE, G.; NOSTEN, F. Malaria in children. **Lancet**, v. 375, n.9724, p. 1468-1481, 2010.

COX-SINGH, J. et al. *Plasmodium knowlesi* malaria in humans is widely distributed and potentially life threatening. **Clinical infectious diseases**, v. 46, n.2, p.165-171. 2008.

D'ALESSANDRO, S. et al. *Plasmodium falciparum* screening assay for anti-gametocyte drugs based on parasite lactate dehydrogenase detection. **Analytical Chemistry**, v.86, n.17, p. 8814-821, 2014.

DA CRUZ, F. P. et al. Drug screen targeted at *Plasmodium* liver stages identifies a potent multistage antimalarial drug. **Journal of Infect Diseases**, v.205, n.8, p.1278-86, 2012.

DECHY-CABARET, O.; BENOIT-VICAL, F. Effects of antimalarial molecules on the gametocyte stage of *Plasmodium falciparum*: the debate. **Journal of Medicinal Chemistry**, v.55, n.23, p.10328-10344, 2012.

DRONAMRAJU, K. R.; ARESE, P.; RICH, S. M.; AYALA, F. J. Evolutionary origins of human malaria parasites. **Malaria: genetic and evolutionary aspects**. USA: Ed. Springer Science, 2006.

EGAN, T. J.; ROSS, D.C.; ADAMS, P.A. Quinoline anti-malarial drugs inhibit spontaneous formation of beta-haematin (malaria pigment). **FEBS Letters**, v.352, p.54-57,1994.

EGAN, T. J.; MAVUSO, W.W.; ROSS, D. C.; MARQUES, H. M. Thermodynamic factors controlling the interaction of quinoline antimalarial drugs with ferriprotoporphyrin IX**. Journal of Inorganic Biochemistry,** v.68, p.137-145,1997.

EKENGARD, E. et al. Antimalarial activity of ruthenium(ii) and osmium(ii) arene complexes with mono- and bidentate chloroquine analogue ligands. **Dalton Transactions**, v. 44, p.19314-19329, 2015.

FERREIRA, M. U.; CASTRO, M. C. Challenges for malaria elimination in Brazil. **Malaria Journal**, v. 15, n.1, p. 284, 2016.

FRANKE-FAYARD, B. et al. *Plasmodium berghei* reference line that constitutively expresses GFP at a high level throughout the complete life cycle. **Molecular Biochemical Parasitology**, v. 137, n.1, p. 23-33, 2004.

FRY, M; PUDNEY, M. Site of action of the antimalarial hydroxynaphthoquinone, 2-[trans-4-(4#-chlorophenyl) cyclohexyl]-3-hydroxy-1, 4-naphthoquinone (566C80). **Biochem Pharmacol**, v. 43, p.1545–53, 1992.

GARCIA, C. R.; MARKUS, R. P.; MADEIRA, L. Tertian and quartan fevers: temporal regulation in malaria infection. **Journal of Biological Rhythms,** v. 16, n. 5, p. 436-443, 2001.

GIL, J. P. Amodiaquine pharmacogenetics. **Pharmacogenomics**, v. 9, n.10, p. 1385-1390, 2008.

GOLDBERG, D. E.; SLATER, A. F.; CERAMI, A.; HENDERSON, G. B. Hemoglobin degradation in the malaria parasite *Plasmodium falciparum*: An ordered process in a unique organelle. **Proceedings of the National Academy of Sciences,** v. 87, n.8, p.2931–2935, 1990.

HEMPELMANN, E.; MOTTA, C.; HUGHES, R.; WARD, S.A.; BRAY, P.G. *Plasmodium falciparum*: sacrificing membrane to grow crystals? **Trends in Parasitology,** v.19, n.1, p. 23–26. 2003.

HERNANDES, M. Z.; PONTES, F. J.; COELHO, L. C.; MOREIRA, D. R.; PEREIRA, V. R.; LEITE, A. C. Recent insights on the medicinal chemistry of metal-based compounds: hints for the successful drug design. **Current Medicinal Chemistry**, v. 17, n.31, p. 3739-3750, 2010.

HUTA B. P.; MEHLENBACHER, M. R.; NIE, Y.; LAI, X.; ZUBIETA, C.; BOU-ABDALLAH, F.; DOYLE, R. P. The lysosomal protein saposin B binds chloroquine. **Chem Med Chem**, v. 11, n. 3, p. 277-282, 2016.

KOVACS, J.; KARPATI, A. P. Regression of autophagic vacuoles in mouse pancreatic cells: a morphometric study of the effect of methylamine and chloroquine followed by cycloheximide treatment. **Cell Biology International Report**, v.13, n.9, p.805-811, 1989.

LE MANACH, C. et al. Fast *in vitro* methods to determine the speed of action and the stage-specificity of anti-malarials in *Plasmodium falciparum*. **Malaria Journal**, v. 12, p. 424, 2013.

LEE, S. et al. Discovery of carbohybrid-based 2-aminopyrimidine analogues as a new class of rapid-acting antimalarial agents using image-based cytological profiling assay. **Journal of Medicine Chemistry,** v. 57, n.17, p. 7425−7434, 2014.

LEWIS, M.D. et al. Toward a novel metal-based chemotherapy against tropical diseases. 3. Synthesis and antimalarial activity in vitro and in vivo of the new gold-chloroquine complex [Au(PPh3)(CQ)]PF6. **Journal of Medicine Chemistry,** v. 40, p1937-1939, 1997.

LÖDIGE, M. et al. A primaquine–chloroquine hybrid with dual activity against *Plasmodium* liver and blood stages. **International Journal of Medical Microbiology,** v. 303, n.8, p. 539– 547, 2013.

LOOAREESUWAN, S. et al. Clinical studies of atovaquone, alone or in combination with other antimalarial drugs, for treatment of acute uncomplicated malaria in Thailand. **The American Journal of Tropical Medicine and Hygiene**, v. 54, n.1, p.62-6,1996.

MACKINTOSH, C. L.; BEESON, J. G.; MARSH, K. Clinical features and pathogenesis of severe malaria. **Trends in Parasitology**, v. 20, n.12, p. 597-603, 2004.

MBOGO, G.W. et al. Temporal changes in prevalence of molecular markers mediating antimalarial drug resistance in a high malaria transmission setting in Uganda. **The American Journal of Tropical Medicine and Hygiene**, v. 91, n.1, p.54-61, 2014.

MILLER, L. H.; ACKERMAN, H. C.; SU, X.; WELLEMS, T. E. Malaria biology and disease pathogenesis: insights for new treatments. **Nature Medicine**, v.19, n.2, p.156-167, 2013.

NAVARRO, M. et al. Metal-chloroquine derivatives as possible anti-malarial drugs: evaluation of anti-malarial activity and mode of action. **Malaria Journal,** v.13, p. 471, 2014.

NAVARRO, M. et al. Synthesis, characterization and biological activity of trans-platinum(II) complexes with chloroquine. **Journal of Inorganic Biochemistry,** v. 105, n.12, p.1684-1691, 2011.

NILSEN, A. et al. Quinolone-3-diarylethers: a new class of antimalarial drug. **Science Translational Medicine**, v. 20;5, n.177, p. 177, 2013.

OLAFSON, K. N.; KETCHUM, M. A.; RIMER, J. D.; VEKILOV, P. G. Mechanisms of hematin crystallization and inhibition by the antimalarial drug chloroquine. **Proceedings of the National Academy of Sciences**, v.112, n.16, p. 4946-4951, 2015.

OLIVER, M. et al. New use of primaquine for malaria. **Médecine et Maladies Infectieuses**, v.38, n.169-179, 2008.

OMS. Organização Mundial da Saúde. Global Malaria Programme. **World Malaria Report 2013**. Geneva: Organização Mundial da Saúde, 2013. Disponível em: < http://www.who.int/malaria/publications/world_malaria_report_2015/en/> Acesso em: 10 de março de 2014.

OMS. Organização Mundial da Saúde. Global Malaria Programme. **World Malaria Report 2015**. Geneva: Organização Mundial da Saúde, 2015. Disponível em: < http://www.who.int/malaria/publications/world_malaria_report_2015/en/> Acesso em: 4 de janeiro de 2016.

PEACOCK, A.F.; SADLER, P.J. Medicinal organometallic chemistry: designing metal arene complexes as anticancer agents. **Chemistry Asian Journal,** v. 3, p.1890-1189, 2008.

PEATEY, C.L.; LEROY. D.; GARDINER, D.L.; TRENHOLME, K.R. Anti-malarial drugs: how effective are they against *Plasmodium falciparum* gametocytes? **Malaria Journal**, v. 11, p. 34, 2012.

PETERS, W. The prevention of antimalarial drug resistance. **Pharmacology & Therapeutics**, v. 47, n. 3, p.499-508, 1990.

RAINSFORD, K. D.; PARKE, A. L.; CLIFFORD-RASHOTTE, M.; KEAN, W. F. Therapy and pharmacological properties of hydroxychloroquine and chloroquine in treatment of systemic lupus erythematosus, rheumatoid arthritis and related diseases. **Inflammopharmacology**, v. 23, n.5, p.231-269, 2015.

ROCHA, V. P.; NONATO, F. R.; GUIMARÃES, E. T.; RODRIGUES-DE-FREITAS, L. A.; SOARES, M. B. Activity of antimalarial drugs in vitro and in a murine model of cutaneous leishmaniasis. **Journal of Medical Microbiology,** v. 62, n.7, p.1001-1010, 2013.

RODRIGUES, T.; PRUDÊNCIO, M.; MOREIRA, R.; MOTA, M. M.; LOPES, F. Targeting the liver stage of malaria parasites: a yet unmet goal. **Journal of Medicinal Chemistry**, v. 55, n.3, p. 995-1012, 2012.

SALAS, P. F.; HERRMANN, C.; ORVIG, C. Metalloantimalarials. **Chemical Reviews**, v.113, n.5, p.3450–3492, 2013.

SALAS, P. F. et al. Structural characteristics of chloroquine-bridged ferrocenophane analogues of ferroquine may obviate malaria drug-resistance mechanisms. **Journal Medicine Chemistry**, v.56, n.54, p.1596-1613, 2013.

SANCHEZ, C. P.; DAVE, A.; STEIN, W. D.; LANZER, M. Transporters as mediators of drug resistance in *Plasmodium falciparum*. **International Journal for Parasitology,** v. 40, n.10, p. 1109–1118, 2010.

SANTOS, C. A.; SILVA, N. C. J. C.; COSTA, S. V.; MACEDO, M. R. A. Mapeamento espacial e epidemiológico da malária no estado do Pará. **Anais XVI Simpósio Brasileiro de Sensoriamento Remoto – SBSR**. Foz do Iguaçu, PR, Brasil, 13 a 18 de abril de 2013, INPE. 8546-8553.

SANZ, L. M. et al. *falciparum in vitro* killing rates allow to discriminate between different antimalarial mode-of-action. **PLoS One**, v. 7, n. 2, p.30949, 2012.

SCHLAGENHAUF, P. Malaria: from prehistory to present. **Infectious Disease Clinics of North America**, v.18, p.189–205. 2004.

STURM, A. et al. Manipulation of host hepatocytes by the malaria parasite for delivery into liver sinusoids. **Science**, v. 313, n.5791, p. 1287-1290, 2006.

TAVARES, J. et al. Role of host cell traversal by the malaria sporozoite during liver infection. **The Journal of Experimental Medicine**, v. 210, n.5, p. 905-915, 2013.

TUTEJA, R. Malaria – an overview. **FEBS Journal**, v. 274, n. 18, p. 4670-4679, 2007.

VANDERBERG, J. P.; FREVERT, U. Intravital microscopy demonstrating antibody-mediated immobilization of *Plasmodium berghei* sporozoites injected into skin by mosquitoes. **International Journal for Parasitology**, v. 34, n.9, p. 991–996, 2004.

VENKATESAN, M.et al. Polymorphisms in *Plasmodium falciparum* chloroquine resistance transporter and multidrug resistance 1 genes: Parasite risk factors that affect treatment outcomes for *P. falciparum* malaria after artemether-lumefantrine and artesunate-amodiaquine. **The American Journal of Tropical Medicine and Hygiene, v.** 91, n.4, p. 833-843, 2014.

WANG, X.; WANG, X.; GUO, Z. Functionalization of Platinum Complexes for Biomedical Applications. **Accounts Chemical Research**, v. 48, n. 9, p. 2622-2631, 2015.

WASSMER, S. C. et al. Investigating the pathogenesis of severe malaria: A multidisciplinary and cross-geographical approach. **The American Journal of Tropical Medicine and Hygiene**, v. 93, n.3, p.42-56, 2015.

WINSTANLEY, P. Modern chemotherapeutic options for malaria. **The Lancet Infectious Diseases**, v.1, n.4, p. 242-250, 2001.

WHITE, N. J. Manson's Tropical Diseases. **Elsevier Science**. 21 th edition: 1205-1295. 2003.

WHITE, N. J. Antimalarial drug resistance. **The Journal of Clinical Investigation**, v. 113, n.8, p.1084-1092, 2004.

WHITE, N. J. Primaquine to prevent transmission of falciparum malaria. **Lancet Infection Disease.** v.13, n.2, p.175-81, 2013.

YEH, I.; ALTMAN, R. B. Drug targets for *Plasmodium falciparum*: A post-genomic review/survey. **Mini-Reviews in Medicinal Chemistry**, v.6, n.2, p.177-202, 2006.

APÊNDICE

Journal of Inorganic Biochemistry 136 (2014) 33–39

Contents lists available at ScienceDirect

Journal of Inorganic Biochemistry

journal homepage: www.elsevier.com/locate/jinorgbio

Antiparasitic activities of novel ruthenium/lapachol complexes

Marília I.F. Barbosa [a], Rodrigo S. Corrêa [a], Katia Mara de Oliveira [a], Claudia Rodrigues [a], Javier Ellena [b], Otaciro R. Nascimento [b], Vinícius P.C. Rocha [c], Fabiana R. Nonato [c], Taís S. Macedo [c], José Maria Barbosa-Filho [e], Milena B.P. Soares [c,d], Alzir A. Batista [a,*]

[a] Departamento de Química, Universidade Federal de São Carlos, CP 676, CEP 13565-905, São Carlos (SP), Brazil
[b] Instituto de Física de São Carlos, Universidade de São Paulo, CP 369, CEP 13560-970, São Carlos (SP), Brazil
[c] Laboratório de Engenharia Tecidual e Imunofarmacologia, Fiocruz, CEP: 40296-710, Salvador (BA), Brazil
[d] Centro de Biotecnologia e Terapia Celular, Hospital São Rafael, CEP 41253-190, Salvador (BA), Brazil
[e] Universidade Federal da Paraíba Laboratório de Tecnologia Farmacêutica, CEP 58051-900, João Pessoa (PB), Brazil

ARTICLE INFO

Article history:
Received 29 November 2013
Received in revised form 19 March 2014
Accepted 19 March 2014
Available online 27 March 2014

Keywords:
Ruthenium (II) and (III) lapachol complex
Cytotoxicity
Antileishmanial and antiplasmodial activities

ABSTRACT

The present study describes the synthesis, characterization, antileishmanial and antiplasmodial activities of novel diimine/(2,2′-bipyridine (bipy), 1,10-phenanthroline (phen), 4,4′-methylbipyridine (Me-bipy) and 4,4′-methoxybipyridine (MeO-bipy)/phosphine/ruthenium(II) complexes containing lapachol (Lap, 2-hydroxy-3-(3-33 methyl-2-buthenyl)-1,4-naphthoquinone) as bidentate ligand. The $[Ru(Lap)(PPh_3)_2(bipy)]PF_6$ (**1**), $[Ru(Lap)(PPh_3)_2(Me\text{-}bipy)]PF_6$ (**2**), $[Ru(Lap)(PPh_3)_2(MeO\text{-}bipy)]PF_6$ **(3)** and$[Ru(Lap)(PPh_3)_2(phen)]PF_6$ (**4**) complexes, PPh_3 = triphenylphospine, were synthesized from the reactions of *cis*-$[RuCl_2(PPh_3)_2(X\text{-}bipy)]$ or *cis*-$[RuCl_2(PPh_3)_2(phen)]$, with lapachol. The $[RuCl_2(Lap)(dppb)]$ **(5)** [dppb = 1,4-*bis*(diphenylphosphine)butane] was synthesized from the *mer*-$[RuCl_3(dppb)(H_2O)]$ complex. The complexes were characterized by elemental analysis, molar conductivity, infrared and UV–vis spectroscopy, $^{31}P\{^1H\}$ and ^1H NMR, and cyclic voltammetry. The Ru(III) complex, $[RuCl_2(Lap)(dppb)]$, was also characterized by the EPR technique. The structure of the complexes $[Ru(Lap)(PPh_3)_2(bipy)]PF_6$ and $[RuCl_2(Lap)(dppb)]$ was elucidated by X-ray diffraction. The evaluation of the antiparasitic activities of the complexes against *Leishmania amazonensis* and *Plasmodium falciparum* demonstrated that lapachol–ruthenium complexes are more potent than the free lapachol. The $[RuCl_2(Lap)(dppb)]$ complex is the most potent and selective antiparasitic compound among the five new ruthenium complexes studied in this work, exhibiting an activity comparable to the reference drugs.

1. Introduction

Leishmaniasis and malaria are diseases caused by protozoan parasites and are characterized by high morbidity. It is estimated that leishmania disease causes about seventy thousand deaths annually and malaria kills around 1 million children only in Africa [1]. The first line treatment for leishmaniasis still relies on the use of pentavalent antimonials, although other drugs are also used for the treatment of *Leishmania* infection, such as pentamidine isethionate, amphotericin B and miltefosine [2,3]. Malaria treatment relies on the use of quinoline-based drugs, such as chloroquine, primaquine and mefloquine, as well as antifolates and artemisinin derivatives, depending on the parasite's susceptibility [4]. Common problems with these antiparasitic drugs are severe side effects and development of drug resistance. Based on this scenery, the research of new active compounds against these parasites is pivotal.

The *Tabebuia* genus, belonging to the bignoniaceae plant family, is widely used in the traditional medicine in South America [5,6]. Among the active secondary metabolites present in this genus, 2-hydroxy-3-(3-methyl-2-buthenyl)-1,4-naphthoquinone (lapachol, Fig. 1) is one of the most studied. Lapachol is endowed with anticancer and antimicrobial properties [7,8]. Because of its antiproliferative activity, lapachol has been employed as a prototype for the design and synthesis of new anticancer and antimicrobial agents. This has led to the identification of fewer lapachol derivatives with an enhanced activity [9–12].

Like other naphthoquinones [13,14], lapachol is a feasible ligand for the preparation of coordinating or organometallic compounds. In fact, there are some findings showing that lapachol–metal complexes are biologically more active than the free molecule [15–18]. Ruthenium complexes are considered to be one of the most promising types of metal compounds for cancer treating, due its interesting chemical properties, such as: versatility in ligand exchange, octahedral geometry and variability of oxidation states [19,20]. Recently it was observed that the lapachol–Ru(II) complex is a more potent anticancer agent than lapachol–Os(II) and Rh(III) complexes [18], suggesting that the use of ruthenium is promising to improve the biological activity of lapachol.

* Corresponding author. Tel.: +55 1633518285; fax: +55 1633518350.
E-mail address: daab@power.ufscar.br (A.A. Batista).

http://dx.doi.org/10.1016/j.jinorgbio.2014.03.009
0162-0134/

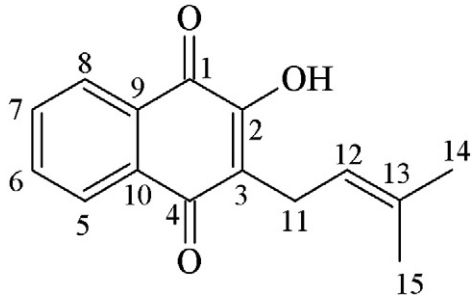

Fig. 1. Lapachol structure.

Therefore, the present study describes the synthesis, characterization, antileishmanial and antiplasmodial activities of novel diimines (2,2′-bipyridine (bipy), 1,10-phenantroline (phen), 4,4′-methylbipyridine (Me-bipy) and 4,4′-methoxybipyridine (MeO-bipy) and monophosphine ruthenium(II) and (III) complexes containing lapachol as a bidentate ligand.

2. Experimental section

2.1. Materials for synthesis

Solvents were purified by standard methods. All chemicals used were of reagent grade or comparable purity. The $RuCl_3 \cdot 3H_2O$ was purchased from Degussa or Aldrich. The ligands 1,4-*bis*(diphenylphosphino)butane (dppb), triphenylphosphine (TPP), bipy, Me-bipy, MeO-bipy and phen were used as received from Aldrich.

2.2. Instrumentation

Elemental analyses were performed in a Fisons EA 1108 model (Thermo Scientific). The IR spectra of the powder complexes were recorded using CsI pellets in the 4000–200 cm^{-1} region in a Bomen–Michelson FT MB-102 instrument. The UV–Visible (UV–vis) spectra of the complex were recorded in CH_2Cl_2 solution, in a Hewlett Packard diode array—8452A. The electron paramagnetic resonance (EPR) spectrum was measured in solid state at −160 °C using a Varian E-109 instrument, recorded at the X band frequency, within a rectangular cavity (E-248) fitted with a temperature controller. Cyclic voltammetry (CV) experiments of the complexes in solution were promoted in an electrochemical analyzer BAS model 100B. These experiments were carried out at room temperature, in CH_2Cl_2 containing 0.10 M $Bu_4N^+ClO_4^-$ (TBAP) (FlukaPurum) as support electrolyte, and using an one-compartment cell, with both working and auxiliary electrodes, which were stationary Pt foils, while the reference electrode was Ag/AgCl, 0.10 M TBAP in CH_2Cl_2. Under these conditions, the ferrocene is oxidized at 0.43 V (Fc^+/Fc).

All NMR experiments were run on a BRUKER, DRX400 MHz equipment, in a BBO 5 mm probe, at 298 K, and TMS (tetramethylsilane) for internal reference. For ^1H and ^{13}C NMR, DMSO-d_6 was used as solvent, while CH_2Cl_2 was used as solvent for ($^{31}P\{^1H\}$) NMR. The splitting of proton, carbon and phosphorus resonances was reported as s = singlet and m = multiplet.

2.3. X-ray crystallography

Blue single crystals of complexes **(1)** and **(5)** were grown by slow evaporation of a dichloromethane/*n*-hexane solution. X-ray diffraction experiments were carried out using a suitable crystal mounted on glass fiber, and positioned on the goniometer head. Intensity data were measured with the crystal at room temperature on an Enraf–Nonius Kappa-CCD diffractometer with graphite monochromated MoKα radiation (λ = 0.71073 Å). The cell refinements were performed using the software Collect [21] and Scalepack [22], and the final cell parameters were obtained on all reflections. Data reduction was carried out using the software Denzo-SMN and Scalepack [22]. The structures were solved by the Direct method using SHELXS-97 [15] and refined using the software SHELXL-97 [23]. A Gaussian method implemented was used for the absorption corrections [24]. Non-hydrogen atoms of the complexes were unambiguously located, and a full-matrix, least-square refinement of these atoms with anisotropic thermal parameters was carried out. The aromatic C–H hydrogen atoms were positioned stereochemically and were refined with fixed individual displacement parameters [$U_{iso}(H) = 1.2\ U_{eq}(Csp^2)$] using a riding model with an aromatic, C–H bond length fixed at 0.93 Å. Methylene groups of the dppb ligand in the complex **(5)**, and methine group of the lapachol were set as isotropic with a thermal parameter 20% greater than the equivalent isotropic displacement parameter of the atom to which each one was bonded, whereas methyl groups were set with $U_{iso}(H)$ values of $1.5U_{eq}(C_{methyl})$. Tables were generated by WinGX [25] and the structure representations by ORTEP-3 [18] and MERCURY [21]. The main crystal data collections and structure refinement parameters for **(1)** and **(5)** are summarized in Table 1.

2.4. Synthesis

All the solvents used in this work were of reagent quality and used without further purification. Lapachol was obtained according to the procedure described in [24]. The precursors *cis*-[$RuCl_2(PPh_3)_2$(X-bipy)] (X = H, methyl (Me) and methoxy (MeO)) and *cis*-[$RuCl_2(PPh_3)_2$ (phen)] were prepared according to literature [26,27]. Typically [100.0 mg; 0.1 mmol] of the [$RuCl_2(PPh_3)_3$] was dissolved in degassed 20 mL of dichloromethane (Merck) and N-heterocyclic (X-bipy or

Table 1
Crystal data and structure refinement for complex [Ru(Lap)$(PPh_3)_2$(bipy)]PF_6 **(1)** and [$RuCl_2$(Lap)(dppb)] **(5)**.

	[Ru(Lap)$(PPh_3)_2$(bipy)]PF_6	[$RuCl_2$(Lap)(dppb)]
Empirical formula	$[RuC_{61}H_{51}N_2O_3P_2]PF_6$	$[RuC_{43}H_{41}Cl_2O_3P_2]$
Formula weight	1168.02	839.67
Crystal system	Monoclinic	Monoclinic
Space group	$P2_1/c$	$P2_1/c$
Unit cell dimensions		
a (Å)	15.950(5)	9.1790(1)
b (Å)	16.744(5)	29.6950(5)
c (Å)	20.316(5)	14.7120(3)
β (°)	93.151(5)	104.564(1)
Volume ($Å^3$)	5418(3)	3881.20(11)
Z	4	4
Density calculated (Mg/m^3)	1.432	1.437
μ (mm^{-1})	0.447	0.663
F(000)	2392	1724
Crystal size (mm^3)	0.26 × 0.28 × 0.53	0.11 × 0.19 × 0.29
θ range (°)	2.96 to 26.76°	2.94 to 26.75°
Index ranges	−20 ≤ h ≤ 20 −19 ≤ k ≤ 21 −25 ≤ l ≤ 23	−11 ≤ h ≤ 8 −37 ≤ k ≤ 37 −18 ≤ l ≤ 18
Reflections collected	36,197	27,401
Independent reflections	11,479 [R(int) = 0.0423]	8251 [R(int) = 0.0617]
Completeness to θ	99.4%	99.7%
Max. and min. transmission	0.942 and 0.795	0.947 and 0.867
Data/restraints/parameters	11,479/0/687	8251/0/462
Goodness-of-fit on F^2	1.209	1.129
Final R indices [I > 2sigma(I)]	R1 = 0.0566, wR2 = 0.1321	R1 = 0.0376, wR2 = 0.0724
R indices (all data)	R1 = 0.0669, wR2 = 0.1386	R1 = 0.0692, wR2 = 0.0776
$\Delta\rho_{max.}$ and $\Delta\rho_{min.}$ ($e.Å^{-3}$)	0.553 and −0.641	0.557 and −0.541

phen) [22.0 mg; 0.11 mmol] ligand was added. The reaction mixture was stirred for 30 min at room temperature and the volume of the resulting blue solution was reduced, under vacuum, to ca. 2 mL and diethyl ether (Merck) was then added to precipitate a red solid, which was filtered off, washed several times with diethyl ether, and dried under vacuum. Yield: ~78 mg (80–90%).

Microanalyses suggested the formation of the complexes with general formula $[Ru(Lap)(PPh_3)_2(bipy)]PF_6$ **(1)**, $[Ru(Lap)(PPh_3)_2$(Me-bipy)$]PF_6$ **(2)**, $[Ru(Lap)(PPh_3)_2$(MeO-bipy)$]PF_6$ **(3)**, $[Ru(Lap)(PPh_3)_2$(phen)$]PF_6$ **(4)** and $[RuCl_2(Lap)(dppb)]$ **(5)**. The molar conductivity data reveal that the complex **5** (3.46 μS cm^{-1}) is non-electrolyte and complexes **1**–**4** (129.1, 146.8, 166.2 and 125.0 μS cm^{-1} respectively) are 1:1 electrolytes (CH_2Cl_2), in accordance with the proposed formulations.

2.4.1. [Ru(Lap)(PPh$_3$)$_2$(X-bipy)] and [Ru(Lap)(PPh$_3$)$_2$(phen)]

The ruthenium(II) complexes with N-N = bipy**(1)**, Me-bipy**(2)**, MeO-bipy**(3)** and phen**(4)** were prepared by reacting an excess of lapachol ligand (0.137 mmol; 33.0 mg), previously dissolved in degassed mixture of CH_2Cl_2:MeOH (50:50) solvent, and the same equivalent of triethylamine Et_3N, and the *cis*-$[RuCl_2(PPh_3)_2$(N-N)] precursors (0.114 mmol; ≅100.0 mg). The reaction mixture was refluxed and stirred for about 72 h, under Ar atmosphere. The final blue solutions were concentrated to *ca.* 2 mL and 10 mL of water was added in order to obtain dark blue precipitates. The solids were filtered off, well rinsed with water and diethyl ether and dried *in vacuum*.

2.4.1.1. [Ru(Lap)(PPh$_3$)$_2$(bipy)]PF$_6$ (1). Yield: 121 mg (88%). Anal. calcd for $C_{61}H_{51}F_6N_2O_3P_3Ru$: exptl (calc) C, 62.30 (62.72); H, 4.20 (4.40); N, 2.18 (2.40). $^{31}P\{^1H\}$ NMR: δ(ppm) 29.3 (s); ^1H NMR (400.21 MHz, DMSO-d_6, 298 K): δ(ppm) 9.80–7.00 (overlapped signals, 30H aromatic hydrogen for PPh_3 and 14H aromatic hydrogen for bipy and Lap) 4.88 (m, 1H, CH of Lap); 3.22 (m, 2H, CH_2 of Lap); 1.83 (s, 3H, CH_3 of Lap); 1.56 (s, 3H, CH_3 of Lap). ^{13}C NMR (400.21 MHz, DMSO-d_6, 298 K): δ(ppm) 198.1 (C_1═O of Lap), 180.6 (C_4═O of Lap), 167.2 (C_2 – O of Lap). UV–vis (CH_2Cl_2, 10^{-5} M): λ/nm (ε/M^{-1} L cm^{-1}) 370 (shoulder), 573 (6.30×10^3).

2.4.1.2. [Ru(Lap)(PPh$_3$)$_2$(Me-bipy)]PF$_6$.CH$_3$OH (2). Yield: 115 mg (84%). Anal. calc. for $C_{64}H_{59}F_6N_2O_4P_3Ru$: exp (calc) C, 62.70 (62.59); H, 4.61 (4.84); N, 2.32 (2.28). $^{31}P\{^1H\}$ NMR: δ(ppm) 29.1 (s); ^1H NMR (400.21 MHz, DMSO-d_6, 298 K): δ(ppm)2.30 (s, 3H, CH_3); 2.42 (s, 3H, CH_3') (aliphatic hydrogen for Me-bipy); 8.09–7.00 (overlapped signals, 30H aromatic hydrogen for PPh_3 and 8H aromatic hydrogen of Me-bipy); 4.87 (m, 1H, CH of Lap); 3.19 (m, 2H, CH_2 of Lap); 1.81 (s, 3H, CH_3 of Lap); 1.55 (s, CH_3 of Lap).^{13}C NMR (400.21 MHz, DMSO-d_6, 298 K): δ(ppm) 198.7 (C_1═O of Lap), 182.3 (C_4═O of Lap), 168.0 (C_2 – O of Lap). UV–vis (CH_2Cl_2, 10^{-5} M): λ/nm (ε/M^{-1} cm^{-1}) 297 (shoulder), 572 (6.40×10^3).

2.4.1.3. [Ru(Lap)(PPh$_3$)$_2$(MeO-bipy)]PF$_6$ (3). Yield: 110 mg (84%). Anal. calcd for $C_{63}H_{55}F_6N_2O_5P_3Ru$: exp.(calc) C, 61.97 (61.61); H, 4.39 (4.51); N, 2.43 (2.28). $^{31}P\{^1H\}$ NMR: δ(ppm) 29.8 (s). ^1H NMR (400.21 MHz, DMSO-d_6, 298 K):δ(ppm) 3.91 (s, 3H, CH_3); 3.84 (s, 3H, CH_3') (aliphatic hydrogen of MeO-bipy); 9.45–7.00 (overlapped signals, 30H aromatic hydrogen for PPh_3 and 12H aromatic hydrogen for MeO-bipy and Lap); 4.85 (m, 1H, CH of Lap); 3.16 (m, 2H, CH_2 of Lap); 1.80 (s, 3H, CH_3 of Lap); 1.54 (s, CH_3 of Lap).^{13}C NMR (400.21 MHz, DMSO-d_6, 298 K): δ(ppm) 198.2 (C_1═O of Lap), 180.4 (C_4═O of Lap), 167.6 (C_2 – O of Lap). UV–vis (CH_2Cl_2, 10^{-5} M): λ/nm (ε/M^{-1} cm^{-1}) 297 (shoulder), 586 (6.11×10^3).

2.4.1.4. [Ru(Lap)(PPh$_3$)$_2$(phen)]PF$_6$(4). Yield: 128 mg (94%). Anal. calcd for $C_{63}H_{51}F_6N_2O_3P_3Ru$: exp.(calc) C, 63.97 (63.48); H, 3.99 (4.31); N, 2.39 (2.35). $^{31}P\{^1H\}$ NMR: δ(ppm) 32.6 (s). ^1H NMR (400.21 MHz, DMSO-d_6, 298 K):δ(ppm)10.00–7.00 (overlapped signals, 30H aromatic hydrogen of PPh_3 and 18H aromatic hydrogen for phen and Lap); 4.91 (m, 1H, CH of Lap); 3.26 (m, 2H, CH_2 of Lap); 1.83 (s, 3H, CH_3 of Lap); 1.55 (s, CH_3 of Lap).^{13}CNMR (400.21 MHz, DMSO-d_6, 298 K): δ(ppm) 198.4 (C_1═O of Lap), 180.6 (C_4═O of Lap), 167.4 (C_2 – O of Lap). UV–vis (CH_2Cl_2, 10^{-5} M): λ/nm (ε/M^{-1} L cm^{-1}) 290 (shoulder), 300 (2.66×10^4), 408 (5.25×10^3).

2.4.1.5. [RuCl$_2$(Lap)(dppb)], (5). The ruthenium (III) complex $[RuCl_2$(Lap)(dppb)] **(5)** was prepared dissolving (0.137 mmol; 33.0 mg) of lapachol ligand in a mixture of CH_2Cl_2:MeOH (50:50) solvent and the same equivalent of triethylamine (Et_3N) and then added the *mer*-$[RuCl_3(dppb)(H_2O)]$ [28] precursor (0.137 mmol; 33.0 mg). The reaction mixture was refluxed and stirred for 24 h, under Ar atmosphere. The final purple solution was concentrated to ca. 2 mL, and 10 mL of diethyl ether was added in order to obtain dark purple precipitate. The solid was filtered off, well rinsed with diethyl ether and dried *in vacuo*. Yield: 189 mg (98%). Anal. calc. for $C_{43}H_{41}Cl_2O_3P_2Ru$: exp. (calc) C, 61.40 (61.50); H, 4.80 (4.92). UV–vis (CH_2Cl_2, 10^{-5} M): λ/nm (ε/M^{-1} L cm^{-1}) 315 (shoulder), 330 (shoulder), 356 (2.77×10^3) and 558 (5.6×10^3).

2.5. Biological experiments

2.5.1. Cells and cultures

Antiparasitic activity was performed with *Leishmania amazonensis* (MHOM/BR88/BA-125) and W2 strain *Plasmodium falciparum*, while hemolysis assays were done using O^+ human erythrocytes and cytotoxicity assays were done in J774 macrophages. The *L. amazonensis* promastigotes were maintained in Schneider's insect medium (Sigma-Aldrich, St. Louis, USA) supplemented with 10% fetal bovine serum (Gibco Laboratories, Gaithersburg, USA) and 50 μg/mL of gentamicin (Hipolabor, Belo Horizonte, Brazil). J774 macrophages were cultivated in RPMI-1640 medium (Sigma-Aldrich, St. Louis, USA) supplemented with 10% fetal bovine serum and 50 μg/mL of gentamicin. W2 strain *P. falciparum* was maintained in continuous culture of human erythrocytes (blood group O^+) using RPMI-1640 medium supplemented with 10% human plasma without hypoxanthine.

2.5.2. Cytotoxicity assays

J774 macrophages (5×10^4 cells/mL) were distributed in 96-well plate (100 μL/well) and incubated for 24 h at 37 °C in 5% CO_2. Each drug was solubilized in DMSO as a stock solution and diluted in culture media in the tested concentrations ranging from 0.1 to 10 μg/mL (100 μL/well). The final concentration of DMSO was 0.1%. Each concentration was tested in triplicate. After incubation for 72 h, 20 μL of Alamar blue (Invitrogen, CA, USA) was added to each well and incubated for 24 h in the dark. Gentian violet was used as control. The absorbance was evaluated at 570 and 600 nm according to manufacturer's instructions. The LC_{50} values were calculated using a non-linear regression curve fit in the Prism version 5.03 (GraphPad Software).

For the hemolysis assay, human erythrocytes type O^+ were washed three times in phosphate buffered saline and 100 μL of this suspension (1% hematocrit) was distributed into a 96-well plate. Then, 100 μL of each drug, previously dissolved in phosphate buffered saline, was added in triplicate to the plate and incubated for 1 h. Saponin (Sigma-Aldrich, St. Louis, USA) was used as reference drug at 1% *v*/*v*. After incubation the cells were centrifuged (1500 rpm for 10 min) and 100 μL of each supernatant was transferred to another microtiter plate. Released haemoglobin was monitored by measuring the absorbance at 540 nm in a spectrophotometer. The percentage of hemolysis was determined in comparison to untreated cells.

2.5.3. Antileishmanial activity against promastigotes

L. amazonensis promastigotes (2×10^6 cells/mL) in stationary growth phase were distributed in a 96-well plate (100 μL/well) at 24 °C. Each drug was solubilized in DMSO as described above,

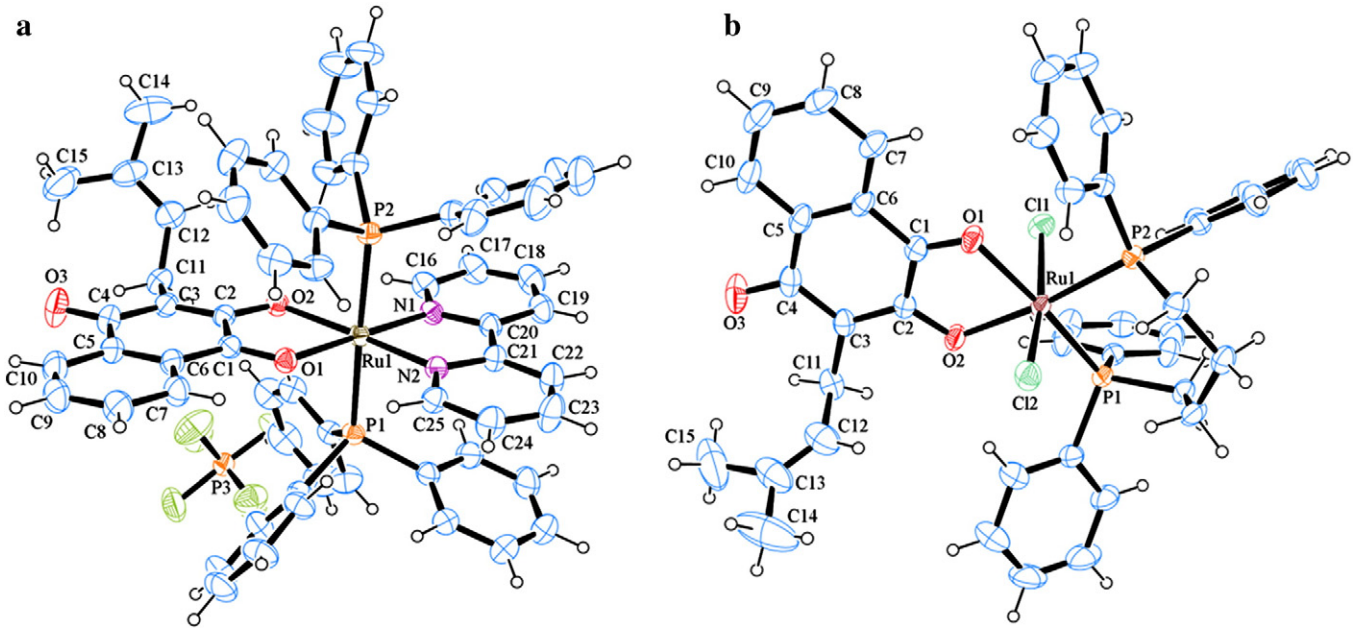

Fig. 2. X-ray structures for (a) $[Ru(Lap)(PPh_3)_2(bipy)]PF_6$ (1) and (b) $[RuCl_2(Lap)(dppb)]$ (5), showing atoms labeling and 50% of probability ellipsoids.

diluted in the culture medium and added in serial dilution from 0.1 to 10 μg/mL (100 μL/well). The final DMSO concentration was 0.1%. Amphotericin B (Gibco Laboratories, Gaithersburg, USA) was used as reference drug. After 72 h incubation at 24 °C, the number of viable parasites was counted in a Neubauer chamber. The IC_{50} values were calculated in Prism version 5.03 (GraphPad Software) using non-linear regression.

2.5.4. In vitro leishmania infection

J774 macrophages (2×10^5cells/mL) were plated in 96-well plate (100 μL/well) and incubated overnight at 37 °C in 5% CO_2. *L. amazonensis* promastigotes in the stationary growth phase were added to the cell culture (100 μL/well) at a parasite/macrophage ratio of 10:1 and incubated for 24 h. Plates were washed to remove non-phagocytosed parasites. Each drug, solubilized as described above, was added and incubated for 72 h. Amphotericin B was used as reference drug. Infected macrophages were lysed by addition of 0.01% sodium dodecyl sulfate (Sigma-Aldrich, St. Louis, USA) in PBS (phosphate-buffered saline) at 37 °C for 30 min.

Amastigotes from lysed macrophages were incubated at 24 °C for 48 h, which then differentiated in promastigotes. The number of viable promastigotes was determined by adding Alamar Blue (20 μL/well) and incubated for 24 h. The absorbance was evaluated at 570 and 600 nm according to the manufacturer's instructions. The IC_{50} values were calculated in Prism version 5.03 (GraphPad Software) using non-linear regression.

2.5.5. Antimalarial activity

The antimalarial effects of the compounds were measured with the [^{3}H]-hypoxanthine (PerkinElmer, Boston, USA) incorporation assay. W2 *P. falciparum* grown at 1–2% parasitemia and 2.5% hematocrit were aliquoted in a 96-well plate. Drugs were solubilized as described above in a concentration range of 0.1 to 10 μg/mL; each concentration was performed in triplicates. Mefloquine (Farmanguinhos, Rio de Janeiro, RJ, Brazil) was used as reference drug. After 24 h of incubation with the tested compounds, 25 μL of medium containing [^{3}H]hypoxanthine (0.5 μCi/well) was added per well, followed by another 24 h of incubation. The parasites were harvested using a cell harvester to evaluate the [^{3}H]-hypoxanthine incorporation in a β-radiation counter (Multilabel Reader; Hidex, Turku, Finland). Inhibition of parasite growth was evaluated by comparing the [^{3}H]-hypoxanthine uptake in untreated versus treated cells. IC_{50} values were calculated in a Graph Pad Prism version 5.03 (Graph Pad Software, San Diego, CA) using non-linear regression.

Table 2
Selected bond length (Å) and angles (°) for complexes (**1**) and (**5**).

Fragment	Complex (1)	Complex (5)
Ru(1)–O(1)	2.0710(19)	2.1707(15)
Ru(1)–O(2)	2.133(2)	2.0580(15)
Ru(1)–P(2)	2.3952(11)	2.3728(6)
Ru(1)–P(1)	2.4104(10)	2.2910(6)
Ru(1)–N(2)	2.038(2)	–
Ru(1)–N1(1)	2.050(2)	–
Ru(1)–Cl(1)	–	2.3308(7)
Ru(1)–Cl(2)	–	2.3343(7)
O(1)–C(1)	1.250(3)	1.235(3)
O(2)–C(2)	1.308(3)	1.309(3)
O(3)–C(4)	1.236(4)	1.230(3)
O(2)–Ru(1)–O(1)	76.22(7)	77.85(6)
O(1)–Ru(1)–P(1)	174.56(5)	91.69(6)
O(2)–Ru(1)–P(2)	90.02(6)	171.11(5)
O(1)–Ru(1)–P(2)	89.95(6)	93.39(5)
P(1)–Ru(1)–P(2)	178.25(3)	92.01(2)
Cl(1)–Ru(1)–Cl(2)	–	168.99(3)

3. Results and discussion

In this work the lapachol acted as bidentate ligand and monoanionic species, coordinating with the ruthenium atoms through its *ortho* oxygens (O1, O2—Fig. 1). The structures of the complexes $[Ru(Lap)(PPh_3)_2(bipy)]PF_6$ **(1)** and $[RuCl_2(Lap)(dppb)]$ **(5)** were confirmed based on X-ray diffraction data (see Fig. 2). These compounds crystallize in the

Table 3
Cyclic voltammetry data for complexes (**1**)–(**4**) (TBAP 0.1 M; CH_2Cl_2; Ag/AgCl; work electrode Pt; 100 mVs^{-1}).

Complex	E_{pa} (V)	$E_{1/2}$ (V)	pKa (N–N)
$[Ru(Lap)(PPh_3)_2(bipy)]PF_6$ (**1**)	1.03	0.99	4.86
$[Ru(Lap)(PPh_3)_2(Me\text{-}bipy)]PF_6$ (**2**)	0.96	0.87	4.92
$[Ru(Lap)(PPh_3)_2(MeO\text{-}bipy)]PF_6$ (**3**)	0.77	0.71	5.74
$[Ru(Lap)(PPh_3)_2(phen)]PF_6$ (**4**)	1.08	1.00	4.44

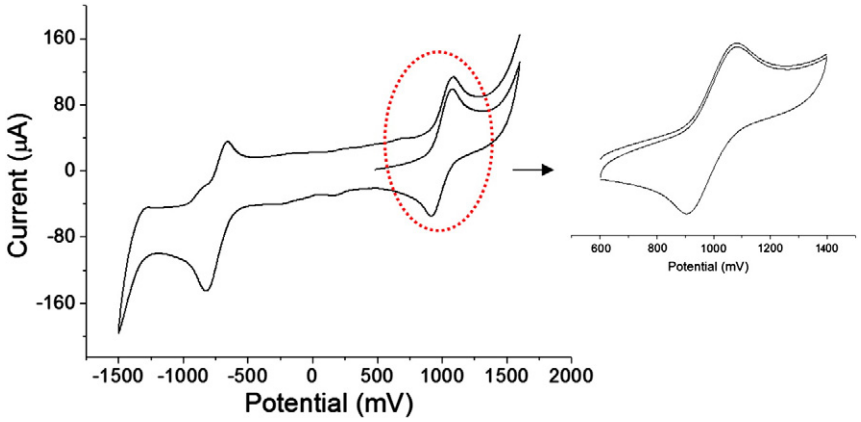

Fig. 3. Cyclic voltammogram of $[Ru(Lap)(PPh_3)_2(phen)]PF_6$ (4) (TBAP 0.1 M; CH_2Cl_2; Ag/AgCl; work electrode Pt; 100 $mV.s^{-1}$).

monoclinic system, with the space group $P2_1/c$. It is observed that the O1 and O2 atoms are involved in the coordination, where O2, is negatively charged and O1, is neutral. A distorted octahedral geometry is observed for both crystal structures, as observed by the bond angles (Table 2).

Some distance and selected angles in the X-ray structure of complex **(1)** and **(5)** are shown in Table 2, which are, in general, in accordance with values expected for similar phosphine complexes of Ru(II) and Ru(III) for Ru–N, Ru–P and Ru–Cl [28–30]. But, it is interesting to point out that the distances of Ru(II)–O for complex **(1)** are also in accordance with the expected values, where the distance Ru–O2 [2.133(2) Å] is longer than the distance Ru–O1 [2.0710(19) Å], since the O2 has charge minus one and its radius is bigger than the one for the neutral species. Therefore, the same was not observed for complex **(5)**, where the distance Ru–O1 [2.1707(15) Å] is longer than the distance Ru–O2 [2.0580(15) Å]. Probably in this case the strong *trans* effect of phosphorus atoms is more effective when it is *trans* to neutral atoms, and not when it is *trans* to negatively charged atoms. As it can be seen in Table 2 the distance of Ru(III)–O1 is 0.1 Å longer than Ru(II)–O1, showing the strong *trans* effect phosphorus atoms. On other hand the distance Ru(III)–O1, is shorter than Ru(II)–O1, as expected, considering the size of the radius of Ru(III) and Ru(II).

In the $^{31}P\{^1H\}$ NMR spectra of the complexes **(1–4)** just one singlet at about 30 ppm is observed in all cases, indicating the magnetic equivalence of the two *trans* phosphorus atoms, as expected. Also, each $^{31}P\{^1H\}$ NMR spectra exhibit a heptet signal at −144 ppm, corresponding to the phosphorus atoms of the PF_6^- counter ion. The EPR spectra in solid state, for complex **(5),** confirms the presence of Ru (III) paramagnetic species, showing $g_1 = 2.578$, g_2 2.128 and $g_3 = 1.822$ typical of ruthenium (III) complexes [29].

Cyclic voltammograms of Ru(II) complexes (**1**–**4**) show a quasi-reversible process between 0.71 and 1.0 V, which correspond to the redox pair Ru(III)/Ru(II), as can be seen from the Table 3, and Fig. 3 for the case of complex **(4)**. In the negative region a quasi-reversible one-electron reduction process was observed in all cases, which most probably correspond to the ligand reduction to the semiquinone form [31]. As can be seen in Table 3 the redox potential of 1–4 decreases when the diimine basicity is increased. Analyzing the complex $[RuCl_2(Lap)(dppb)]$ (5), in the same experimental conditions, it is observed a Ru(III)/Ru(II) reversible process with E1/2 of 0.18 V.

The IR spectra of complexes **(1–5)** confirm the presence of the lapachol ligand coordinated to the metal. The band located at 3351 cm^{-1} in the free lapachol [31,32] assigned to OH, disappears upon coordination, as expected. The characteristic ν(C═O) stretching bands, found at $\nu(C_1{=}O)$ 1664 and $\nu(C_4{=}O)$ 1641 cm^{-1} in free lapachol [11] shifted to lower frequencies in complexes, 1561–1591 cm^{-1} and 1581–1533 cm^{-1}, respectively. This behavior was also observed for other complexes like Ru(II), Co(II), Ni(II) and Cu(II) containing the lapachol as ligand [5,11,12]. The characteristic $\nu(C_2-O)$ stretching band found in 1028 cm^{-1} in the free lapachol shifted to higher frequencies in complexes (1065–1079 cm^{-1}). Finally, new bands of medium intensities, located below 500 cm^{-1} are present in the spectra of complexes, which may be related to metal–ligand vibrations.

The antiparasitic and toxicity of host cell were evaluated. For comparison, the metal-free lapachol was included in the pharmacological evaluation. Firstly, compounds were evaluated on their ability to inhibit the *L. amazonensis* promastigote proliferation, as well as against intracellular amastigotes, according to standard methodology [33]. Secondly, the antimalarial activity of the complexes was determined against the erythrocytic stage of W2 strain *P. falciparum*. Host cell cytotoxicity in J774 macrophages as well as the hemolysis in uninfected erythrocytes was determined [34,35]. The results were expressed in terms of IC_{50} and LC_{50} values. Amphotericin B and mefloquine were respectively

Table 4
Antiparasitic activity and cytotoxicity for the ruthenium complexes.

Compounds	*L. amazonensis*, IC_{50} ± SEM(μM)		*P. falciparum*[c] IC_{50} ± SEM(μM)	Cytotoxicity[d] LC_{50} ± SEM(μM)	SI[e]
	Promastigotes[a]	*In vitro* infection[b]			
Lapachol	12.4 ± 0.69	>10	11.3 ± 4.1	>10	N.D.
(**1**)	>10	0.07 ± 0.002	43.5 ± 0.71	0.33 ± 0.08	4.7
(**2**)	0.18 ± 0.04	0.17 ± 0.01	0.35 ± 0.26	1.0 ± 0.46	5.9
(**3**)	0.42 ± 0.03	>10	0.53 ± 0.28	6.7 ± 1.3	N.D.
(**4**)	1.6 ± 0.44	N.D.	0.19 ± 0.17	1.9 ± 1.3	N.D.
(**5**)	0.14 ± 0.04	0.57	0.21 ± 0.10	>10	17.5
Mefloquine	–	–	0.04 ± 0.01	–	N.D.
Amphotericin B	0.13 ± 0.01	0.23 ± 0.09	–	>10	N.D.
Gentian Violet	–	N.D.	N.D.	0.60 ± 0.07	–

[a]Values determined 72 h after incubation with drugs. [b]Values determined for infected macrophages 72 h after incubation with drugs [c]Determined against W2 strain *P. falciparum* (erythrocytic stage) 24 h after incubation with drugs. [d]Cytotoxicity was determined in J774 macrophages after 72 h incubation with drugs. [e]SI value is given from the ratio LC_{50} in J774/IC_{50} (*L. amazonensis*, *in vitro* infection). IC_{50} and LC_{50} values were determined from two independent experiments, concentration in triplicates. SEM = standard error of the mean; N.D. = not determined. SI = selectivity index.

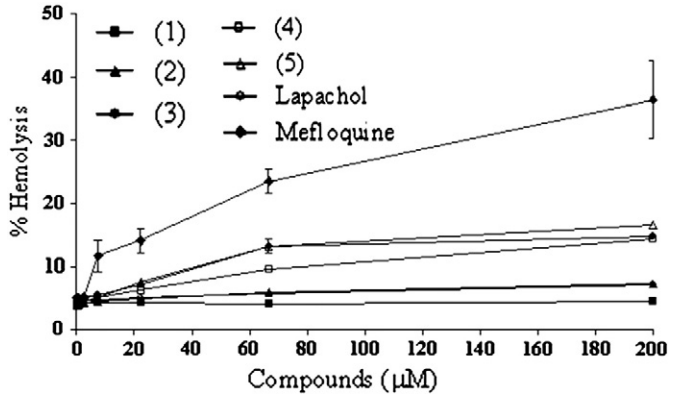

Fig. 4. Hemolytic activity of lapachol and complexes. The hemolytic activity of the compounds was assayed in fresh human erythrocytes type O^+. Saponin was used as hemolytic drug at 1% *v*/*v*. Released hemoglobin was monitored by measuring the absorbance at 540 nm in a spectrophotometer. Results shown are mean ± SD of one experiment performed in triplicate.

used as reference drugs for *Leishmania* and *Plasmodium* tests respectively, while gentian violet was used as control in host cell cytotoxicity.

Amphotericin B, which was used as a reference drug, exhibited an $IC_{50} = 0.13 \pm 0.01$ μM, while lapachol was in practice, inactive against *L. amazonensis* promastigotes. Complex **(1)** was inactive to inhibit promastigotes, while complexes (**2**–**5**) were able to inhibit their proliferation. Specifically, complexes (**2**) and (**5**) exhibited activity against promastigotes similar to the observed for amphotericin B. Regarding the inhibitory activity in *L. amazonensis*-infected macrophages, amphotericin B displayed an $IC_{50} = 0.23 \pm 0.09$ μM, while lapachol was inactive. In this assay, complexes (**3**) and (**4**) were also inactive. In contrast, complexes (**1**), (**2**) and (**5**) were able to reduce the *Leishmania* infection in macrophages, with similar potency to the observed for amphotericin B.

The cytotoxicity towards host cells was also determined for all five complexes, including lapachol. Gentian violet had a $LC_{50} = 0.60 \pm 0.07$, while lapachol was non-toxic, having a $LC_{50} > 10$ μM for J774 macrophages. In comparison to lapachol, complexes **(1–4)** were more cytotoxic, while complex (**5**) was not cytotoxic. The selectivity index was calculated and shown in Table 4. Considering the antileishmania activity, complex (**5**) exhibited high selectivity index, while complexes (**1**–**2**) showed indexes lower than complex (**5**).

Next, the antimalarial activity for these complexes was evaluated. Lapachol displayed a weak activity to inhibit *P. falciparum* in comparison to mefloquine. It was observed that complex (**1**) showed a poor activity, while the complexes (**2**–**5**) were several times more potent than free lapachol. The most potent complexes against *P. falciparum* were **(4)** and **(5)**. These complexes were fifty times more potent than free lapachol and only five times less potent than mefloquine. In addition, the effects of complexes **(1–5)**, as well as of free lapachol, in causing hemolysis were evaluated and the percentage of hemolysis was calculated. Saponin, was used as the reference drug to cause hemolysis to the erythrocytes (Fig. 4). Lapachol did not cause hemolysis. The complexes **(1–5)** failed to cause not even 50% of hemolysis at 200 μM. This suggests that the reported anti-*P. falciparum* activity was not caused by the red blood cells lyses.

4. Conclusions

In summary, five new ruthenium (II) and (III) complexes containing lapachol as ligand were synthesized and characterized by a combination of NMR, EPR, FTIR, and X ray diffraction techniques. The evaluation of antiparasitic activities of the complexes against *L. amazonensis* and *P. falciparum* demonstrated that the lapachol–ruthenium complexes are more potent than the free lapachol. The $[RuCl_2(Lap)(dppb)]$ complex is the most potent and selective antiparasitic compound among the five new ruthenium complexes studied in this work, exhibiting an activity comparable to the one of reference drugs. Specifically, lapachol–ruthenium complexes displayed potent and selective antileishmanial activity.

Acknowledgments

This study received support from CNPq, FAPESP, FAPESB and CAPES. T.S.M. holds a FAPESB scholarship. R.S.C. thanks FAPESP for a PhD fellowship (Grant number 2009/08131-1). The authors acknowledge the assistance of Diogo Rodrigo de Magalhães Moreira for helpful discussions during the preparation of the manuscript.

Appendix A. Supplementary data

Coordinates and other crystallographic data have been deposited with the CCDC, deposition codes CCDC 973562 and 973365, for the complexes (**1**) and (**5**), respectively. Copies of this information may be obtained from The Director, CCDC, 12 Union Road, Cambridge, CB2 1EZ, UK, Fax: +44 1233 336033, E-mail: deposit@ccdc.cam.ac.uk or www.ccdc.cam.ac.uk. Supplementary data to this article can be found online at http://dx.doi.org/10.1016/j.jinorgbio.2014.03.009.

References

[1] P. Baiocco, G. Colotti, S. Franceschini, A. Ilari, J. Med. Chem. 52 (2009) 2603–2612.
[2] B. Monge-Maillo, R. López-Vélez, Drugs 73 (2013) 1889–1920.
[3] S. Sundar, J. Chakravarty, Expert. Opin. Pharmacother. 14 (2013) 53–63.
[4] J.K. Baird, N. Engl. J. Med. 352 (2005) 1565–1577.
[5] H. Hussain, K. Krohn, V.U. Ahmad, G.A. Miana, I.R. Green, Arkivoc 3 (2007) 145–171.
[6] F. Epifano, S. Genovese, S. Fiorito, V. Mathieu, R. Kiss, Phytochem. Rev. 13 (2014) 37–49.
[7] J.J. Lu, J.L. Bao, G.S. Wu, W.S. Xu, M.Q. Huang, X.P. Chen, Y.T. Wang, Anticancer Agents Med. Chem. 13 (2013) 456–463.
[8] P. Guiraud, R. Steiman, G.M. Campos-Takaki, F. Seigle-Murandi, Planta Med. 60 (1994) 373–374.
[9] N.M. Lima, C.S. Correia, L.L. Leon, G.M. Machado, M.F. Madeira, A.E. Santana, M.O. Goulart, Mem. Inst. Oswaldo Cruz 99 (2004) 757–761.
[10] E. Pérez-Sacau, R.G. Díaz-Peñate, A. Estévez-Braun, A.G. Ravelo, J.M. García-Castellano, L. Pardo, M. Campillo, J. Med. Chem. 50 (2007) 696–706.
[11] M.A. Souza, S. Johann, L.A. Lima, F.F. Campos, I.C. Mendes, H. Beraldo, E.M. de Souza-Fagundes, P.S. Cisalpino, C.A. Rosa, T.M. Alves, N.P. de Sá, C.L. Zani, Mem. Inst. Oswaldo Cruz 108 (2013) 342–351.
[12] E.N. da Silva, C.F. de Deus, B.C. Cavalcanti, C. Pessoa, L.V. Costa-Lotufo, R.C. Montenegro, M.O. de Moraes, M.C. Pinto, C.A. de Simone, V.F. Ferreira, M.O. Goulart, C.K. Andrade, A.V. Pinto, J. Med. Chem. 53 (2010) 504–508.
[13] S. Oramas-Royo, C. Torrejón, I. Cuadrado, R. Hernández-Molina, S. Hortelano, A. Estévez-Braun, B. de Las Heras, Bioorg. Med. Chem. 21 (2013) 2471–2477.
[14] A.P. Neves, M.X. Pereira, E.J. Peterson, R. Kipping, M.D. Vargas, F.P. Silva Jr., J.W. Carneiro, N.P. Farrell, J. Inorg. Biochem. 119 (2013) 54–64.
[15] M.N. Rocha, P.M. Nogueira, C. Demicheli, L.G. de Oliveira, M.M. da Silva, F. Frézard, M.N. Melo, R.P. Soares, Bioinorg. Chem. Appl. 2013 (2013) 1–7.
[16] L.G. Oliveira, M.M. Silva, F.C. Paula, E.C. Pereira-Maia, C.L. Donnici, C.A. Simone, F. Frézard, E.N. Silva, C. Demicheli, Molecules 16 (2011) 10314–10323.
[17] G.L. Parrilha, R.P. Vieira, P.P. Campos, G.D. Silva, L.P. Duarte, S.P. Andrade, H. Beraldo, Biometals 25 (2012) 55–62.
[18] W. Kandioller, E. Balsano, S.M. Meier, U. Jungwirth, S. Göschl, A. Roller, M.A. Jakupec, W. Berger, B.K. Keppler, C.G. Hartinger, Chem. Commun. 49 (2013) 3348–3350.
[19] G.-J. Lin, G.-B. Jiang, Y.-Y. Xie, H.-L. Huang, Z.-H. Liang, Y.-J. Liu, J. Biol. Inorg. Chem. 18 (2013) 873–882.
[20] Y.-Y. Xie, H.-L. Huang, J.-H. Yao, G.-J. Lin, G.-B. Jiang, Y.-J. Liu, Eur. J. Med. Chem. 63 (2013) 603–610.
[21] Enraf-Nonius,COLLECT. Nonius BV, Delft, The Netherlands, 1997–2000.
[22] Z. Otwinowski, W. Minor, Methods Enzymol. 276 (1997) 307–326.
[23] G.M.A. Sheldrick, Acta Crystallogr. A Found. Crystallogr. 64 (2008) 112–122.
[24] P. Coppens, L. Leiserowitz, D. Rabinovich, Acta Crystallogr. 18 (1965) 1035–1038.
[25] L.J. Farrugia, J. Appl. Crystallogr. 32 (1999) 837–838.
[26] E.R. dos Santos, M.A. Mondelli, L.V. Pozzi, R.S. Corrêa, H.S. Salistre-de-Araújo, F.R. Pavan, C.Q.F. Leite, J. Ellena, V.R.S. Malta, S.P. Machado, A.A. Batista, Polyhedron 51 (2013) 292–297.
[27] A.A. Batista, M.O. Santiago, C.L. Donicci, I.S. Moreira, P.C. Healy, S.J. Berners-Price, S.L. Queiroz, Polyhedron 20 (2001) 2123–2128.
[28] L.R. Dinelli, A.A. Batista, K. Wohnrath, M.P. de Araujo, S.L. Queiroz, M.R. Bonfadini, G. Oliva, O.R. Nascimento, P.W. Cyr, K.S. MacFarlane, B.R. James, Inorg. Chem. Commun. 38 (1999) 5341–5345.
[29] A.A. Batista, K. Wohnrat, E.E. Castellano, I.S. Moreira, J. Elena, L.R. Dinelli, M.P. Araujo, J. Chem. Soc. Dalton Trans. 19 (2000) 3383–3386.
[30] Q.A. de Paula, R.W. Franco, M.B. Ribeiro, J. Ellena, E.E. Castellano, O.R. Nascimento, A. A. Batista, J. Mol. Struct. 891 (2008) 64–74.

[31] P.A.L. Ferraz, F.C. de Abreu, A.V. Pinto, V. Glezer, J. Tonholo, M.O.F. Goulart, J. Electroanal. Chem. 507 (2001) 275–286.
[32] R. Hernández-Molina, I. Kalinina, P. Esparza, M. Sokolov, J. Gonzalez-Platas, A. Estévez-Braun, E. Pérez-Sacau, Polyhedron 26 (2007) 4860–4864.
[33] V.P. Rocha, F.R. Nonato, E.T. Guimarães, L.A.R. de Freitas, M.B.P. Soares, J. Med. Microbiol. 62 (2013) 1001–1010.
[34] R. Dejardins, C. Canfield, J. Haynes, J. Chulay, Antimicrob. Agents Chemother. 16 (1979) 710–718.
[35] C. Wang, X. Qui, B. Huang, F. He, C. Zeng, Biochem. Biophys. Res. Commun. 402 (2010) 773–777.

FeSBE
FEDERAÇÃO DE SOCIEDADES DE BIOLOGIA EXPERIMENTAL

X Reunião Regional
Salvador - BA

Certificamos que

o trabalho 05.029 intitulado AVALIAÇÃO DA ATIVIDADE ANTIMALÁRICA DE NOVOS COMPLEXOS DE RUTÊNIO COM CLOROQUINA. Paixao MJ, Macedo TS, Moreira DRM, Batista AA, Vegas LAC, Soares MBP - Departamento de Química - UFSCar Laboratório de Engenharia Tecidual e Imunofarmacologia - CPqGM - FIOCRUZ, foi apresentado sob a forma de painel na

X Reunião Regional da Federação de Sociedades de Biologia Experimental - FeSBE, realizada de 04 a 06 de junho de 2015, no Instituto de Ciências da Saúde - UFBA, Salvador - BA.

Comissão Organizadora

CAPES

CNPq
Conselho Nacional de Desenvolvimento Científico e Tecnológico

fapesb
Fundação de Amparo à Pesquisa do Estado da Bahia

FeSBE
FEDERAÇÃO DE SOCIEDADES DE BIOLOGIA EXPERIMENTAL

X Reunião Regional
Salvador - BA

Certificamos que

O trabalho 05.029 intitulado AVALIAÇÃO DA ATIVIDADE ANTIMALÁRICA DE NOVOS COMPLEXOS DE RUTÊNIO COM CLOROQUINA. Paixao MJ, Macedo TS, Moreira DRM, Batista AA, Vegas LAC, Soares MBP - Departamento de Química - UFSCar Laboratório de Engenharia Tecidual e Imunofarmacologia - CPqGM - FIOCRUZ, foi contemplado com Menção Honrosa pela brilhante apresentação

X Reunião Regional da Federação de Sociedades de Biologia Experimental - FeSBE, realizada de 04 a 06 de junho de 2015, no Instituto de Ciências da Saúde - UFBA, Salvador - BA.

Comissão Organizadora

CAPES

CNPq
Conselho Nacional de Desenvolvimento Científico e Tecnológico

fapesb
Fundação de Amparo à Pesquisa do Estado da Bahia